ACTIVATION OF THE PLEIOTROPIC DRUG RESISTANCE REGULON BY THE MOLECULAR CHAPERONES SSZ1 AND ZUO1

by

Jeanette K. Ducett

A dissertation submitted in partial fulfillment of

the requirements for the degree of

Doctor of Philosophy

(Cellular & Molecular Biology)

at the

UNIVERSITY OF WISCONSIN-MADISON

2012

Date of final oral examination: 5/16/12

This dissertation is approved by the following members of the Final Oral Committee:

Elizabeth A Craig, Professor, Biochemistry

Aseem Z Ansari, Professor, Biochemistry

Thomas FJ Martin, Professor, Biochemistry

Catherine A Fox, Professor, Biomolecular Chemistry

Warren Heideman, Professor, Pharmacy

ACKNOWLEDGEMENTS

First, I would like to express my endless gratitude to my advisor, Dr. Elizabeth Craig, for allowing me to the opportunity to work in her lab and providing me with excellent mentorship. Over the past several years I have grown tremendously as a scientist and I know that this is in large part due to her great insights and helpful feedback on my project, her accessibility and patience in guiding me through this process, and her ability to help me learn to "think like a scientist." I would also like to thank my committee members, Dr. Aseem Ansari, Dr. Catherine Fox, Dr. Warren Heideman, and Dr. Thomas Martin, who have been a tremendous source of guidance and support throughout the years. I would like to extend a huge thanks to my "Milwaukee lab", most importantly Dr. Brian Volkman and Dr. Francis Peterson, who have been instrumental in my training as a scientist and to whom I owe much of my success. I also thank them for taking me under their wings once again during graduate school, this time as collaborators. I would also like to express my gratitude to my undergraduate advisor, Dr. Wayne Wiens, who not only taught me an incredibly vast array of scientific knowledge, but also helped instill in me a passion for the sciences.

I send a huge thanks to the members of the Craig lab, both past and present, for their guidance, support, great scientific discussions, and for helping make the lab an enjoyable place to work. In particular I would like to thank Amy Prunuske and Peter Kuhn for serving as excellent partners on the PDR project—providing great scientific insights and contributions as well as guidance and support. I thank Chandan Sahi, Brenda Schilke, Willy Walter, and Justin Hines for always providing great project advice and encouragement. I also send a huge thanks to

Lindsey Hoover, June Pais, and Alison Meyer for many great scientific and not-so-scientific discussions, for their endless encouragement, wonderful friendship, and for making life in the lab a daily joy.

Finally, I cannot imagine doing any of this without the love and support of my friends and family. I owe a huge thanks to my friends, both from my childhood in Moundridge, from mod 9C and my years at Bethel College, and especially from my time in the CMB program in Madison who have supported me and filled my life with laughter. I am forever grateful to my parents, Galen and Kathy Waltner, for everything they have provided me in life, most importantly for their endless love and support, and for instilling in me a love for the sciences at an early age. I thank my siblings, Kristy and Michael, for their amazing support and friendship throughout the years and my newer "siblings", Phil and Amanda, for all of their encouragement. I owe a huge thanks to my in-laws Bill and Diana Ducett and the rest of my "Illinois family", which is quite possibly one of the most supportive, loving, and fun families I can imagine having married into. Finally, I owe so much to my husband, Mike, for being married to a graduate student! I cannot imagine having gone through this process without his constant love, patience, support, and humor. I thank him for always standing by me, for encouraging me when things got rough, for helping me keep things in perspective, for enduring countless "boring" scientific discussions with friends, and for always cooking for me. And finally, thank you to my beautiful daughter, Maya, who helps me keep life in perspective and whose smiles and giggles fill my life with joy every day.

TABLE OF CONTENTS

LIST OF FIGURES

CHAPTER ONE

CHAPTER TWO

CHAPTER THREE

APPENDIX

LIST OF TABLES

CHAPTER ONE

CHAPTER TWO

CHAPTER THREE

APPENDIX

ABBREVIATIONS

3-AT	3-aminotriazole
Å	Angstroms
ABC	ATP-binding cassette
AD	activation domain
ADP	adenosine diphosphate
ATP	adenosine triphosphate
C’	carbonyl carbon
C^{α}	alpha carbon
C^{β}	beta carbon
ChIP	chromatin immunoprecipitation
CHX	cycloheximide
co-IP	co-immunoprecipitation
DBD	DNA binding domain
EDTA	ethylene diamine tetraacetic acid
EGTA	ethylene glycol tetraacetic acid
GAD	Gal4 activation domain
GBD	Gal4 DNA binding domain
GO	gene ontology
GPD	glyceraldehyde-3-phosphate dehydrogenase
GST	glutathione S-transferase

H/D	hydrogen-deuterium
Hsp	heat shock protein
HSQC	heteronuclear single quantum coherence
IgG	immunoglobulin G
IP	immunoprecipitation
kDa	kilodalton
kJ	kilojoule
LB	Luria broth
LMB	Leptomycin B
MDR	multidrug resistance
MFS	major facilitator superfamily
MHz	megahertz
MWCO	molecular weight cutoff
NES	nuclear export signal
NLS	nuclear localization signal
NMR	nuclear magnetic resonance
NOE	Nuclear Overhauser Effect
NOESY	Nuclear Overhauser Enhancement Spectroscopy
OD	optical density
OLI	oligomycin
ORF	open reading frame
pBpa	*p*-benzoyl-L-phenylalanine

PCR	polymerase chain reaction
PDR	pleiotropic drug resistance
PDRE	pleiotropic drug response element
PG	progesterone
PolII	RNA Polymerase II
qPCR	quantitative real-time PCR
PBD	peptide-binding domain
RAC	ribosome-associated complex
RMSD	root mean square deviation
rRNA	ribosomal ribonucleic acid
SDS	sodium dodecyl sulfate
SDS-PAGE	sodium dodecyl sulfate polyacrylamide gel electrophoresis
Ssz1*	Ssz1 containing the hyperactive S295F alteration
TAP	tandem affinity purification
TBS	Tris-buffered saline
TF	transcription factor
WT	wild-type
XBD	xenobiotic binding domain
ZuoC	the C-terminal 69 residues of Zuo1
ZuoC*	ZuoC containing the hyperactive S427G alteration

ACTIVATION OF THE PLEIOTROPIC DRUG RESISTANCE REGULON BY THE MOLECULAR CHAPERONES SSZ1 AND ZUO1

Jeanette K. Ducett

Under the supervision of Professor Elizabeth A. Craig

At the University of Wisconsin-Madison

Ribosome-associated molecular chaperones are conserved throughout evolution and have a well-established role in the folding of nascent polypeptides. Yet, the role of these chaperones in extra-ribosomal cellular signaling events is only beginning to be appreciated. In *Saccharomyces cerevisiae,* the J-protein Zuo1 and the Hsp70-like protein Ssz1 form a stable heterodimer that associates with translating ribosomes and functions in the folding of newly synthesized polypeptides. In addition to this role in protein folding, Ssz1 and Zuo1 have a distinct function in cellular signaling as the N-terminus of Ssz1 or the C-terminus of Zuo1 can independently upregulate genes belonging to the pleiotropic drug resistance (PDR) regulon. In the work presented in this thesis, I aimed to uncover the molecular mechanism Ssz1 and Zuo1 use to activate the PDR regulon as well as to understand the physiological basis of this regulation.

Activation of the PDR regulon by Ssz1 or Zuo1 has previously been shown to render cells resistant to high concentrations of drugs, a phenotype conferred by the upregulation of plasma membrane transporters that facilitate the export of xenobiotics from the cell. Results presented in this thesis are consistent with a model in which Ssz1 and Zuo1 activate the PDR

regulon directly by interacting with Pdr1, the primary nuclear transcription factor controlling this regulon. This activation appears to be highly specific, as genome-wide expression analysis indicates that the PDR regulon is the major target of regulation by either of these proteins. Activation of Pdr1 by Ssz1 or Zuo1 also results in the premature growth arrest of cells at the diauxic shift, while cells lacking these proteins arrest at a higher density than wild-type cells. These results support a model in which Ssz1 and Zuo1 are involved in the regulation of cellular growth via activation of Pdr1-dependent transcription, perhaps by increasing the export of quorum sensing molecules extruded by upregulated plasma membrane transporters.

Previous research indicated that the last 69 residues of Zuo1 were competent to activate the PDR regulon, though this activity was not observed with full-length protein. In this work, I identified a 13-residue peptide at the extreme C-terminus of Zuo1 that is both necessary and sufficient to activate Pdr1-dependent transcription. Structural analysis of the C-terminus revealed that these critical residues are contained within an autoinhibitory four-helix bundle. Key hydrophobic residues required for interaction with Pdr1 are essential to the structural integrity of this domain. Unfolding of this helical bundle *in vitro* correlates strongly with both activation of and interaction with Pdr1 by Zuo1 *in vivo.* These results are consistent with a model in which Zuo1's transcriptional properties are regulated by autoinhibition conferred by the sequestering of critical residues and that unfolding of Zuo1's C-terminal helical bundle results in the activation of Pdr1-dependent transcription.

CHAPTER ONE:

Introduction

Roles of molecular chaperones

A diversity of cellular functions

Molecular chaperones represent a large family of structurally and functionally diverse proteins. Originally discovered as being upregulated under conditions of cellular stress, such as heat shock, these proteins are best known for their role in protein folding. However, molecular chaperones can carry out a multitude of cellular tasks and many of these proteins are constitutively expressed to perform critical roles in cellular maintenance. Chaperones are capable of interacting with unfolded proteins, shielding stretches of exposed hydrophobic residues and preventing them from forming unproductive aggregates (Fink, 1999; Hartl and Hayer-Hartl, 2002). The ability of these proteins to bind to hydrophobic patches of proteins, however, also makes them well suited to perform a wide variety of cellular functions. In addition to their roles in protein folding, chaperones have been shown to be involved in activities such as the translocation of proteins across organelle membranes, the remodeling of multimeric protein complexes, and the degradation of misfolded proteins (Craig et al., 2006; Young et al., 2003). A number of chaperones have also been shown to have roles in transcriptional activation (Eisenman and Craig, 2004; Freeman and Yamamoto, 2002).

Molecular chaperones have been highly conserved throughout evolution and are essential in all organisms. These ubiquitous proteins can be found in all cellular compartments, where they often specialize in roles related to their subcellular localization. Multiple families of chaperones exist that differ in their structure and mechanism of action, conferring further specialization to the chaperone network (Craig et al., 2006; Fink, 1999; Young et al., 2003). The work presented in this thesis focuses on chaperones of the Hsp70 family, which interact with substrate through

ATP-regulated cycles of binding and release (Kampinga and Craig, 2010). Although members of this family share a common structure and mechanism, differences in the abundance and subcellular distribution of these proteins enables them to take on a wide array of cellular tasks. Furthermore, the presence of additional functional domains on these proteins can contribute further specialization to these proteins, as well as result in chaperones that carry out more than one cellular function. The research presented in this thesis focuses on two multifunctional molecular chaperones in yeast, Ssz1 and Zuo1. These proteins have been shown to function both in protein folding and in transcriptional activation, activities that will be covered in more detail in the following sections.

Molecular chaperones in protein folding

In order to carry out their cellular function, proteins must fold from a linear polypeptide into their proper three-dimensional conformation. Although the resulting structure is encoded in the protein's primary amino acid sequence (Anfinsen, 1973), reaching this final conformation in the crowded and dynamic cellular environment is challenging (Ellis, 2001; Gershenson and Gierasch, 2011). An initial complication to this process occurs during protein translation itself. While polypeptide biosynthesis occurs in a vectorial fashion, the tertiary structure of a protein often involves intramolecular interactions that span the entire length of the polypeptide. Therefore, folding of the final tertiary structure cannot be completed until an entire domain, or even the entire protein, has been synthesized and emerges from the ribosome (Gershenson and Gierasch, 2011). The polypeptide exit tunnel is approximately 100Å in length, allowing the protection of only about 30-35 amino acids of the nascent chain (Ban et al., 2000; Malkin and

Rich, 1967). Therefore, stretches of hydrophobic amino acids normally sequestered in the core of the protein may become exposed to the cytosol before folding can be completed. Exposure of these hydrophobic regions renders the proteins highly susceptible to unproductive interactions that can lead to protein misfolding and/or the formation of protein aggregates.

To help prevent misfolding and aggregation during protein synthesis, cells have evolved specialized molecular chaperones that are tethered to the ribosome in close proximity to the polypeptide exit tunnel. These chaperones bind to short segments of exposed hydrophobic residues in the polypeptide chain, preventing the formation of non-native interactions and delaying premature folding until enough of the protein has been synthesized to allow proper folding to take place (Hartl and Hayer-Hartl, 2002). Such ribosome-associated chaperones are highly conserved and appear to exist in all organisms where they participate in early folding events (Craig et al., 2003). In *E. coli*, the ribosome-associated peptidyl-prolyl isomerase Trigger Factor functions together with the Hsp70 DnaK in cotranslational protein folding (Bukau et al., 2000). In *S. cerevisiae*, the Hsp70 Ssb1/2 (Ssb) associates with translating ribosomes and functions along with its co-chaperones Ssz1 and Zuo1 to aid in nascent chain folding (Pfund et al., 1998). In humans, Hsp70L1 and Mpp11 function as a ribosome-associated chaperone complex (Hundley et al., 2005; Otto et al., 2005).

In addition to molecular chaperones physically associated with the ribosome, a number of chaperones exist that aid in post-translational folding of larger and more complex multidomain proteins. For example, chaperones of the Hsp70 family, such as DnaK in *E. coli* and Ssa in *S. cerevisiae,* aid in protein folding in the cytosol (Hartl and Hayer-Hartl, 2002; Kampinga and Craig, 2010). Members of the chaperonin family, including the prokaryotic GroEL/GroES and

the eukaryotic TRiC/CCT, form large, cylindrical complexes that can shield entire domains or proteins within them to promote proper folding (Bukau et al., 2000; Hartl and Hayer-Hartl, 2002). Although a number of diverse families of chaperones participate in this folding network, the work presented in this thesis focuses on chaperones of the Hsp70 family and, therefore, the remainder of the background will focus exclusively on this family of chaperones.

The Hsp70/J-protein chaperone system

Hsp70s are amongst the most abundant and versatile chaperones in the eukaryotic cell. Though their name refers to chaperones upregulated under conditions of stress (Heat shock protein of 70 kDa), both constitutively expressed and stress-induced Hsp70s exist (Albanese et al., 2006). All Hsp70s have been shown to require a co-chaperone, referred to as a J-protein or Hsp40, in order to carry out their function. Though the Hsp70 family of chaperones is diverse in function, these highly conserved proteins share a common structure and mechanism.

Hsp70s function by binding to short, hydrophobic stretches of amino acids in a transient and cyclical manner. This interaction with substrate is regulated by the binding and release of adenosine triphosphate (ATP). Binding of ATP occurs in a nucleotide-binding cleft contained within a highly conserved 44-kDa N-terminal ATPase domain. This domain regulates the conformation of a 25-kDa C-terminal peptide-binding domain (PBD), altering its ability to interact with client proteins. While ATP is bound by the N-terminal domain, the PBD has low affinity for substrate and binding and release occurs rapidly. This interaction becomes stabilized upon hydrolysis of ATP to ADP (Kampinga and Craig, 2010; Young, 2010).

Despite the ability of Hsp70s to both hydrolyze ATP and interact with client proteins, these chaperones do not function independently. This is in large part due to the fact that Hsp70s themselves exhibit low intrinsic ATPase activity (Erbse et al., 2004). These chaperones thus require the assistance of co-chaperones, known as J-proteins or Hsp40s. J-proteins function by stimulating the weak intrinsic ATPase activity of Hsp70s, thereby enhancing the interaction between Hsp70 and client protein. J-proteins contain a highly conserved J-domain of approximately 70 amino acids through which they interact transiently with their partner Hsp70 (Craig et al., 2006). J-domains from multiple J-proteins show high sequence homology and a conserved structure (Li et al., 2009; Walsh et al., 2004). The J-domains of two cytosolic yeast J-proteins, Sis1 and Ydj1, have been shown to be functionally interchangeable (Yan and Craig, 1999). Furthermore, the growth defects caused by deletion of Ydj1, the most abundant J-protein in yeast, can be rescued by the J-domains of many cytosolic J-proteins, suggesting that this domain is sufficient to carry out the major cellular function of this J-protein (Sahi and Craig, 2007).

Beyond the highly conserved J-domain, however, J-proteins show a high degree of sequence divergence and often contain unique domains that contribute to the specialization of these chaperones. The number of J-proteins in the cell is much greater than the number of Hsp70s and multiple J-proteins can work with a single Hsp70. In *S. cerevisiae*, for instance, two classes of Hsp70s (Ssa and Ssb) are present in the cytosol along with 13 J-proteins (Sahi and Craig, 2007). Many of these J-proteins can themselves bind client proteins and deliver them to their partner Hsp70. Thus, J-proteins contribute much of the specificity of the Hsp70 chaperone

system. Furthermore, the presence of J-proteins in different subcellular locations provides an additional level of specificity to these chaperones (Craig et al., 2006; Walsh et al., 2004).

In addition to J-proteins providing specificity to the Hsp70 system, many J-proteins contain additional accessory domains that can contribute to the multifunctionality of these proteins. In some cases, this multifunctionality can even occur in an Hsp70-independent manner. For instance, the yeast J-protein Cwc23 functions in disassembly of the spliceosome, a role for which its J-domain is dispensable (Sahi et al., 2010). The J-protein Zuo1, the focus of the research presented in this thesis, has been implicated both in protein folding activities requiring its conserved J-domain and in transcriptional activation mediated by a unique domain at its C-terminus (Eisenman and Craig, 2004).

The ribosome-associated chaperones Ssz1 and Zuo1

For my thesis work, I have focused specifically on the study of two molecular chaperones in the yeast *Saccharomyces cerevisiae*, Ssz1 and Zuo1. These proteins have been most extensively studied for their role in protein folding as ribosome-associated chaperones. However, both Ssz1 and Zuo1 have also been implicated in cellular signaling activities that can occur independently of their chaperone function. Although this research focuses primarily on the role of these proteins in transcription, I will first provide background on the well-known role of Ssz1 and Zuo1 in protein folding and then cover what is currently known about their ability to function in transcriptional activation, as understanding the cellular function of these proteins will ultimately require knowledge of both of these cellular activities.

The ribosome-associated complex

The yeast ribosome contains an Hsp70-based complex of molecular chaperones that aids in the folding of nascent polypeptides during protein biosynthesis. The J-protein of this system is Zuo1, which is present in a stable heterodimer with the Hsp70-like protein Ssz1. In addition to this complex, the yeast ribosome contains a classical Hsp70, Ssb, which is composed of two family members that share 99% identity, Ssb1 and Ssb2 (Pfund et al., 2001). Several pieces of evidence point to Ssz1, Zuo1, and Ssb functioning together in nascent chain protection. All three proteins have been shown to associate with translating ribosomes, consistent with a role for these chaperones in early protein folding events (Gautschi et al., 2001a; Nelson et al., 1992; Yan et al., 1998a). Furthermore, the Hsp70 Ssb can be crosslinked to short nascent chains in a yeast translation extract (Hundley et al., 2002; Pfund et al., 1998). The ability of Ssb to form these nascent chain complexes is dependent on the presence of both Ssz1 and Zuo1, suggesting that these three chaperones function together in nascent chain protection (Gautschi et al., 2002). Genetic evidence also supports these proteins functioning collectively. Strains lacking Ssz1, Zuo1, or Ssb show similar growth phenotypes, including slow growth and sensitivity to cold and cations (Hundley et al., 2002; Yan et al., 1998a). Strains lacking all three of these proteins do not show enhanced growth defects over those lacking only one of the proteins, suggesting that these proteins function in the same cellular process (Hundley et al., 2002). Together these findings support the idea that Ssz1, Zuo1, and Ssb function cooperatively as a ribosome-associated complex involved in early protein folding events.

The J-protein Zuo1

The J-protein Zuo1 has been shown to function as the co-chaperone of the Hsp70 Ssb (Huang et al., 2005). Like all J-proteins, the ability of Zuo1 to perform this function depends upon a highly conserved J-domain located near its N-terminus (Figure 1-1A). In addition to a J-domain, this 433 amino acid protein contains an N-terminal region required for binding to its heterodimeric partner Ssz1, a central conserved region of unknown function, a charged ribosome-binding domain, and a C-terminal PDR-inducing domain. Deletion of any of these domains, with the exception of the C-terminus, results in the inability of the protein to rescue the growth phenotypes of a strain lacking Zuo1 (Yan et al., 1998). As these phenotypes are shared by the other ribosome-associated molecular chaperones, Ssb and Ssz1, these data suggest that these domains are all essential for Zuo1's function in protein folding. Zuo1's C-terminal domain (residues 365-433), on the other hand, has been shown to be involved in transcriptional regulation (Eisenman and Craig, 2004), a topic that will be discussed in more detail in the following section.

Consistent with its role in nascent chain folding, the majority of Zuo1 in the cell is found associated with translating ribosomes (Yan et al., 1998). A stretch of highly charged amino acids near the C-terminus of the protein (residues 285-364) is required for stable association of Zuo1 with the ribosome. The ability of Zuo1 to bind various types of RNA *in vitro,* an activity dependent on this charged region, suggests that Zuo1's interaction with the ribosome is due, at least in part, to interaction of this highly charged region with ribosomal RNAs. More recently, crosslinking experiments have detected an interaction between Zuo1 and the ribosomal protein Rpl31 (Peisker et al., 2008), a protein located near the polypeptide exit tunnel (Ban et al., 2000;

Ben-Shem et al., 2011). Though these data suggest that Zuo1 may be aptly positioned at the site of nascent chain synthesis, the ability of Zuo1 to bind ribosomes in the absence of Rpl31 indicates that this protein does not simply anchor Zuo1 to the ribosome. Peptide mapping and mutagenesis experiments suggest that Zuo1 contains an extended interface for ribosome binding located primarily within its highly charged RNA-binding region (Peisker et al., 2008). Together these findings suggest that the interaction between Zuo1 and the ribosome may involve multiple contacts with both rRNA and ribosomal proteins that position it in close proximity to the polypeptide exit tunnel.

Although Zuo1 appears to be predominantly associated with ribosomes, it has been implicated in nuclear functions (Albanese et al., 2010b) and shown to effect the transcription of genes of the pleiotropic drug resistance regulon independently of its association with the ribosome (Eisenman and Craig, 2004). Furthermore, a variant of Zuo1 lacking its charged ribosome-binding domain has been observed in the nucleus (Appendix Figure A-4A, (Albanese et al., 2010b)). Thus, the subcellular distribution of Zuo1 or regulation of its localization may be more complex than originally thought based on its predominant co-migration with ribosomal particles.

The atypical Hsp70 Ssz1

Although Zuo1 has been identified as the J-protein partner of the Hsp70 Ssb, Zuo1's ability to function in this manner is dependent upon the presence of its heterodimeric partner, Ssz1 (Huang et al., 2005). Ssz1 shows sequence homology to the Hsp70 family of proteins; however, no evidence points to Ssz1 functioning as a classical Hsp70. Like traditional Hsp70s,

Ssz1 is composed of an N-terminal ATPase domain (residues 1-407) and a C-terminal putative PBD (residues 408-538; Figure 1-1B). Although Ssz1 is competent to bind ATP similar to classical Hsp70s, it shows little to no ATPase activity even in complex with the J-protein Zuo1 (Conz et al., 2007b; Huang et al., 2005). Furthermore, alterations in Ssz1's nucleotide binding cleft have no effect on its ability to rescue the growth defects of a Δ*ssz1* strain, suggesting that nucleotide binding is not required for its *in vivo* function. Unlike other Hsp70s, Ssz1 does not require its putative PBD to carry out its *in vivo* function, as the N-terminal 407 residues of Ssz1 are sufficient to rescue the growth defects of strain lacking Ssz1 (Hundley et al., 2002). These findings suggest that Ssz1 does not function like a classical Hsp70. Yet, Ssz1 is functionally significant in this unique complex, as Zuo1 can only activate the ATPase activity of the Hsp70 Ssb in the presence of Ssz1 (Huang et al., 2005). It is unclear what the precise role of Ssz1 is in this complex. It is possible that Ssz1 plays a regulatory role in modulating Zuo1's co-chaperone activity or that these proteins have a cooperative function in regulating Ssb's activity. More details regarding this unique complex will be discussed below.

In addition to its role in nascent chain folding, Ssz1, like Zuo1, has been shown to function in transcriptional activation of the pleiotropic drug resistance regulon, an activity that will be covered in more detail in the next section. Ssz1's C-terminal putative PBD is also dispensable for this activity (Eisenman and Craig, 2004). Thus, the ATPase domain of Ssz1 appears to be important both for its role in protein folding and for its ability to activate transcription.

RAC structure and function

The heterodimeric complex formed by the J-protein Zuo1 and the non-canonical Hsp70 Ssz1 is referred to as the ribosome-associated complex or RAC. This complex associates with translating ribosomes through interaction of Zuo1's highly charged RNA-binding domain with the ribosome (Gautschi et al., 2001a; Yan et al., 1998a). The Ssz1:Zuo1 heterodimer is highly stable, showing resistance to high levels of salt, and requiring denaturation in order to separate its subunits (Conz et al., 2007b; Gautschi et al., 2001a). The interaction between Ssz1 and Zuo1 is also unaffected by the presence of either ATP or ADP (Gautschi et al., 2001a). This suggests that Zuo1 is not bound by Ssz1 in a substrate-like manner, further supporting the idea that Ssz1 does not function like a classical Hsp70 in this complex. This example of a stable interaction occurring between an Hsp70 and a J-protein is unusual, as the interaction between these families of chaperones is typically transient. Yet, the requirement for both Ssz1 and Zuo1 in stimulation of Ssb's ATPase activity indicates that this heterodimer is of functional importance (Huang et al., 2005). The significance of this unusual complex is further evidenced by its conservation in higher eukaryotes. The human Zuo1 homolog Mpp11 has been shown to form a stable complex with the Ssz1 homolog Hsp70L1 (Otto et al., 2005). This complex also associates with translating ribosomes and can rescue the growth defects of a yeast strain lacking functional RAC, suggesting that it plays an orthologous role to RAC in mammalian cells (Hundley et al., 2005; Otto et al., 2005).

More recent work using deletion mapping and hydrogen-deuterium (H/D) exchange has enabled us to gain a better understanding of the structure and dynamics of the Ssz1:Zuo1 complex. These studies suggest that the C-terminal domain of Ssz1 and the N-terminal domain

of Zuo1 are primarily responsible for the structural stability of this heterodimer. Upon deletion of Ssz1's C-terminus (residues 395-538), the interaction between Ssz1 and Zuo1 can no longer be detected (Conz et al., 2007b). Furthermore, deletion of this C-terminal region strongly impairs Ssz1's ability to interact with ribosomes, consistent with the requirement for this domain in binding to Zuo1. This C-terminal region, however, is not sufficient to mediate complex formation with Zuo1, suggesting that extended interactions may be required or that deletion of the N-terminus results in conformational changes that impair Ssz1's ability to interact with Zuo1. H/D exchange experiments, however, strongly support the importance of the C-terminus of Ssz1 in complex formation. Comparison of Ssz1 with Ssz1 in complex with Zuo1 indicates that RAC provides the strongest protection in Ssz1's C-terminal domain (residues 396-447 and 479-538), consistent with this region serving as the major interaction surface for Zuo1 (Fiaux et al., 2010). Comparison of Zuo1 with Zuo1 in RAC by H/D exchange revealed extensive protection of residues 1-51 of Zuo1's N-terminus when in complex with Ssz1. Consistent with the importance of this N-terminal region in heterodimer formation, Zuo1 lacking its N-terminal 62 residues was unable to interact with Ssz1. Deletion of this N-terminal domain of Zuo1 also prevented association of Ssz1 with the ribosome.

Although the precise role of the RAC heterodimer is unclear, these studies suggest that the presence of Ssz1 may provide structural stability to Zuo1. Levels of Zuo1 were shown to be significantly decreased in a strain lacking Ssz1, suggesting that Zuo1 may be destabilized in the absence of RAC (Gautschi et al., 2001a). Furthermore, the N-terminal region of Zuo1 appears to be largely unfolded and highly flexible in the absence of Ssz1. When not in the RAC complex, this region shows higher susceptibility to tryptic proteolysis and very rapid and near complete

exchange of amide hydrogens in H/D exchange experiments, but shows extensive protection when bound to Ssz1 (Fiaux et al., 2010). Interestingly, the J-domain of Zuo1 actually shows greater accessibility when part of the complex. As this domain is responsible for Zuo1's ability to stimulate Ssb's ATPase activity, it is conceivable that the presence of Ssz1 helps position Zuo1's J-domain to help facilitate its co-chaperone function.

Analytical centrifugation experiments suggest that virtually all of the Ssz1 and Zuo1 in the cell are present in the RAC complex (Gautschi et al., 2001a). When expressed at native levels, the majority of these proteins are found in association with ribosomes (Gautschi et al., 2001a; Yan et al., 1998a). Based on the estimated abundance of Ssz1 and Zuo1 (70,000-90,00 molecules/cell) and the estimated number of ribosomes the yeast cytosol (310,000), the ratio of Ssz1:Zuo1:ribosomes is roughly 1:1:3 (Ghaemmaghami et al., 2003; Raue et al., 2007). This suggests that not every ribosomal particle contains RAC. Interestingly, it has been found that even significantly lower levels of RAC are sufficient for normal growth *in vivo.* When expressed at an estimated 1-2% of endogenous levels, Ssz1 and Zuo1 are able to rescue the growth defects of a strain lacking both proteins. (Hundley et al., 2002). Thus, Ssz1 and Zuo1 appear to be expressed at significantly higher levels than are required for their role in protein folding. It is possible that RAC is required for only a small population of ribosomes or that RAC is able to shuttle between ribosomes. Ssz1 and Zuo1 have also both been implicated in cellular signaling roles that appear to occur off the ribosome, as will be explained in detail in the next section. It is conceivable that this activity could provide a potential explanation for this abundance of RAC in the cell.

Activation of the PDR regulon by Ssz1 and Zuo1

In addition to their well-defined role in the folding of nascent polypeptides, Ssz1 and Zuo1 have been implicated in cellular signaling events, as either the N-terminus of Ssz1 or the C-terminus of Zuo1 can upregulate the transcription of genes belonging to the pleiotropic drug resistance regulon. Current evidence suggests that this transcriptional regulation can occur independently of their ribosomal function in chaperoning nascent chains. The work presented in this thesis aims to better understand this secondary role of Ssz1 and Zuo1 in cellular signaling.

The PDR regulon

Named for its ability to confer resistance to a multitude of diverse drugs, the pleiotropic drug resistance (PDR) regulon has a well-established role in cellular detoxification. In addition to providing resistance to extracellular toxins, however, a number of reports suggest that the PDR regulon may carry out additional cellular functions, possibly relating to membrane maintenance, cell:cell communication, and the regulation of cellular growth (Hlavacek et al., 2009; Shahi and Moye-Rowley, 2009). Though the majority of the literature on the PDR regulon focuses on its role in drug resistance, it is clear that the underlying physiological role of this pathway is not well understood. As the work presented in this thesis focuses on understanding the ability of this regulon to become activated by two intracellular proteins, Ssz1 and Zuo1, rather than extracellular toxins, I think that the smaller subset of literature related to these potential alternative cellular activities might be most relevant. Therefore, this background will focus not only on the well-defined role of the PDR regulon in cellular detoxification, but will also present

more in-depth pieces of data that relate to the involvement of this pathway in other cellular processes.

The PDR regulon represents a highly conserved network of genes that become activated in the presence of xenobiotics. This pathway is found in all organisms and is referred to as multidrug resistance (MDR) in many species, including bacteria and mammals. The PDR regulon is composed primarily of genes encoding plasma membrane transporters and genes involved in lipid biosynthesis (DeRisi et al., 2000; Devaux et al., 2001). Many of the transporters involved in the PDR regulon belong to the ATP-binding cassette (ABC) family. These transporters have a low specificity for substrate and can serve as drug efflux pumps in the plasma membrane. Upregulation of these transporters thus results in the rapid expulsion of a broad range of cytotoxic compounds from the cell and prevents their accumulation at toxic levels. This renders cells resistant to a multitude of diverse drugs, including drugs that differ both in their chemical structure and mechanism of action, giving the regulon its pleiotropic nature (Jungwirth and Kuchler, 2006). In *S. cerevisiae,* the ABC transporters Pdr5, Snq2, and Yor1 are amongst those shown to play a major role in the acquisition of drug resistance. Deletion of the genes encoding these transporters has been shown to result in the sensitivity of yeast to hundreds of different compounds (Kolaczkowski et al., 1998). In humans, the MDR1/P-glycoprotein (Pgp) transporter can recognize diverse classes of structurally unrelated drugs, including a number of chemotherapeutic agents, making it of clinical importance in the fight against multidrug resistance (Sarkadi et al., 2006).

In addition to this well-defined role in the acquisition of drug resistance, however, a number of reports suggest that the PDR regulon may have a more basic physiological function in

the cell, likely unrelated to its ability to become activated by xenobiotics. This idea comes in part from the diverse nature of ABC transporters. In addition to their role in the export of toxic substances, ABC transporters have been shown to be involved in a wide range of cellular activities. In *S. cerevisiae*, there are an estimated 30 ABC transporters (Decottignies and Goffeau, 1997) and an estimated 48 in humans (Dean et al., 2001). These transporters are found in nearly every organelle membrane where they utilize ATP hydrolysis to facilitate the translocation of a wide variety of substrates across biological membranes. In addition to toxic xenobiotics, substrates of ABC transporters include ions, heavy metals, metabolites, steroids, sugars, lipids, amino acids, peptides, and proteins (Bauer et al., 1999). Though some ABC transporters do show preference for different substrates, many show very broad specificity, making them well suited for a wide range of activities. One common characteristic of these substrates is their amphipathic or hydrophobic nature. Thus, it has been proposed that ABC transporters involved in multidrug resistance may have evolved to expand their substrate specificity from endogenous lipids to hydrophobic toxic chemicals (Sarkadi et al., 2006). In both bacteria and fungi, ABC transporters associated with multidrug resistance have been proposed to function in quorum sensing by facilitating the export of signaling molecules involved in regulating cell growth in a density-dependent manner (Hlavacek et al., 2009; Yang et al., 2006). In *S. cerevisiae,* cells lacking the genes encoding the ABC transporters Pdr5 and Snq2 reach significantly higher culture densities as cells approach stationary phase, consistent with the inability of these cells to export signaling molecules involved in regulating cellular growth (Hlavacek et al., 2009). A similar overgrowth is observed in bacterial cells lacking the MDR pump AcrAB (Yang et al., 2006).

In *S. cerevisiae*, the transcription factors (TFs) Pdr1 and Pdr3, which upregulate drug efflux pumps in response to xenobiotics, also upregulate genes encoding enzymes involved in sphingolipid biosynthesis and cell wall maintenance (DeRisi et al., 2000; Hallstrom et al., 2001; Kolaczkowski et al., 2004). In humans, altered lipid profiles have been observed in drug-resistant cells (Sietsma et al., 2001). Furthermore, a number of ABC transporters translocate lipids and have been shown to affect the asymmetric distribution of membrane phospholipids (Pohl et al., 2005; Sietsma et al., 2001). Though the physiological relevance of this altered lipid composition is not currently understood, it suggests that the PDR regulon may play a role in modulating the composition of cellular membranes by facilitating the synthesis of both lipids and lipid-associated transporters. In addition to serving as primary constituents of the plasma membrane, sphingolipids and their metabolites have also been shown to have important roles in signal transduction, specifically in the regulation of cell growth, cell differentiation, and apoptosis (Sietsma et al., 2001). Though direct evidence for a lipid-mediated signaling pathway regulating cell growth in this context is lacking, these data suggest that the PDR regulon may be involved in cellular activities that extend beyond its role in providing resistance to xenobiotics.

Furthermore, there is evidence that the PDR regulon is regulated with the cell cycle. In yeast, mRNA levels of the ABC transporter-encoding gene *PDR5* are highest during mitosis, a phase during which transcription of most genes is significantly reduced (Souid et al., 2006; Spellman et al., 1998). Additionally, serine/threonine kinases involved in the G2 to mitosis transition, such as Elm1, have been shown to be required for the induction of drug resistance (Souid et al., 2006). This type of cell cycle-dependent regulation further supports a role for the PDR regulon in basic physiological functions, such as cellular growth.

It is clear from these studies that the PDR regulon is complex. In addition to its ability to provide cellular cross-resistance to a wide variety of toxic substances, the PDR regulon may be involved in cellular activities that are unrelated to its ability to become activated by xenobiotics. Although a complete picture of the physiological role of the PDR regulon has not emerged from these findings, they do suggest that this pathway may have more fundamental physiological roles underlying the major drug resistance phenotype observed upon its activation.

The yeast PDR network

In *S. cerevisiae*, two highly related TFs, Pdr1 and Pdr3, serve as the predominant regulators of the PDR regulon (Figure 1-2). Deletion of *PDR1* and *PDR3* renders cells sensitive to a wide range of structurally and mechanistically unrelated drugs, including the translation inhibitor cycloheximide (CHX) and the mitochondrial inhibitor oligomycin (OLI) (Balzi et al., 1987; Kolaczkowski et al., 1998). Furthermore, gain-of-function point mutations in both *PDR1* and *PDR3* have been found to result in increased drug resistance (Carvajal et al., 1997; Nourani et al., 1997; Simonics et al., 2000). Pdr1 and Pdr3 can function as both homo- and heterodimers *in vivo* (Mamnun et al., 2002). These TFs regulate the transcription of PDR-responsive genes by binding to one or more conserved pleiotropic drug response elements (PDREs) in the promoters of their target genes (Katzmann et al., 1996). The promoters of *PDR5, SNQ2,* and *YOR1,* which encode ABC transporters that have a well-established role in PDR, each contain at least one PDRE and are regulated by Pdr1/3 (DeRisi et al., 2000; Katzmann et al., 1996). Genome-wide microarray analysis indicates that Pdr1 and Pdr3 not only upregulate genes of the ABC transporter family, as expected given their role in the acquisition of drug resistance, but also

upregulate genes belonging to the major facilitator superfamily (MFS) of transporters and genes involved in cell wall maintenance, sphingolipid biosynthesis, and the stress response (DeRisi et al., 2000; Devaux et al., 2001) (Table 1-1). This suggests that activation of Pdr1/3 may have cellular consequences that extend beyond providing cellular cross-resistance to drugs.

The yeast PDR regulon can be activated by a wide range of structurally and functionally unrelated xenobiotics. Human steroids, such as progesterone (PG), have also been shown to induce the yeast PDR regulon and can serve as substrates of the ABC transporters Pdr5 and Snq2 (Banerjee et al., 2008; Kolaczkowski et al., 1996; Mahe et al., 1996). Despite its ability to become activated by a wide range of diverse molecules, however, the PDR regulon does not appear to function as a general stress response pathway. Levels of *PDR5* mRNA are upregulated in response to xenobiotics; yet, they appear to be unaffected by other cellular stresses, such as high salt, sorbitol, or weak acid treatment (Wolfger et al., 2004). A number of genes in the PDR regulon, however, are upregulated in response to either the presence of xenobiotics or other cellular stresses. The promoter of the gene encoding the ABC transporter Pdr15, for instance, contains a PDRE and its basal activity is regulated by Pdr1/3; yet, it also contains a stress response element (STRE) and is regulated by Msn2/4 under stress conditions. This suggest that, although the PDR regulon is specific in its ability to respond to the presence of xenobiotics, there does appear to be crosstalk between this pathway and other cellular pathways.

The major regulators of the PDR regulon, Pdr1 and Pdr3, belong to the Zn_2Cys_6 zinc cluster family of transcription factors. These TFs are characterized by a DNA-binding motif comprised of six cysteines that coordinate two zinc ions. The most well known member of this family is Gal4, one of the best-characterized eukaryotic transcription factors. In addition to the

Zn_2Cys_6 cluster, members of this family share a conserved domain architecture consisting of an N-terminal DNA binding domain (DBD), a dimerization domain, a central regulatory region, and an acidic C-terminal activation domain (AD) (MacPherson et al., 2006). Like other members of the zinc cluster family, specificity of Pdr1/3 for its cognate genes in encoded in its N-terminal DBD (Figure 1-3). A fusion between Pdr1's DBD and the AD of Gal4 activates a similar set of genes on a genome-wide level as full-length Pdr1 (DeRisi et al., 2000; Devaux et al., 2001). Pdr1/3's C-terminal AD, on the other hand, facilitates general transcriptional activation by enabling the TF to interact with the transcriptional machinery (Kolaczkowska et al., 2002; Thakur et al., 2008). In addition to these two key elements of transcriptional activation, members of the zinc cluster family contain a large central region that is often regulatory in nature and responsive to protein-specific inducing signals. Many of the gain-of-function point mutations identified in *PDR1* and *PDR3* map to this region, suggesting its importance in regulating the activity of these TFs (Carvajal et al., 1997; Nourani et al., 1997). Deletion of the regulatory region of Pdr1 renders the protein hyperactive, a feature common among members of the zinc cluster family (Kolaczkowska et al., 2002). This enhanced activity suggests that the central region of these TFs may be required to keep the AD in an inactive conformation until it becomes activated by a specific inducing signal. Consistent with the regulatory nature of this region, it was discovered more recently that xenobiotics are capable of binding to Pdr1/3 directly and that this binding occurs within this central regulatory region (Thakur et al., 2008). Using a number of Pdr1 and Pdr3 truncations, the region responsible for drug binding was further narrowed to approximately 100-200 amino acids in each of these TFs (Pdr1 residues 352-543; Pdr3 residues 290-420) and termed the xenobiotic binding domain (XBD).

Pdr1 and Pdr3 are predominantly localized to the nucleus (Delahodde et al., 2001). A nuclear localization signal (NLS) has been identified in Pdr1's central regulatory region (residues 725-769) and this protein has been shown to maintain this localization both in the presence and absence of drugs (Delahodde et al., 2001; Hallstrom and Moye-Rowley, 2000a). Genome-wide chromatin immunoprecipitation (ChIP) experiments done in the presence and absence of drug further suggest that Pdr1 is constitutively bound to the promoters of many of its target genes, including *PDR5* (Fardeau et al., 2007). These data are consistent with a model in which Pdr1/3 is present on its target promoters in an inactive state and becomes activated by the direct binding of drugs to its XBD. Interaction of Pdr1's AD with Gal11, a subunit of the Mediator complex involved in general transcriptional activation, was enhanced in the presence of drug (Thakur et al., 2008). Thus, interaction of Pdr1/3 with drug likely facilitates a conformational change that exposes its C-terminal AD, allowing it to interact with the general transcriptional machinery and initiate transcription (Figure 1-3).

Though both Pdr1 and Pdr3 can be activated by the binding of xenobiotics, these TFs do show differences in their ability to become activated by alternative inducing signals. Pdr3, but not Pdr1, has been shown to activate the PDR regulon in response to the absence of the mitochondrial genome (Hallstrom and Moye-Rowley, 2000b). Importantly for this work, Ssz1 has been shown to require Pdr1, but not Pdr3, to activate the PDR regulon (Hallstrom et al., 1998).

Ssz1 and Zuo1 as activators of the PDR regulon

Though it has been well established that the PDR regulon can be activated by extracellular toxins, far less is known about its ability to become activated by intracellular factors. The proteins Ssz1 and Zuo1, which have a defined role in protein folding, have each been identified as activators of the PDR regulon (Eisenman and Craig, 2004; Hallstrom et al., 1998). Though Ssz1 and Zuo1 are known to function together as ribosome-associated chaperones, they are capable of activating PDR independently of this function.

SSZ1 was first implicated in PDR regulation when it was isolated from a multicopy library screen for factors that give rise to enhanced resistance to the drug oligomycin upon overexpression (Hallstrom et al., 1998). This Ssz1-induced drug resistance was found to occur through the upregulation of genes of the PDR regulon, including those encoding the ABC transporters Pdr5 and Yor1. A single amino acid alteration in Ssz1, substitution of serine 295 with phenylalanine, enhances this upregulation. The fact that only *SSZ1* and the ABC-transporter-encoding gene *YOR1* were identified in this screen suggests that the number of intracellular proteins that can activate the PDR regulon is limited (Hallstrom et al., 1998; Katzmann et al., 1995). Although the mechanism by which Ssz1 activates the PDR regulon is not known, deletion of the TF Pdr1 has been shown to be sufficient to abolish this transcriptional activation. Deletion of the homologous TF Pdr3, on the other hand, has no effect on Ssz1's activity (Hallstrom et al., 1998). Thus, activation of the PDR regulon by Ssz1 appears to occur upstream of transcription, likely through regulation of Pdr1's activity by an unknown mechanism.

Zuo1, the heterodimeric partner of Ssz1, has also been found to activate the PDR regulon. Although transcriptional activation of PDR target genes was not observed upon overexpression of full-length protein, Zuo1 lacking the highly charged domain required for its association with ribosomes (residues 285-364, Figure 1-1A) was found to be capable of inducing PDR (Eisenman and Craig, 2004). A 69-amino acid region at the extreme C-terminus of Zuo1 (residues 365-433) was discovered to be both necessary and sufficient to induce PDR. As a common measure of PDR activation, cells expressing Zuo1's C-terminal domain (referred to as ZuoC or $Zuo1_{365-433}$ throughout) showed enhanced resistance to the drug CHX similar to cells expressing high levels of Ssz1 (Figure 1-4). Cells expressing ZuoC also showed enhanced transcriptional activation of the ABC transporter genes *PDR5* and *YOR1*, consistent with the observed drug resistance resulting from activation of the PDR regulon (Eisenman and Craig, 2004).

Although both Ssz1 and Zuo1 have well-established roles as ribosome-associated molecular chaperones, these proteins are capable of activating the PDR regulon independently of this function. Interestingly, both Ssz1 and Zuo1 can activate PDR independently of one another, despite their cooperative function in stimulation of the Hsp70 Ssb. In fact, overexpression of either Ssz1 or Zuo1 lacking its charged ribosome-binding domain was sufficient to induce a PDR phenotype even in cells lacking all three of the of the ribosome-associated chaperones, Ssz1, Zuo1, and Ssb (Eisenman and Craig, 2004). Thus, the chaperone complex required for nascent chain folding appears to be dispensable for PDR activation. Furthermore, Zuo1's conserved J-domain, which is required to activate its Hsp70 partner Ssb (Gautschi et al., 2002; Yan et al., 1998a), is dispensable for activation of the PDR regulon (Eisenman and Craig, 2004). Conversely, the C-terminal region of Zuo1 required to induce PDR appears to be dispensable for

Zuo1's chaperone function (Yan et al., 1998a). Thus, Zuo1 may contain a unique accessory domain at its C-terminus that enables this J-protein to function in transcriptional activation. Deletion of Ssz1's C-terminal putative peptide binding domain has no affect on its ability to activate PDR, indicating that Ssz1 does not bind client protein and function as a classical Hsp70 in PDR activation (Eisenman and Craig, 2004).

Activation of the PDR regulon by Ssz1 and Zuo1 also appears to occur independently of their association with ribosomes, suggesting that dissociation of these proteins from the ribosome may be a critical aspect of this activation process. Only constructs of Zuo1 lacking its charged ribosome-binding domain have been shown to be capable of activating the PDR regulon (Eisenman and Craig, 2004). Overexpression of *SSZ1,* which causes activation of genes of the PDR regulon, also results in some Ssz1 free from ribosomes. When expressed at native levels, Ssz1 containing the hyperactive S295F alteration is unable to activate PDR. However, when this construct is expressed in a strain lacking *ZUO1,* PDR induction is observed. Since Zuo1 is required to tether Ssz1 to the ribosome, this suggests that Ssz1 can activate the PDR regulon even when expressed at endogenous levels if the protein is not associated with ribosomes. Thus, both Ssz1 and Zuo1 can activate the PDR regulon independently of their interaction with the ribosome, further supporting a possible distinction between their transcriptional activity and their role in nascent chain remodeling.

Thesis plan

My thesis research has focused on understanding the role of the molecular chaperones Ssz1 and Zuo1 in transcriptional regulation of the yeast PDR regulon. Previous research proposed a role for these proteins in cellular signaling, as overexpression of either the N-terminus of Ssz1 or the C-terminus of Zuo1 was found to induce drug resistance and upregulate genes belonging to the PDR regulon (Eisenman and Craig, 2004; Hallstrom et al., 1998). However, the mechanism by which this occurs naturally was not known and, thus, prompted further investigation. Initial research into the mechanism of this regulation suggested that both Ssz1 and Zuo1 were capable of activating transcription independently of their well-established function in protein folding as ribosome-associated molecular chaperones (Eisenman and Craig, 2004). Yet, mechanistic details regarding this transcriptional activation and the physiological relevance of this signaling were not understood.

Ssz1 has previously been shown to require the nuclear TF Pdr1 for activation of the PDR regulon (Hallstrom et al., 1998). Though activation of Pdr1 by Ssz1 appears to occur independently of its association with ribosomes (Eisenman and Craig, 2004), it was unclear whether this predominantly cytosolic protein could activate Pdr1 directly or whether this activation requires the transduction of an unknown signal from the cytosol to the nucleus. During my investigations into the mechanism of regulation, it was discovered that xenobiotics bind directly to the TFs Pdr1 and Pdr3 to activate the PDR regulon (Thakur et al., 2008). I thus became interested in determining whether Ssz1 and Zuo1 utilize a similarly direct mechanism to activate the PDR regulon or whether these proteins employ an alternative mechanism for this regulation. As the PDR regulon is best known for its role in cellular detoxification in response to

extracellular xenobiotics, it was also unclear why these two intracellular proteins are capable of activating this transcriptional response. Therefore, another focus of this work has been to gain an understanding of the physiological relevance of PDR activation by the molecular chaperones Ssz1 and Zuo1.

In chapter two, I present work related to the mechanism of PDR activation by Ssz1 and Zuo1 and present a possible model for the physiological basis of this signaling. I found that, like Ssz1, Zuo1 requires the TF Pdr1 for activation of the PDR regulon. Regulation of Pdr1 activity by either Ssz1 or Zuo1 appears to be highly specific, as whole-genome microarray analysis indicates that the PDR regulon is the primary target of transcriptional activation by either of these proteins. Using a yeast two-hybrid system, I detected an interaction between the TF Pdr1 and the domains of both Ssz1 and Zuo1 responsible for transcriptional activation. Chromatin immunoprecipitation (ChIP) analysis further revealed an enrichment of Ssz1 at the promoter of the ABC transporter-encoding gene *PDR5*. These data are consistent with a model in which activation of Pdr1 by either Ssz1 or Zuo1 occurs via a direct mechanism. Furthermore, activation of Pdr1 by Ssz1 or Zuo1 promotes premature growth arrest of cells at the diauxic shift and cells lacking *SSZ1* and *ZUO1* grow to a higher culture density than wild-type (wt) cells. These data support a model in which Ssz1 and Zuo1 function in cell:cell communication through the upregulation of membrane transporters which export quorum sensing molecules involved in the regulation of cellular growth.

Previously it was found that the C-terminal 69 residues of Zuo1 were sufficient to activate the PDR regulon (Eisenman and Craig, 2004). Although activity was observed with this C-terminal fragment, as well as with a construct of Zuo1 lacking its charged ribosome-binding

domain, full-length Zuo1 has not been shown to activate PDR. In chapter three, I present research focused on understanding the mechanism of activation of Pdr1 by Zuo1's C-terminal domain and investigate the possibility of autoinhibition regulating Zuo1's transcriptional activity. In this work, I found that dissociation of Zuo1 from the ribosome is not sufficient to activate Pdr1-dependent transcription. Rather, NMR analysis revealed that Zuo1 contains an autoinhibitory C-terminal domain that folds into a left-handed four-helix bundle. Residues required for activation of PDR target genes and for interaction with Pdr1 are sequestered within the hydrophobic core of this domain and critical to its structural integrity. Unfolding of this helical bundle is required to activate autoinhibited Zuo1 constructs, suggesting that autoinhibition is conferred by C-terminal structure and that exposure of key residues is a requisite step to activation of Pdr1-dependent transcription by Zuo1.

In chapter four, I discuss the major conclusions of this work and present possible future directions to further understand the role of the molecular chaperones Ssz1 and Zuo1 in cellular signaling.

Figures, Tables, and Legends

Figure 1-1. The J-protein Zuo1 and the non-canonical Hsp70 Ssz1. (A) Zuo1 contains an N-terminal domain required for stable interaction with its heterodimeric partner Ssz1, a highly conserved J-domain required for stimulation of Ssb's ATPase activity, and a charged domain near its C-terminus that facilitates interaction with the ribosome. The C-terminal 69 residues (365-433) are necessary and sufficient for Zuo1 to activate the PDR regulon. (B) The atypical Hsp70 Ssz1 contains an N-terminal ATPase domain that is required for its ability to function with Zuo1 in activation of Ssb's ATPase activity and is also sufficient to activate the transcription factor Pdr1. Ssz1's C-terminal putative peptide binding domain (PBD) is required for heterodimer formation with Zuo1.

Figure 1-1

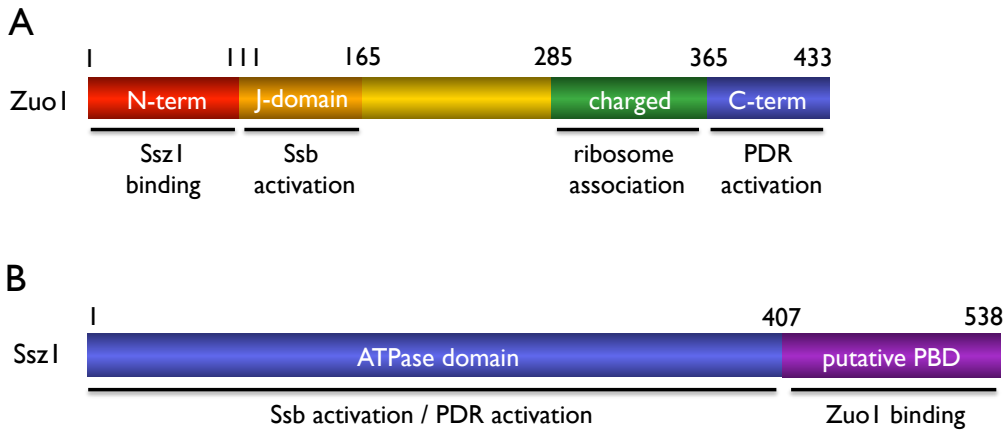
A
1
111
165
285
365
433
Zuo1
N-term
J-domain
charged
C-term
Ssz1 binding
Ssb activation
ribosome association
PDR activation
B
1
407
538
Ssz1
ATPase domain
putative PBD
Ssb activation / PDR activation
Zuo1 binding

Figure 1-2. The yeast PDR network. The transcription factors Pdr1 and Pdr3 control the PDR regulon by upregulating transcription of genes encoding ATP-binding cassette (ABC) transporters, such as Pdr5 and Snq2, by binding to conserved PDR response elements (PDREs) in the promoters of these genes. The subsequent increase in plasma membrane transporters leads to an enhanced efflux of drugs from the cell. The molecular chaperones Ssz1 and Zuo1 can also activate the PDR regulon by a yet unknown mechanism.

Figure 1-2

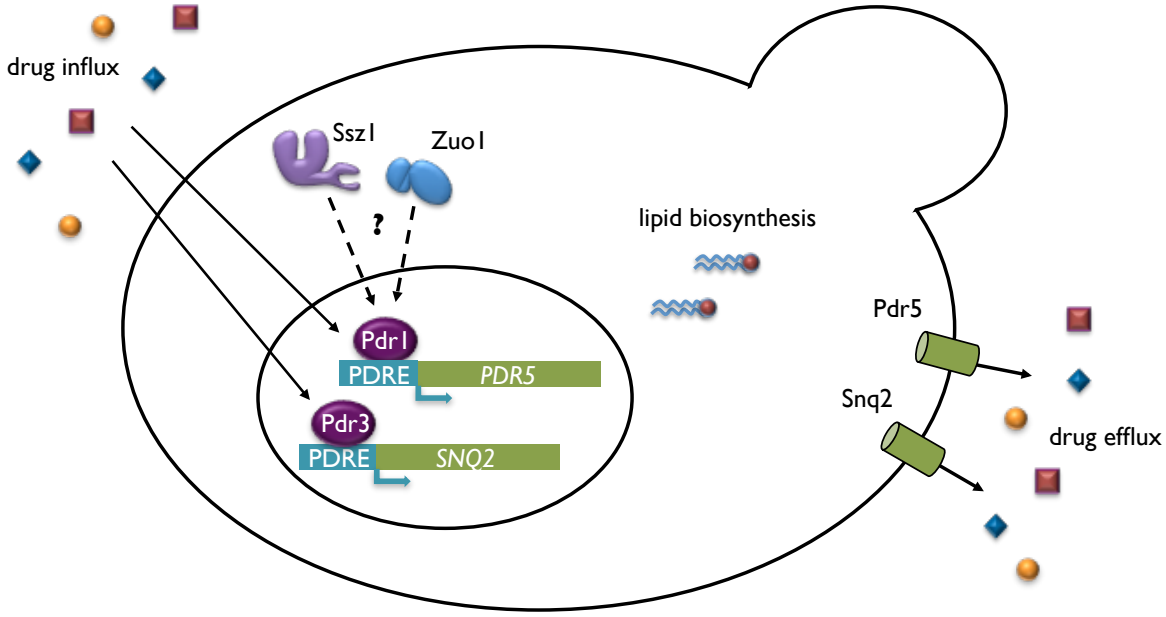
drug influx
Ssz1
Zuo1
?
lipid biosynthesis
Pdr1
PDRE
PDR5
Pdr3
PDRE
SNQ2
Pdr5
Snq2
drug efflux

Figure 1-3. Model of Pdr1 activation by xenobiotics. The transcription factor Pdr1 contains an N-terminal DNA binding domain (DBD), through which it binds constitutively to promoters of its target genes, such as the ABC transporter-encoding gene *PDR5*. Drugs, which enter the nucleus by passive diffusion, bind directly to a xenobiotic binding domain (XBD) within Pdr1's central regulatory region. This binding facilitates the interaction of Pdr1's transcriptional activation domain (AD) with the Gal11 subunit of the Mediator complex, which recruits the RNA Polymerase II (PolII) complex, resulting in transcriptional activation.

Figure 1-3

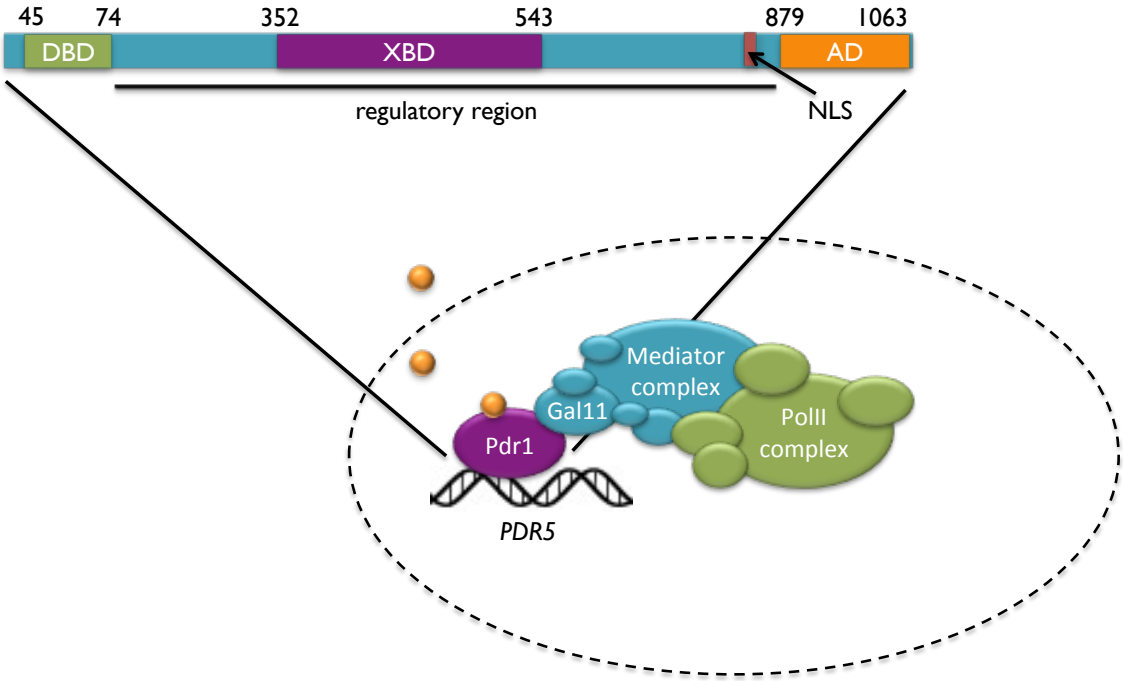
45
74
352
543
879
1063
DBD
XBD
AD
regulatory region
NLS
Mediator complex
Gal11
PolII complex
Pdr1
PDR5

Figure 1-4. Activation of the PDR regulon by Ssz1 or the C-terminus of Zuo1. Overexpression of the Hsp70-like protein Ssz1 or the C-terminus of the J-protein Zuo1 renders cells resistant to high levels of the drug cycloheximide. Cells were transformed with vector containing DNA encoding a tandem affinity purification tag (vector) or the same tag fused to residues 365-433 of Zuo1 behind a high-expression promoter (↑ZuoC) or with DNA encoding Ssz1 on either a low (Ssz1) or high (↑Ssz1) copy plasmid. Drug resistance was observed by plating transformants in serial dilutions onto media without (-) or with (+) cycloheximide.

Figure 1-4

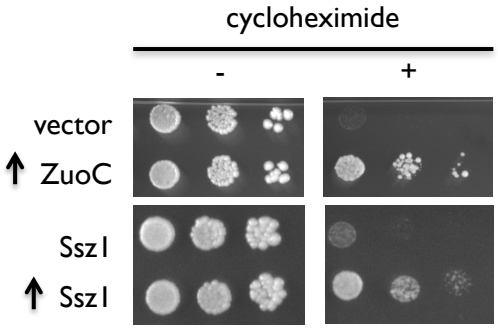

Table 1-1. Genes upregulated by the transcription factor Pdr1

Name	SGD Description	PDRE
SNQ2	ABC transporter protein involved in multidrug resistance	yes
GRE2	NADPH-dependent methylglyoxal reductase	yes
PDR5	ABC transporter involved in steroid transport, cellular detoxification	yes
YOR1	Plasma membrane ABC transporter	yes
YGR035C	Putative protein of unknown function	yes
ICT1	Lysophosphatidic acid acyltransferase, involved in phospholipid synthesis	yes
YMR102C	Putative protein of unknown function	yes
PDR16	Phosphatidylinositol transfer protein, may regulate lipid synthesis	yes
YLR346C	Putative protein of unknown function	yes
YPL088W	Putative aryl alcohol dehydrogenase	yes
PDR15	Plasma membrane ABC transporter implicated in cellular detoxification	yes
YCR061W	Protein of unknown function	yes
RPN4	Transcription factor that stimulates expression of proteasome genes	yes
YAL061W	Putative medium-chain alcohol dehydrogenase	yes
YLL056C	Putative protein of unknown function	yes
RSB1	Putative integral membrane transporter or flippase, may transport LCBs	yes
IPT1	Inositolphosphotransferase 1, involved in sphingolipid biosynthesis	yes
TPO1	Polyamine transporter	yes
IMA5	Alpha-glucosidase with specificity for isomaltose, maltose, and palatinose	yes
PDR10	ABC membrane pump involved in pleiotropic drug resistance	yes
FSP2	Protein of unknown function, induced during nitrogen limitation	yes
IMA3	Alpha-glucosidase	yes
HXT9	Putative hexose transporter, has similarity to MFS transporters	yes
HXT11	Putative hexose transporter, has similarity to MFS transporters	yes
HXT8	Protein of unknown function with similarity to hexose transporters	yes
PGA3	Essential protein required for maturation of Gas1p and Pho8p	yes
URA1	Dihydroorotate dehydrogenase, involved in pyrimidines biosynthesis	no
YOR152C	Putative protein of unknown function	no
HSP26	Small heat shock protein with chaperone activity	no
HXK1	Hexokinase isoenzyme 1,involved in glucose metabolism	no
INO1	Inositol 1-phosphate synthase, involved in phospholipid biosynthesis	no

ABC: ATP-binding cassette
MFS: Major facilitator superfamily
LCB: long chain base

Data based on genome-wide expression arrays reported in (DeRisi et al., 2000; Devaux et al., 2001).

CHAPTER TWO:

Role for the molecular chaperones Zuo1 and Ssz1 in quorum sensing via activation of the transcription factor Pdr1

This chapter has been published as Prunuske AJ, Waltner JK, Kuhn P, Gu B, and Craig EA (2012) Role for the molecular chaperones Zuo1 and Ssz1 in quorum sensing via activation of the transcription factor Pdr1. *Proceedings of the National Academy of Sciences U S A* 109(2):472-477 with AJ Prunuske and myself as co-first authors. I performed the yeast two-hybrid and chromatin immunoprecipitation experiments. The expression arrays, isolation of the hyperactive *ZUO1* allele and yeast growth arrest assays were carried out by AJ Prunuske. Cloning, yeast genetics, drug resistance assays, and ß-galactosidase assays were performed by both AJ Prunuske and myself. P Kuhn performed qPCR and assisted with the yeast two-hybrid and growth arrest assays. B Gu assisted with the yeast growth curves. The manuscript was written by AJ Prunuske, EA Craig, and myself. Some of the figures have been modified from the published version to include supplementary materials for the purpose of this thesis.

Abstract

Zuo1 functions as a J-protein co-chaperone of its partner Hsp70. In addition, the C-terminus of Zuo1 and the N-terminus of Ssz1, with which Zuo1 forms a heterodimer, can independently activate the *Saccharomyces cerevisiae* transcription factor Pleiotropic drug resistance 1 (Pdr1). Here we report that activation of Pdr1 by Zuo1 or Ssz1 causes premature growth arrest of cells during the diauxic shift, as they adapt to the changing environmental conditions. On the other hand, cells lacking Zuo1 or Ssz1 overgrow, arresting at a higher cell density, an effect overcome by activation of Pdr1. Cells lacking the genes encoding plasma membrane transporters Pdr5 and Snq2, two targets of Pdr1, also overgrow at the diauxic shift. Adding conditioned medium harvested from cultures of wild-type cells attenuated the overgrowth of both *zuo1*Δ *ssz1*Δ and *pdr5*Δ *snq2*Δ cells, suggesting the extracellular presence of molecules that signal growth arrest. In addition, our yeast two-hybrid analysis revealed an interaction between Pdr1 and both Zuo1 and Ssz1. Together, our results support a model in which (*i*) membrane transporters, encoded by Pdr1-target genes act to promote cell-cell communication by exporting quorum sensing molecules, in addition to playing a role in pleiotropic drug resistance and (*ii*) molecular chaperones function at promoters to regulate this intercellular communication through their activation of the transcription factor Pdr1.

Introduction

Eukaryotes, from fungi to humans, have a conserved, Hsp70-based molecular chaperone system best known for its function near the exit site of the ribosome tunnel from which nascent polypeptide chains emerge (Hundley et al., 2005; Otto et al., 2005). The J-protein of this system, called Zuo1/DNAJC2 in fungi/humans, is required for stimulation of the ATPase activity of its partner Hsp70, facilitating efficient interaction of Hsp70's peptide-binding domain with client proteins. Although the majority of Zuo1/DNAJC2 is found in the cytosol, associated with ribosomes, reports from both fungi and metazoans (Albanese et al., 2010a; Richly et al., 2010; von Plehwe et al., 2009), indicate that it also has functions off the ribosome and/or in the nucleus. Zuo1/DNAJC2 is found in a heterodimer with Ssz1/Hsp70L1(Otto et al., 2005). Although Ssz1/Hsp70L1 shares sequence similarity with the Hsp70 family of proteins, no evidence points to its binding to client proteins. Rather, Ssz1, as the heterodimer partner of Zuo1, facilitates the ability of Zuo1 to function as a J-protein, that is to stimulate the ATPase activity of its partner Hsp70 (Huang et al., 2005; Hundley et al., 2005).

In addition to their roles tied to their molecular chaperone activity, Ssz1 and Zuo1 have been shown to independently have the capacity to enhance the transcription of genes of the pleiotropic drug resistance (PDR) regulon (Eisenman and Craig, 2004; Hallstrom et al., 1998). The PDR regulon is predominately composed of genes encoding membrane transporters, such as Pdr5 and Snq2, and enzymes involved in lipid biosynthesis and membrane remodeling (Shahi and Moye-Rowley, 2009). As suggested by the PDR designation, this regulon was first identified because upregulation renders cells resistant to a variety of toxic xenobiotics by increasing their export from cells. Two related Zn_2-Cys_6 cluster transcription factors (TF), Pdr1 and Pdr3, are the

major regulators of this regulon. Some PDR targets, such as *PDR5*, are transcribed by both Pdr1 and Pdr3; others, such as *YOR1*, are only activated by Pdr1 (Shahi and Moye-Rowley, 2009). Pdr1 and Pdr3 can activate PDR in response to different signals. Ssz1 activates Pdr1, but not Pdr3 (Hallstrom et al., 1998); Pdr3, but not Pdr1, responds to the absence of the mitochondrial genome (Hallstrom and Moye-Rowley, 2000b). However, both are activated by a variety of xenobiotics, which directly bind Pdr1/3, likely causing a conformational change exposing a C-terminal transcription activation domain (Thakur et al., 2008).

Here we report the results of experiments designed to understand the physiological role of activation of the PDR regulon by Zuo1 or Ssz1. Activation of Pdr1 promotes the arrest of cell growth in the diauxic shift. Our results are consistent with a model in which Pdr1 is activated via direct interaction with Zuo1 and Ssz1, and the resulting upregulation of transporters in the plasma membrane increases export of signaling molecules involved in cell:cell communication.

Results

Activation of the PDR regulon by Zuo1 requires Pdr1

As a first step in our analysis of Zuo1 activation of PDR, we isolated a hyperactive *ZUO1* allele. Since the C-terminal 69 residues of Zuo1 are sufficient for induction of PDR (Eisenman and Craig, 2004), a library of randomly generated mutations within these 69 codons was screened for enhanced growth on plates containing the drug cycloheximide, relative to unmutagenized controls. From this screen we identified a single amino acid alteration, S427G. Cells expressing a fusion between a tandem affinity purification (TAP) tag and Zuo1's C-terminal 69 residues containing the S427G alteration (ZuoC*) displayed greater resistance to two mechanistically distinct drugs, cycloheximide and oligomycin, than cells expressing the wild-type (wt) fragment (ZuoC), even though the fusions were expressed at the same level (Figure 2-1A,B). That the observed upregulation was due to enhanced transcription was supported by the higher levels of mRNAs of Pdr5 and Yor1, known PDR target genes encoding drug transporters, in cells expressing ZuoC* compared to cells expressing ZuoC (Figure 2-1C). In addition, ZuoC* expressing cells harboring a PDR5 promoter-lacZ reporter had twice the ß-galactosidase activity of ZuoC-expressing cells (Figure 2-1D).

Given that Zuo1 and Ssz1 can independently activate PDR, we next tested whether Zuo1, like Ssz1, operated through the Pdr1 transcription factor. PDR induction by ZuoC* in wt, *pdr1*Δ and *pdr3*Δ cells was compared by assessing growth on plates containing drugs and by activation of *PDR5* and *YOR1* promoter-*lacZ* fusions. Similar levels of drug resistance were observed for wt and *pdr3*Δ cells, while no growth in the presence of drug was observed in *pdr1*Δ cells (Figure 2-2A). ZuoC* activated the *PDR5-lacZ* and *YOR1-lacZ* reporters on the order of 10-fold and 4-

fold, respectively, in wt cells and *pdr3*Δ cells. In contrast, no activation of *PDR5-lacZ* or *YOR1-lacZ* was observed in *pdr1*Δ cells expressing ZuoC* (Figure 2-2B, Table 2-1). This Pdr1-dependent induction was not specific to the hyperactive allele, as induction by wt ZuoC was also dependent upon Pdr1 (Figure 2-2C). Thus, we conclude that Zuo1 activation of the promoters of PDR genes, like that of Ssz1, is dependent on Pdr1.

The PDR regulon is a primary target of activation by Ssz1 and Zuo1

The results discussed above indicate that both Zuo1 and Ssz1 can activate PDR in a Pdr1-dependent manner. However, whether PDR is the primary pathway activated is not known. Therefore, we carried out whole genome microarray analysis (GEO accession #GSE31693) to provide an unbiased assessment, using ZuoC* and a previously identified hyperactive variant $Ssz1_{S295F}$ (Ssz1*) (Hallstrom et al., 1998). The gene expression pattern of cells expressing ZuoC* or Ssz1* were strongly correlated with an R^2 value of 0.9886, indicating that similar mRNAs were up and downregulated in these strains. The transcription factor consensus motifs and gene ontology of the upregulated and downregulated genes were identified (Tables 2-2, 2-3, 2-4). The major classes of genes upregulated were part of the PDR regulon. The target genes of two other TFs, Msn2/4 and Gcr1, were also identified as significantly upregulated. While the relationship between Ssz1/Zuo1 and Gcr1, which has been linked to growth control and filamentation (Willis et al., 2003), is not obvious, previous microarray analysis revealed that xenobiotic compounds inducing PDR upregulated Msn2/4 targets in a Pdr1/3 dependent manner (Willis et al., 2003). The major gene ontology classes that were enriched in upregulated genes included those associated with the plasma membrane, budding, transporters, and polarized growth (Table 2-3).

The major pathways downregulated are involved in ribosome synthesis (Table 2-4), consistent with the identification of the PAC element as a down-regulated TF binding site (Table 2-2) and previous results assessing effects of xenobiotic compounds (Willis et al., 2003). Based on this analysis, we conclude that ZuoC* and Ssz1* activate a similar set of genes, a major class of which are PDR associated.

Zuo1 and Ssz1 interact with Pdr1 in a yeast two-hybrid assay

Since the PDR regulon was a target of Zuo1 and Ssz1, we decided to test for their interaction with Pdr1 using a two-hybrid system. We generated a fusion of the Gal4 DNA binding domain (GBD) to Pdr1 to use as bait. To avoid confusion in interpretation of results, we used a Pdr1 fragment lacking its DNA binding (DBD) and activation (AD) domains, yielding GBD-Pdr1$_{\Delta DBD\Delta AD}$. As prey, the Gal4 activation domain (GAD) was fused to ZuoC* or Ssz1*$_{1-407}$, generating GAD-ZuoC* and GAD-Ssz1*$_{1-407}$. Positive signals were obtained. Cells expressing GBD-Pdr1$_{\Delta DBD\Delta AD}$ and GAD-ZuoC* or GAD-Ssz1*$_{1-407}$, but not GAD alone, grew in the absence of histidine, indicating activation of the *Gal1p-HIS3* reporter. The *Gal7p-lacZ* reporter was activated, as GAD-ZuoC* and GAD-Ssz1*$_{1-407}$ expressing cells had 6- and 5-fold higher β-galactosidase activity, respectively, than cells expressing GAD alone (Figure 2-3A, Table 2-5).

When setting up the two-hybrid system we intended to also carryout two-hybrid testing using ZuoC and Ssz1 fused to GBD as bait. However, GBD-ZuoC strongly auto-activated reporter genes in the absence of the Gal4 activation domain. GBD-ZuoC expressing cells grew in the absence of histidine and adenine, indicating activation of both *Gal1p-HIS3* and *Gal2p-ADE2*

reporters. β-galactosidase activity was 50-fold higher in cells expressing GBD-ZuoC than GBD alone (Figure 2-3B, Table 2-6). In addition, cells expressing GBD-ZuoC* grew more robustly on plates lacking histidine and adenine and showed approximately 2-fold higher β-galactosidase activity than those expressing GBD-ZuoC. We confirmed that the enhanced activity of GBD-ZuoC* was not due to increased expression (data not shown). We reasoned that an interaction between GBD-ZuoC and Pdr1 might eliminate the requirement for the Gal4 activation domain leading to auto-activation. Consistent with this idea, GBD-ZuoC cells containing an extra plasmid copy of *PDR1* grew more robustly on medium lacking histidine and adenine and had 2-fold higher β-galactosidase activity than cells having a single *PDR1* gene. In addition, *pdr1*Δ cells expressing GBD-ZuoC did not grow on medium lacking histidine and adenine. β-galactosidase activity was reduced to 19 units compared to 48 units in cells containing Pdr1. This residual activity indicates some Pdr1-independent activity. However, together, these results indicate that auto-activation of *GAL* promoters by GBD-ZuoC is largely dependent on Pdr1.

The fusion between GBD and Ssz1*$_{1\text{-}407}$, also auto-activated the *GAL* reporter constructs in a Pdr1-dependent manner (Figure 2-3C, Table 2-6), but to a lesser extent than the GBD-ZuoC fusion. No growth on selective plates was observed in *pdr1*Δ cells and the β-galactosidase activity was at the basal level found in cells expressing GBD alone. Together, these two-hybrid results are consistent with an interaction of Zuo1 and Ssz1 with Pdr1. To support the idea that the activation of Pdr1by Ssz1/Zuo1 likely occurs by direct action, chromatin immunoprecipitation (ChIP) was carried out using strains expressing Ssz1*. The presence of Ssz1 at the *PDR5* promoter, and as a control, a region 1.5 kB upstream, was evaluated by precipitating DNA using Ssz1-specific antibodies followed by quantitative PCR (qPCR). Increased levels of Ssz1 were

detected at the *PDR5* promoter compared to the upstream region relative to a control strain deleted for *SSZ1* (Figure 2-3D). This increase was dependent on the presence of Pdr1, as no precipitation above background levels was found in *pdr1*Δ cells. Together, these results support the idea that Ssz1/Zuo1 function at the *PDR5* promoter in a Pdr1-dependent manner.

Activation of the PDR regulon promotes early growth arrest at the diauxic shift

The ability of Zuo1 and Ssz1 to activate the PDR regulon in a Pdr1-dependent manner led us to ask whether such induction plays a physiological role. During our investigations, we noted that overnight cultures of cells expressing ZuoC* attained a lower cell number during the diauxic shift, the time during which glucose becomes depleted and growth arrests as cells transition to the utilization of nonfermentable carbon sources (DeRisi et al., 1997). We compared the growth of cells expressing ZuoC* with that of control cells. Overnight culture of cells were diluted and grown in synthetic media at 30°C, with samples removed periodically over the next 25 hours (Figure 2-4A). The cultures grew at the same rate over the first 10 hours. However, growth of ZuoC* expressing cells transiently plateaued at an optical density at 600 nm (OD) of approximately 2.8 after 13 hours. Cells expressing the control vector continued dividing for an additional 2-3 hours, plateauing at an OD of approximately 3.3. To confirm that the lower OD in the cells expressing the PDR inducing construct corresponded to a lower cell number, cells present in the cultures 15 hours after dilution were counted. Cultures expressing ZuoC* had 19% fewer cells than those carrying the control vector. Early growth arrest was also seen in cultures of cells expressing Ssz1* (data not shown). To address whether this difference in cell number as cells arrest at the diauxic shift was dependent on Pdr1, we also tested a *pdr1*Δ strain. Both

control and ZuoC* expressing *pdr1*Δ cells reached the diauxic shift plateau at an OD_{600} of 3.3, similar to wt cells (Figure 2-4A). Although the exact plateau OD reading varied slightly between batches of media, consistently, the plateau value for the PDR activating strain was lower than that of the three other strains. Thus, we conclude that the earlier transient growth arrest that occurs when ZuoC* is expressed is due to the activation of Pdr1.

Overgrowth of cells lacking Zuo1/Ssz1 is mitigated by Pdr1 activation

Since Pdr1 activation by Zuo1 or Ssz1 leads to growth arrest at a lower cell density, we asked whether the absence of these two proteins affected the density at which growth plateaued. Although *zuo1*Δ *ssz1*Δ cells grew more slowly than wt cells in exponential phase, they entered the diauxic shift at a higher OD (4.0 compared to 3.5) (Figure 2-4B). Consistent with the higher OD, 29% more cells were present in the *zuo1*Δ *ssz1*Δ culture than the wt culture after 25 hours of growth, when both cultures had reached the diauxic shift. To test the effect of Pdr1 activity on the response of cells to the absence of Zuo1 and Ssz1, *zuo1*Δ *ssz1*Δ cells were treated, 10 hours after dilution, with progesterone, a xenobiotic known to activate Pdr1 (Thakur et al., 2008) (Figure 2-4B). Overgrowth was mitigated; *zuo1*Δ *ssz1*Δ cells treated with progesterone plateaued at an OD of approximately 3.4, similar to wt cells.

Addition of conditioned medium alters growth at the diauxic shift

The results presented above suggested to us that activation of Pdr1 by Zuo1 and Ssz1 plays a role in regulating the timing of growth arrest as cells approach the diauxic shift. Since Pdr1 regulates the expression of membrane transporters that extrude small molecules from cells,

we decided to test the idea that the media of wt cells contained molecules that signal growth arrest, that is play a role in "quorum sensing". Wt and *zuo1*Δ *ssz1*Δ cells were diluted to an OD of 0.2 and grown for 14 hours. Cells were then pelleted. As controls, wt and *zuo1*Δ *ssz1*Δ cells were resuspended in medium in which they were grown (Figure 2-5A) and further growth monitored. As expected, *zuo1*Δ *ssz1*Δ cells attained an OD of approximately 4.1, while wt cells plateaued at 3.4. However, the growth of Δ*zuo1* Δ*ssz1* cells resuspended in "conditioned" medium from wt cells, rapidly plateaued, only reaching an OD at the diauxic shift of 3.5. This cessation of growth is consistent with the presence of factors in the wt-conditioned medium that signal arrest.

Cells lacking the membrane transporters Pdr5 and Snq2, whose expression is regulated by Pdr1, have been reported to overgrow at the diauxic shift (Hlavacek et al., 2009). Therefore, we extended our analysis to test whether these specific transporters play a role in signaling growth arrest. Cultures of wt and *pdr5*Δ *snq2*Δ cells approaching the diauxic shift were harvested at an OD of 2.5 and resuspended, either in the medium in which they were grown or the conditioned medium retrieved from the other culture (Figure 2-5B). The overgrowth of the *pdr5*Δ *snq2*Δ cells when resuspended in the medium in which they were grown was more dramatic than that of *zuo1*Δ *ssz1*Δ cells; they attained an OD of 6.8 after 11 hours of further incubation. When resuspended in conditioned medium from wt cells, however, growth of *pdr5*Δ *snq2*Δ cells plateaued at an OD of 3.2, only slightly higher than wt cells. On the other hand, wt cells resuspended in *pdr5*Δ *snq2*Δ conditioned media continued to grow slowly, reaching an OD of 4 after 11 hours. These results are consistent with the presence of a factor(s) in the wt conditioned media that promotes inhibition of cell division and that media in which *zuo1*Δ *ssz1*Δ

or *pdr5*Δ *snq2*Δ cells have been grown contain a lower concentration of this factor(s). As a preliminary assessment of the nature of these factors, media harvested from wt cells was subjected to one of two treatments, boiling or dialysis, prior to adding to *pdr5*Δ *snq2*Δ. Consistent with the factor(s) being small molecules, cells resuspended in dialyzed media overgrew, reaching an OD of 4.5 10 hours after addition, compared to 5 and 3 for *pdr5*Δ *snq2*Δ and wt media, respectively (Figure 2-6). On the other hand, boiled media was as efficient as untreated media in suppressing overgrowth.

Discussion

As discussed below, a picture emerges from the results presented here consistent with the ideas that: (*i*) activation of Pdr1 by Zuo1 and Ssz1 plays a role in regulating cell growth upon nutrient depletion at the diauxic shift and (*ii*) transporters of the plasma membrane, encoded by Pdr1-target genes, export quorum molecules sensed by other cells in the culture leading to growth arrest.

Activation of Pdr1 by Ssz1 and Zuo1

Expression of either the C-terminal 69 amino acids of Zuo1 or the ATPase domain of Ssz1 affects gene expression in very similar ways. Both cause the upregulation of genes of the PDR regulon in a Pdr1-dependent manner. The two-hybrid and ChIP data reported here suggest that this activation may be direct, involving an interaction of these proteins with Pdr1, leading to mobilization of its transcription activation domain that is normally sequestered by its endogenous inhibitory region. Such a mechanism is reminiscent of the activation of Pdr1 by xenobiotics, which bind Pdr1/Pdr3 in the internal "xenobiotic binding domain" (Thakur et al., 2008), releasing the inhibition of the transcriptional activation domain.

The specificity of the activation of Pdr1 by Zuo1 and Ssz1 is intriguing. While, xenobiotics activate both Pdr1 and Pdr3 (Thakur et al., 2008), Zuo1 and Ssz1 activate Pdr1, but not Pdr3. On the other hand, Pdr3, but not Pdr1, is activated by a yet-to-be defined signal present in cells lacking a functional mitochondrial genome (Hallstrom and Moye-Rowley, 2000b). Analysis of the genome organization surrounding the *PDR1* and *PDR3* genes indicates that this gene pair is a product of the whole genome duplication that occurred in an ancestral genome of

S. cerevisiae (Lelandais and Devaux, 2010). The differences between Pdr1 and Pdr3 may represent specialization for physiologically important signaling events, while both transcription factors retained the basic property of being activated by xenobiotics.

It is also worth noting that domains of Zuo1 and Ssz1 are independently capable of activating Pdr1. Since Ssz1 and Zuo1 form a very stable heterodimer (Conz et al., 2007a; Gautschi et al., 2001b), it is reasonable to posit that under normal physiological conditions they activate Pdr1 as a complex. It is also possible that the heterodimer is destabilized in response to some yet unknown signal, allowing them to act independently. Further work is required to understand the complexities of the relationship between the activation of Pdr1 by Zuo1 and by Ssz1.

Physiological role of activation of Pdr1 at the diauxic shift by Ssz1/Zuo1

Based on the results presented here, which link Pdr1 activation to the transition point of the diauxic shift, we propose a model in which the density at which yeast cells arrest growth, transitioning to an environment of less favorable nutrients, depends in part on the level of small molecules in the surrounding medium. The efflux of these quorum sensing molecules from cells in which they were synthesized is mediated by plasma membrane transporters such as Snq2 and Pdr5. According to this model, the concentration of these regulatory molecules in the medium is dependent upon the level of such transporters. Consistent with this model, *pdr5*Δ *snq2*Δ cells arrest at a very high cell density. As expression of these transporters is regulated in part by Pdr1, activation by either Zuo1/Ssz1 or by xenobiotics results in growth arrest at a lower cell density, because more autoregulatory molecules are exported from cells. Interestingly, a recent

bioinformatics analysis of several genome wide studies identified Pdr1 as one of handful of transcription factors predicted to be involved in quorum sensing (Wuster and Babu, 2010).

Sensing of signals in response to cell density has been extensively studied in bacteria. In fact, cell:cell signaling related to regulating the cell density attained by bacterial cultures has been linked to multidrug transporters in *Escherichia coli* (Yang et al., 2006). Studies on cell:cell communication in eukaryotic unicellular organisms are more limited. Nevertheless, several intercellular signal transduction pathways have been identified in fungi. In the dimorphic fungal human pathogen *Candida albicans* aromatic alcohols have been linked to nitrogen limitation and yeast-to-filamentous growth transition (Hornby et al., 2001). The very limited number of reports of quorum sensing in *S. cerevisiae* is likely due to the fact that standard yeast strains, such as those used here, do not undergo filamentous growth because of a mutation in the *FLO8* gene, which is needed for invasive and filamentous growth (Liu et al., 1996). However, using a truly wt strain, Fink and colleagues uncovered a quorum sensing signaling pathway responsive to aromatic alcohols that regulates filamentation in response to both cell density and nutrient availability (Chen and Fink, 2006). Interestingly, in this strain background, *ZUO1* was identified in a screen for genes involved in filamentous growth (Palecek et al., 2000). Future studies in such truly wt strains may be required to determine whether the role of the Ssz1 and Zuo1 chaperones in quorum sensing relates to the regulation of filamentous growth and nitrogen metabolism, an unappreciated cellular response to glucose deprivation or an unknown signaling pathway.

Universal role of Zuo1:Ssz1 orthologs in transcriptional regulation in eukaryotes

The C-terminal regions of Zuo1 and Ssz1 in fungi differ from that of other eukaryotic orthologs (Braun and Grotewold, 2001b). However, it is intriguing that Zuo1 orthologs in most other eukaryotes have Myb/SANT domains, well-established DNA binding domains, at their C-termini. These domains of Zuo1 orthologs have been implicated in regulation of asymmetric cell division in blue-green algae (Pappas and Miller, 2009) and in nematodes (Hatzold and Conradt, 2008). In yeast, our evidence supports the idea that molecular chaperones regulate cell:cell communication through modulation of the pleiotropic drug resistance pathway. Future study will be required to define the similarities and differences in mechanisms of action of these molecular chaperones in cell:cell communication in diverse organisms. Regardless, this conserved connection between the ribosome, the cellular center of protein synthesis, and the regulation of growth control/development, raises the intriguing possibility of regulatory connections coordinating the regulation of protein synthesis and growth control/development.

Figures, Tables, and Legends

Figure 2-1. Enhancement of drug resistance in the C-terminus of Zuo1. Wt cells were transformed with vector containing DNA encoding a TAP tag (-) or TAP tag fused to either amino acids 365-433 of wt Zuo1 (ZuoC) or ZuoC having the S427G alteration (ZuoC*). (A) Serial dilutions of wt cells harboring the indicated plasmids were spotted onto media without (-) or with (+) cycloheximide (CHX) or oligomycin (OLI). (B) Cell extracts prepared from indicated cells were subjected to immunoblot analysis using IgG to detect TAP-ZuoC and TAP-ZuoC* fusions. (C) RNA isolated from wt cells harboring the indicated plasmids was subjected to Northern blot analysis using probes against *PDR5* or *YOR1*. An *ACTIN* probe was used as a loading control. (D) Wt yeast containing an integrated *PDR5* promoter-*lacZ* fusion were transformed with the indicated plasmids and β-galactosidase activity was measured. The average activity of three transformants of each was measured on two independent occasions and averaged and the fold activation of experimental/control (ZuoC/TAP) was plotted.

Figure 2-1

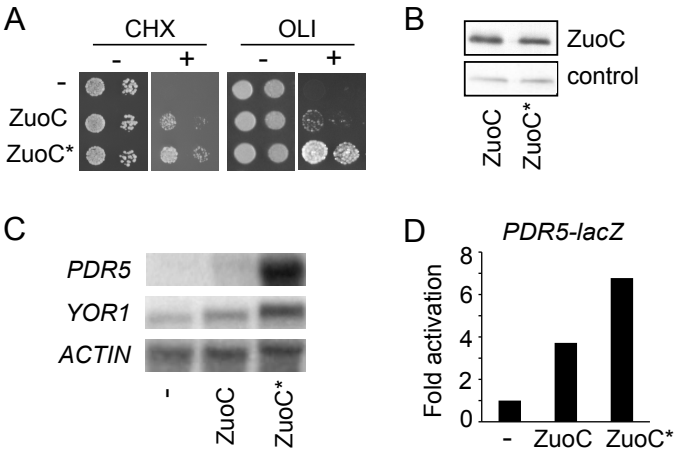
A
CHX
OLI
-
+
-
+
-
ZuoC
ZuoC*
B
ZuoC
control
ZuoC
ZuoC*
C
PDR5
YOR1
ACTIN
-
ZuoC
ZuoC*
D
PDR5-lacZ
Fold activation
8
6
4
2
0
-
ZuoC
ZuoC*

Figure 2-2. Activation of the PDR regulon by Zuo1 is specific for Pdr1. (A) Serial dilutions of WT, *pdr1*Δ and *pdr3*Δ cells transformed with either vector containing DNA encoding a TAP tag (-) or the TAP-ZuoC* plasmid (+) were spotted onto media without (-) or with (+) cycloheximide (CHX) or oligomycin (OLI). (B) Cells harboring either the control (TAP) or TAP-ZuoC* (ZuoC*) plasmid were transformed with a second plasmid encoding either a *PDR5* or *YOR1* promoter-*lacZ* fusion. The average ß-galactosidase activity of 3 transformants of each was quantified as Miller units and plotted. (C) Serial dilutions WT, *pdr1*Δ and *pdr3*Δ cells transformed with either the control (-) or TAP-ZuoC plasmid (+) were spotted onto media without (-) or with (+) cycloheximide (CHX).

Figure 2-2

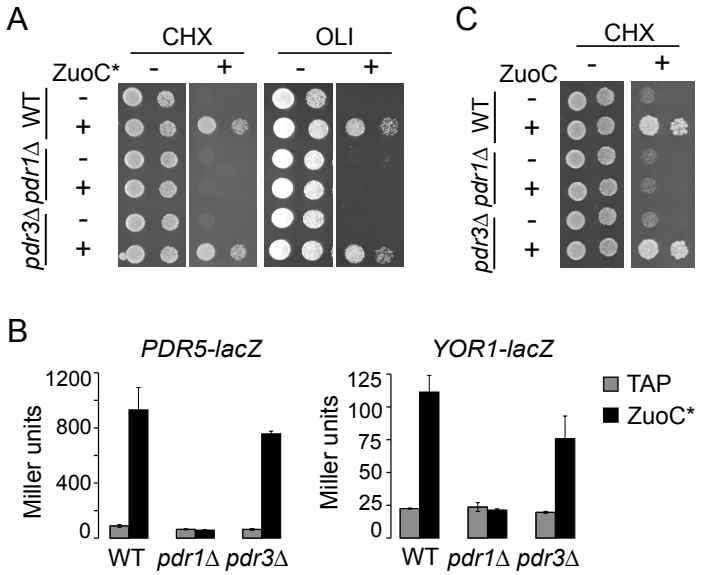
A
CHX
OLI
ZuoC*
-
+
-
+
WT
pdr1Δ
pdr3Δ
C
CHX
ZuoC
B
PDR5-lacZ
YOR1-lacZ
Miller units
1200
800
400
0
125
100
75
50
25
TAP
ZuoC*
WT
pdr1Δ
pdr3Δ

Figure 2-3. Interaction of ZuoC, ZuoC* and Ssz1*$_{1-407}$ with Pdr1. (A-C) Yeast two-hybrid. (A) Interaction between Pdr1 and Ssz1/Zuo1. Wt PJ69 cells were transformed with a plasmid containing DNA encoding the Gal4 DNA binding domain (GBD) fused to residues 76-965 of Pdr1 (GBD-Pdr1) and a second plasmid containing either DNA encoding the Gal4 activation domain (GAD, -) or GAD fused to ZuoC* or Ssz1*$_{1-407}$. Serial dilutions of cells containing the indicated plasmids were spotted onto media lacking histidine (-his). The average ß-galactosidase activity of three transformants of each was measured and reported as fold activation of experimental/control (GAD fusion/GAD). (B and C) ZuoC, ZuoC* and Ssz1*$_{1-407}$ tethered to GBD activate *GAL* promoters in a Pdr1-dependent manner. Cells carrying varying copies of *PDR1* were created by transforming WT cells with either empty vector (+) or a centromeric plasmid containing *PDR1* (++) or transforming *pdr1Δ* cells with empty vector (−). These cells were transformed with a second plasmid containing DNA encoding GBD (-) or GBD fused to codons for residues 365-433 of wt Zuo1 (ZuoC), ZuoC having the S427G alteration (ZuoC*), or 1-407 of Ssz1 containing the S295F alteration (Ssz1*$_{1-407}$). Serial dilutions of cells harboring the indicated plasmids were spotted onto media lacking histidine (-his) or histidine and adenine (-his -ade). The average ß-galactosidase activity of 2-3 transformants of each was measured and reported as fold activation of experimental/control (GBD fusion/GBD). (D) Chromatin immunoprecipitation (ChIP). DNA precipitated by Ssz1-specific antibodies from strains having (+) or lacking (-) *PDR1* and expressing Ssz1* was analyzed by qPCR using primer pairs designed to amplify the *PDR5* promoter (*PDR5*) and a region 1.5 kB upstream (control). The IP signal relative to input DNA was calculated for each location. The mean and SEs of the resulting IP/input from three PCR measurements are plotted.

Figure 2-3

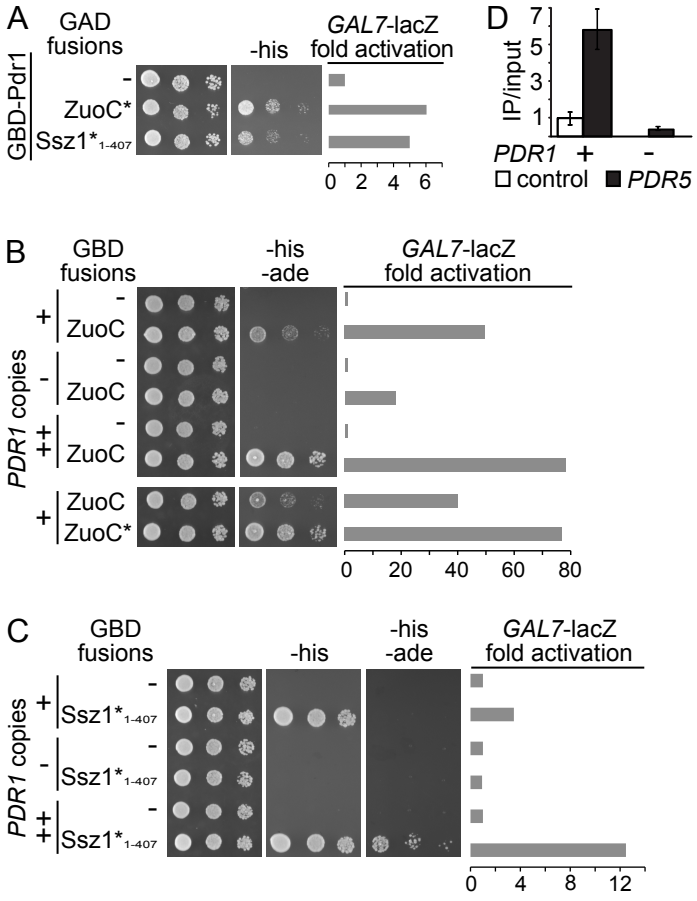
A
GAD fusions
-his
GAL7-lacZ fold activation
GBD-Pdr1
-
ZuoC*
Ssz1*1-407
0 2 4 6
D
IP/input
7
5
3
1
PDR1 + -
control
PDR5
B
GBD fusions
-his -ade
GAL7-lacZ fold activation
PDR1 copies
+
-
++
ZuoC
ZuoC*
0 20 40 60 80
C
GBD fusions
-his
-his -ade
GAL7-lacZ fold activation
PDR1 copies
Ssz1*1-407
0 4 8 12

Figure 2-4. Effect of Pdr1 activation on the cell density at which growth arrest occurs at the diauxic shift. Indicated cells were diluted to an OD_{600} of 0.2 in synthetic media and the OD monitored for the subsequent 25 hours. (A) WT or *pdr1*Δ cells were transformed with the control vector containing DNA encoding the TAP tag (no designation) or vector encoding TAP-ZuoC* (ZuoC*). (B) Two cultures of WT and *zuo1*Δ *ssz1*Δ cells were grown as above. One of each was treated with progesterone (PG) 10 hours after dilution of the culture.

Figure 2-4

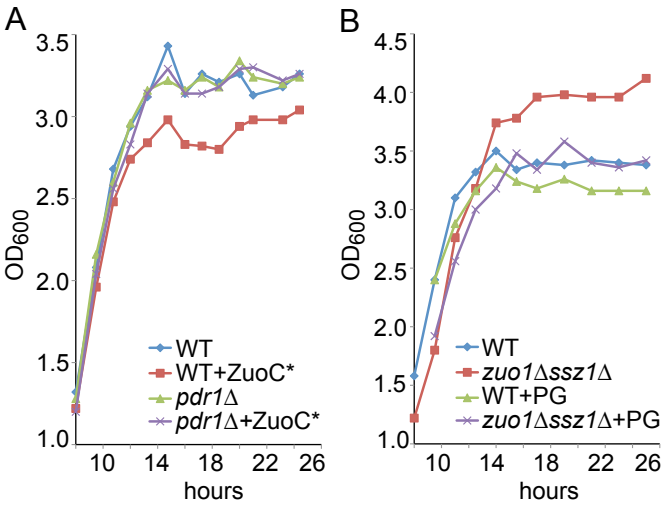
A
3.5
3.0
2.5
2.0
1.5
1.0
OD600
10
14
18
22
26
hours
WT
WT+ZuoC*
pdr1Δ
pdr1Δ+ZuoC*
B
4.5
4.0
3.5
3.0
2.5
2.0
1.5
1.0
OD600
10
14
18
22
26
hours
WT
zuo1Δssz1Δ
WT+PG
zuo1Δssz1Δ+PG

Figure 2-5. Addition of conditioned medium alters growth at the diauxic shift. WT, *zuo1*Δ*ssz1*Δ, or *pdr5*Δ*snq2*Δ cells were diluted to an OD_{600} of 0.2. After 14 (A) or 15 (B) hours, cultures were spun down and the conditioned media harvested. Cells were resuspended in the indicated conditioned medium and growth monitored for the ensuing 11 (A) or 10 (B) hours.

Figure 2-5

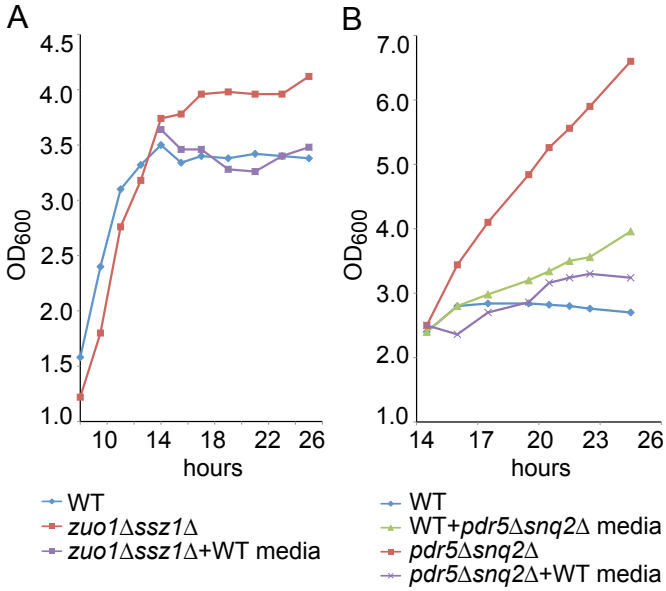
A
4.5
4.0
3.5
3.0
2.5
2.0
1.5
1.0
OD600
10
14
18
22
26
hours
WT
zuo1Δssz1Δ
zuo1Δssz1Δ+WT media
B
7.0
6.0
5.0
4.0
3.0
2.0
1.0
OD600
14
17
20
23
26
hours
WT
WT+pdr5Δsnq2Δ media
pdr5Δsnq2Δ
pdr5Δsnq2Δ+WT media

Figure 2-6. Altered growth in conditioned medium is abrogated by dialysis. Wt and *pdr5*Δ*snq2*Δ strains were diluted to an OD_{600} of 0.2 with a second dilution of the *pdr5*Δ*snq2*Δ strain started 4 hours later. After 15 hours, cultures were spun down and the conditioned media harvested. Conditioned media was either dialyzed, boiled, or untreated prior to resuspending the second culture of the *pdr5*Δ*snq2*Δ strain in each media treatment. Growth was monitored over the subsequent 11 hours.

Figure 2-6

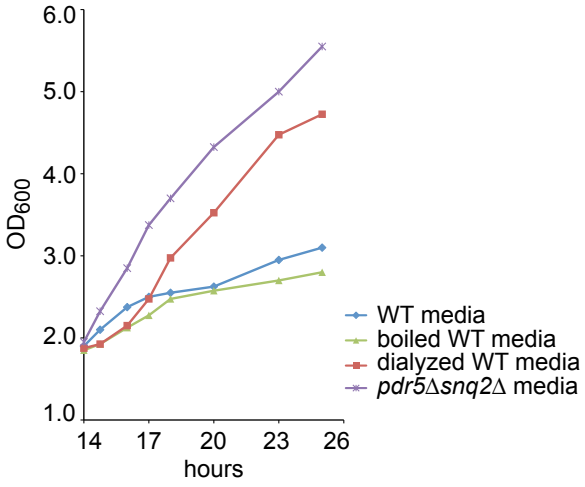
6.0
5.0
4.0
3.0
2.0
1.0
OD600
14
17
20
23
26
hours
WT media
boiled WT media
dialyzed WT media
pdr5Δsnq2Δ media

Table 2-1. Induction of PDR reporters by ZuoC*

ß-galactosidase activity of reporter gene fusions[†]			
Strain	**Plasmid**	***PDR5-lacZ***	***YOR1-lacZ***
WT	vector	88.9 ± 9.7	22.5 ± 0.4
WT	ZuoC*	931.0 ± 162.4	111.3 ± 9.7
*pdr1*Δ	vector	64.1 ± 3.6	23.6 ± 3.4
*pdr1*Δ	ZuoC*	58.7 ± 2.9	21.4 ± 0.8
*pdr3*Δ	vector	63.9 ± 5.7	19.6 ± 0.7
*pdr3*Δ	ZuoC*	757.2 ± 19.8	75.8 ± 17.3

[†]The average ß-galactosidase activity of three independent transformants was measured and reported in Miller units.

Table 2-2. Transcription factor motifs enriched in ZuoC* and Ssz1* expression arrays

Name	**Motif**	***t*-value**[†]		
		ZuoC*	Ssz1*	ZuoC* + Ssz1*
PDR1/3	TCCGYGGA	**4.62**	**3.82**	**4.21**
PDR like	TCCGYGGR	**4.43**	**3.79**	**4.11**
Msn2/4	CCCCT	3.50	**4.76**	**4.26**
GCR1	CWTCC	**3.82**	**4.06**	**4.00**
PAC	CGATGAG	-2.26	**-4.08**	-3.34

[†] *t*-values considered significant are indicated in bold.

Table 2-3. GO categories significantly upregulated in ZuoC* and Ssz1* expression arrays

GO category	*t*-value	E-value[†]	Mean	# of ORFs
phosphotransferase activity, alcohol groups as acceptor	6.39	2.30E-07	0.264	166
plasma membrane	6.36	2.80E-07	0.240	212
protein kinase activity	6.21	7.36E-07	0.287	128
kinase activity	5.49	5.58E-05	0.222	198
catalytic activity	5.11	4.47E-04	0.108	1744
carrier activity	4.84	1.80E-03	0.238	128
physiological process	4.69	3.79E-03	0.084	4024
transcription factor activity	4.66	4.38E-03	0.330	52
transporter activity	4.58	6.44E-03	0.154	416
regulation of biological process	4.56	7.08E-03	0.154	412
bud	4.52	8.55E-03	0.226	131
transcription regulator activity	4.36	1.79E-02	0.165	309
regulation of metabolism	4.29	2.45E-02	0.155	363
site of polarized growth	4.13	4.91E-02	0.208	137

Normalized array data were combined using ArrayStar and Gene Ontology categories were identified using t-profiler http://www.t-profiler.org.
[†]E-values <0.05 were considered significant.

Table 2-4. GO categories significantly downregulated in ZuoC* and Ssz1* expression arrays

GO category	*t*-value	E-value[†]	Mean	# of ORFs
nucleolus	-4.25	2.93E-02	-0.054	191
small ribosomal subunit	-4.41	1.43E-02	-0.120	90
cytosolic ribosome	-4.48	1.03E-02	-0.079	148
biological process unknown	-4.95	1.03E-03	0.026	1620
molecular function unknown	-5.10	4.72E-04	0.034	2217
mitochondrial matrix	-5.45	7.00E-05	-0.118	137
organellar large ribosomal subunit	-5.60	2.98E-05	-0.286	42
large ribosomal subunit	-6.35	2.99E-07	-0.162	122
structural molecule activity	-6.76	1.92E-08	-0.079	324
ribosome	-6.76	1.92E-08	-0.100	250
ribonucleoprotein complex	-6.82	1.27E-08	-0.066	393
organellar ribosome	-6.98	4.10E-09	-0.257	75
structural constituent of ribosome	-7.84	6.32E-12	-0.147	207

Normalized array data were combined using ArrayStar and Gene Ontology categories were identified using t-profiler http://www.t-profiler.org.
[†]E-values <0.05 were considered significant.

Table 2-5. Activation of yeast two-hybrid system by GBD-Pdr1$_{\Delta DBD\Delta AD}$ and GAD-ZuoC* and GAD-Ssz1*$_{1-407}$ fusions

ß-galactosidase activity of *GAL7-lacZ*[†]		
GBD fusion	**GAD fusion**	**Activity**
Pdr1$_{\Delta DBD\Delta AD}$	-	0.38 ± 0.04
Pdr1$_{\Delta DBD\Delta AD}$	ZuoC*	2.26 ± 0.06
Pdr1$_{\Delta DBD\Delta AD}$	Ssz1*$_{1-407}$	1.88 ± 0.13

[†]The average ß-galactosidase activity of three independent transformants was measured and reported in Miller units.

Table 2-6. Pdr1-dependent auto-activation of the yeast two-hybrid system by GBD-ZuoC, GBD-ZuoC*, and GBD-Ssz1*$_{1-407}$ fusions

ß-galactosidase activity of *GAL7-lacZ*[†]		
***PDR1* copies**	**GBD fusion**	**Activity**
+	-	0.97
+	ZuoC	47.88
+	Ssz1*$_{1-407}$	3.36
-	-	1.52
-	ZuoC	19.19
-	Ssz1*$_{1-407}$	1.42
++	-	1.25
++	ZuoC	97.43
++	Ssz1*$_{1-407}$	15.53
+	-	1.35
+	ZuoC	54.17
+	ZuoC*	103.91

[†]The average ß-galactosidase activity of 2-3 independent transformants was measured and reported in Miller units. Data shown below the solid line were collected as an independent experiment.

Material and Methods

Genetic methods

Most yeast strains used were isogenic with DS10 (*his3-11, 15 leu2-3, 112 lys1 lys2 trp1*Δ *ura3-52*). *zuo*Δ*1*::*HIS3 ssz1*Δ::*LYS2* was previously published (Hundley et al., 2002)*; pdr5*Δ*::URA3 snq2*Δ*::TRP1*, *pdr1*Δ*::TRP1* and Δ*pdr3::HIS3* were made by transforming a PCR product generated from amplifying the *URA3* marker from pRS306, the *TRP1* marker from pRS304, or the *HIS3* marker from pRS303 using primers that contain homology immediately upstream and downstream of the gene to be deleted. Integration was confirmed by PCR. *PDR5-lacZ* and *YOR1-lacZ* were previously described (Hallstrom et al., 1998). TAP and TAP-ZuoC plasmids were created by PCR amplifying codons for an N-terminal TAP tag and Zuo1 residues 365-433 and cloning into pRS415-GPD using SpeI and BamHI (TAP) and BamHI and SalI (ZuoC). ZuoC* was created by site directed mutagenesis using S427G mutagenic primers. Full length Ssz1 (BamHI and SalI) was cloned into the pRS415-GPD vector using BamHI and SalI. Ssz1* was created by introducing S295F into this vector using site directed mutagenesis.

To obtain a hyperactive *ZUO1* allele, mutagenic PCR with high magnesium was used to generate PCR products in the codons encoding the C-terminal 69 residues. These products were then used in a QuickChange reaction to generate a library of plasmids in pRS315-Zuo1$_{\Delta 285\text{-}364}$ (Yan et al., 1998b). The library was transformed into DS10 and candidates able to grow in the presence of 1 μg/ml cycloheximide selected. Plasmid from each candidate was recovered, sequenced, retransformed and then assayed for induction of the *PDR5-lacZ* reporter.

To assay drug resistance, approximately equal numbers of cells were subjected to 10-fold serial dilutions and spotted on media: selective minimal glucose, containing either 0, 0.7 or 1

μg/ml cycloheximide or YPGE (1% yeast extract, 2% peptone, 3% glycerol and 2% ethanol) containing 0 or 1.5 μg/ml oligomycin. Plates were incubated at 30°C for 2-3, 4 or 7-11 days on minimal, YPGE, or YPGE + oligomycin media, respectively, before photographing. β-galactosidase assays were performed as previously described (Eisenman and Craig, 2004); average of three independent transformants was reported.

Northern blot

RNA was isolated from 5-ml cultures by the hot phenol method (Ausubel et al., 1997). Ten micrograms of total RNA was separated on a 1% MOPS-formaldehyde gel, transferred to a nylon membrane, and hybridized in ULTRAhyb (Ambion, Austin, TX) overnight with radiolabeled double-stranded DNA probes. Probes were generated by random priming with [-^{32}P]dCTP (6000 Ci/mmol; Perkin Elmer-Cetus, Boston, MA), using the Prime-A-Gene kit (Promega), and PCR products containing the coding region of each gene. After stringent washes, membranes were exposed using a PhosphorImager detection screen (GE Healthcare, Piscataway, NJ), and visualized on a Typhoon 941 (GE Healthcare)). For reprobing, blots were boiled in 1% SDS and rehybridized with a new probe.

Tiled microarray

20 μg samples of total RNA (prepared by pooling equal quantities of 3 biological replicates) were digested with RQ1 DNase (Promega). Reactions were extracted with phenol/chloroform/isoamyl alcohol, followed by chloroform and then precipitated. RNA quality was assessed using the Agilent 2100 Bioanalyzer. 10 μg RNA was used to prepare labeled

cDNA using SuperScript II (Invitrogen) followed by the one-color Cy3 labeling kit (NimbleGen). Labeled sample was hybridized to a 12x137K NimbleGen *S. cerevisiae* array (05543835001) using the manufacturers recommended conditions. Arrays were scanned using the MS 200 Microarray Scanner and MS 200 Data Collection Software. Probes were averaged and samples quantile normalized with a log2 transformation and analyzed using ArrayStar (DNAstar). T-profiler (http://www.t-profiler.org/) was used to identify transcription factor binding motifs and gene ontogeny (Boorsma et al., 2005).

Yeast Two-Hybrid and ChIP

Strain background PJ69, a derivative of W303, was used. GBD and GAD plasmids and the two-hybrid methods are previously published (James et al., 1996). *pdr1*Δ*::TRP1* was created by amplifying the integrated *pdr1*Δ*::TRP1* cassette from DS10 *pdr1*Δ*::TRP1* genomic DNA and transforming into PJ69. GBD-ZuoC and GBD-Ssz1*$_{1\text{-}407}$ plasmids were created by PCR amplification of DNA encoding Zuo1 residues 365-433 and Ssz1 residues 1-407 containing the S295F mutation and cloning into pGBDU-C1 using BamHI and PstI. GBD-ZuoC* was created by site-directed mutagenesis using S427G primers. GBD-Pdr1$_{\Delta DBD}$ was created by PCR amplification of DNA encoding Pdr1 residues 76-1063 and cloning into pGBD-C1 using ClaI and SmaI. *pdr1*$_{\Delta DBD\Delta AD}$ was created by removing DNA encoding residues 965-1063. GAD-ZuoC* and GAD-Ssz1*$_{1\text{-}407}$ were created by PCR amplification of each and cloning into pGAD-C1 using BamHI and SacI. Cells were grown for 2 days at 30˚C on minimal media lacking uracil, leucine, or tryptophan to select for the respective plasmids and lacking either histidine and adenine or histidine and containing 2 mM 3-aminotriazole (3-AT) to detect activation of *Gal2p*-

ADE2 and Gal1p-HIS3 reporters. At least two independent transformants were measured for β-galactosidase activity of the *GAL7-lacZ* reporter and averaged.

ChIP was carried out as described previously (Tietjen et al., 2010). Strains used were deleted for *ZUO1* to ensure that Ssz1 was not ribosome-associated and carrying Ssz1* on pRS316. Briefly, cultures at 0.6 OD were treated with formaldehyde to induce crosslinking. Lysates were sonicated to shear genomic DNA and then incubated with Ssz1-specific antibody followed by precipitation with Protein A-agarose beads. After washing, cross-linking was reversed by incubation overnight at 65°C. DNA was then precipitated and subjected to qPCR. The background signal from a control experiment using cells lacking *SSZ1* was subtracted from experimental values obtained. Target DNA in the sample was quantified by generating a standard curve with a 4-fold dilution series of the input DNA for each sample.

Growth curves

Overnight cultures were diluted to an OD of 0.2 into synthetic complete media (0.67% yeast nitrogen base with ammonium sulfate and without amino acids, 2% dextrose, supplemented with all amino acids). Leucine was omitted in the case of TAP vectors. 5 mL cultures were grown at 30°C with shaking and OD measured between 8 and 25 hour after dilution. Each experiment was performed a minimum of 5 times. Progesterone (Sigma) was diluted to 0.1 M in ethanol and added to the yeast culture after 10 hours of growth for a final concentration of 100 μM.

Media swap time course

Overnight cultures of the wt and *pdr5*Δ *snq2*Δ strains were diluted to an OD_{600} of 0.2 (50 ml final volume) into synthetic complete media (0.67% yeast nitrogen base with ammonium sulfate and without amino acids, 2% dextrose, supplemented with all amino acids). Four hours later a second 50 ml culture of the *pdr5*Δ *snq2*Δ strain was diluted under the same conditions. The initial cultures were grown at 30°C with shaking for 15 hours to "condition" media. Cells were then pelleted and the supernatant/media was spun again at 6000xg for 10 minutes to remove any remaining cells. 10 ml of wt-conditioned media was dialyzed against 500 ml of TBS (50 mM Tris-HCl pH 7.4, 150 mM NaCl) for 3 hours at 25°C, replacing the TBS every hour. Dialysis was performed in 12 ml Slide-A-Lyzer cassettes (Thermo Scientific) with a 2K MWCO. Additional wt-conditioned media and *pdr5*Δ *snq2*Δ-conditioned media were stored at 25°C during dialysis. Just before resuspending cells in treated media a portion of the wt-conditioned media was boiled for 10 minutes. Four hours after the initial cultures were stopped, the cells in the second culture of the *pdr5*Δ *snq2*Δ strain were pelleted and washed 3x in 10 ml of TBS. The fresh *pdr5*Δ *snq2*Δ pellets were then resuspended in one of the four media treatments to an OD_{600} of 2.0 and growth was assessed for 11 hours.

Acknowledgments

We thank Scott Moye-Rowley for plasmids and Jeffrey Lewis and Audrey Gasch for help with microarray analysis. This work was supported by National Institutes of Health Grants GM31107 (EAC) and GM080931 (AJP).

CHAPTER THREE:

Unfolding of the C-terminal domain of the J-protein Zuo1 releases autoinhibition and activates Pdr1-dependent transcription

The work presented in this chapter is being prepared as a manuscript that will be submitted to *Nature Structural & Molecular Biology.* This work was done in collaboration with Dr. Brian Volkman's lab at the Medical College of Wisconsin, Milwaukee, WI. I solved the NMR structure of Zuo1's C-terminal domain with the assistance of Dr. Francis Peterson. F Peterson collected the NMR and circular dichroism data and I performed all remaining experiments presented in this chapter. (Note: The fragment of Zuo1's C-terminus referred to as "ZuoC" in the previous chapter will be referred as "$Zuo1_{365\text{-}433}$" in this chapter to denote its residue boundaries and avoid confusion as more C-terminal constructs are introduced.)

Abstract

The C-terminus of Zuo1, a ribosome-associated J-protein co-chaperone, is sufficient to activate the transcription factor pleiotropic drug resistance 1 (Pdr1), consequently playing a role in quorum sensing during nutrient limitation by increasing the expression of membrane transporters. Here we report that dissociation of Zuo1 from the ribosome is not sufficient for this activation because the C-terminal 86 residues fold into an autoinhibitory left-handed four-helix bundle. Hydrophobic residues at the extreme C-terminus required for Pdr1 activation are integral to the domain structure, suggesting that sequestering of these key residues may be a critical aspect of Zuo1 autoinhibition. Experimentally, unfolding propensity *in vitro* correlates with both activation of and interaction with Pdr1, as monitored by *in vivo* assays. Thus, our results are consistent with a model in which response to yet to be determined physiological signals results in unfolding of the C-terminal domain of ribosome-dissociated Zuo1 and activation of Pdr1 in a manner analogous to its activation by xenobiotics.

Introduction

The eukaryotic-specific J-protein Zuo1 is an Hsp70 co-chaperone that is primarily associated with ribosomes and has a widely accepted role in the folding of nascent polypeptides (Gautschi et al., 2002; Hundley et al., 2002; Yan et al., 1998a). However, evidence from several organisms indicates that Zuo1 also has a direct role in transcriptional regulation (Inoue et al., 1999; Richly et al., 2010). In *Saccharomyces cerevisiae,* Zuo1 has been identified as an activator of the zinc cluster transcription factor (TF) Pdr1 (Eisenman and Craig, 2004; Prunuske et al., 2012). Pdr1, like many TFs, has a C-terminal activation domain that has minimal activity until activated by a specific signal (Kolaczkowska et al., 2002; Thakur et al., 2008). Activation of Pdr1 by either Zuo1 or by a variety of xenobiotics initiates a highly specific transcriptional response, upregulating a set of genes belonging to the pleiotropic drug resistance (PDR) regulon (DeRisi et al., 2000; Devaux et al., 2001; Prunuske et al., 2012). The name PDR originated because the regulon includes genes encoding plasma membrane ATP-binding cassette (ABC) transporters, such as Pdr5 and Snq2, which extrude xenobiotics from cells, rendering them resistant to a variety of toxic compounds (Jungwirth and Kuchler, 2006; Kolaczkowski et al., 1998). However, evidence indicates that the PDR pathway plays additional roles. Pdr5 and Snq2 also function in regulating the transient growth arrest that occurs at the diauxic shift as cells preferred carbon sources and other nutrients become depleted, suggesting a role for the PDR system in growth regulation, perhaps by extruding small molecules sensed by neighboring cells (Hlavacek et al., 2009; Prunuske et al., 2012).

Zuo1 is a 433 amino acid protein consisting of three regions known to be important for its ribosome-associated role in protein folding: an N-terminal region required for interaction with its

heterodimeric partner Ssz1; an adjacent J-domain, a conserved domain found in all J-proteins critical for functional interaction with their Hsp70 partners; and a positively charged RNA-binding region necessary for association with the ribosome (Fiaux et al., 2010; Gautschi et al., 2002; Yan et al., 1998a). The 69 residues at Zuo1's C-terminus ($Zuo1_{365-433}$), on the other hand, have been shown to be sufficient to activate Pdr1-dependent transcription (Eisenman and Craig, 2004; Prunuske et al., 2012).

Evidence indicates that activation of Pdr1 by Zuo1's C-terminus is specific and direct. The Pdr1-related TF Pdr3, though activated by many of the same xenobiotics as Pdr1, is not activated by Zuo1. PDR is not induced by the C-terminus of Zuo1 in a Δ*pdr1* strain, however, suggesting specificity of Zuo1 for the TF Pdr1 (Prunuske et al., 2012). As Zuo1 lacking its charged ribosome-binding region is capable of inducing PDR, it suggests that this transcriptional activation occurs off the ribosome (Eisenman and Craig, 2004). Furthermore, Zuo1's C-terminus has been shown to interact with the nuclear TF Pdr1 in yeast two-hybrid analyses, suggesting a direct role for Zuo1 in PDR activation (Prunuske et al., 2012).

In this work we set out to better understand the means by which Zuo1 activates Pdr1. We found that dissociation of Zuo1 from the ribosome is not sufficient for PDR activation. Rather, the C-terminal 86 residues of Zuo1 form a four-helix bundle that sequesters hydrophobic residues essential for interaction with and activation of Pdr1. Thus, a key to this activation is the unfolding of Zuo1's C-terminal domain, releasing autoinhibition.

Results

The C-terminal 13 residues of Zuo1 are necessary and sufficient for Pdr1 activation

The 69 C-terminal residues of Zuo1 ($Zuo1_{365-433}$) were previously shown to be capable of activating Pdr1. To determine if a smaller region was sufficient for activation, a series of truncation mutants were constructed, starting at residues 388, 403 and 421, and each was fused to a tandem affinity purification (TAP) tag. Cells expressing the control fusion, TAP-$Zuo1_{365-433}$, or one of the truncated constructs were plated on media containing cycloheximide to assess their resistance to this drug as a measure of the induction of the PDR regulon. As expected, cells expressing TAP-$Zuo1_{365-433}$ formed colonies on cycloheximide-containing plates, while those expressing only the TAP tag did not (Figure 3-1A). Cells expressing TAP-$Zuo1_{388-433}$, TAP-$Zuo1_{403-433}$, and TAP-$Zuo1_{421-433}$ grew similarly to those expressing TAP-$Zuo1_{365-433}$, indicating that the 13 most C-terminal residues of Zuo1 are sufficient to induce PDR. To further test the sufficiency of the C-terminal 13 residues, we assessed the ability of the TAP-Zuo1 fusions to activate the transcription of a Pdr1 target gene, *PDR5,* using a *PDR5* promoter-*lacZ* reporter. ß-galactosidase activities in cells expressing TAP-$Zuo1_{421-433}$ or TAP-$Zuo1_{365-433}$ were statistically indistinguishable, 2.7-3.0-fold higher than in cells expressing the TAP tag alone (Figure 3-1A). These results indicate that residues 421 to 433 of Zuo1 are sufficient for PDR activation.

We carried out three additional experiments to determine the necessity and sufficiency of these 13 residues at the C-terminus for activation. First, to confirm that the 13 C-terminal residues are necessary for activation by $Zuo1_{365-433}$, we generated a construct that lacks the codons for these 13 residues, TAP-$Zuo1_{365-420}$. Cells expressing TAP-$Zuo1_{365-420}$ did not form colonies on cycloheximide-containing plates and had ß-galactosidase activity similar to the basal

level found in cells expressing only the TAP tag (Figure 3-1A). Second, we constructed three additional TAP fusions having even smaller segments of the extreme C-terminus of Zuo1, generating TAP-Zuo1$_{425-433}$, TAP-Zuo1$_{428-433}$ and TAP-Zuo1$_{430-433}$. None of these shorter C-terminal fragments were able to support growth on drug-containing plates (Figure 3-1B) even though all fusions were expressed at expected levels (Figure 3-1C). Third, to ensure that sequences in the TAP tag were not contributing to the activity of the shorter fragment by compensating for loss of native residues, we made a construct such that glutathione-S-transferase (GST) was fused to Zuo1$_{421-433}$. Cells expressing GST-Zuo1$_{421-433}$ showed similar growth to those expressing GST-Zuo1$_{365-433}$ on plates containing cycloheximide (data not shown). Thus, we conclude that the extreme C-terminal 13 residues of Zuo1 are both necessary and sufficient for induction of PDR.

To identify residues within the extreme C-terminus required for Pdr1 activation, we performed alanine scanning mutagenesis of the 13 residues shown to be sufficient for activation. Cells expressing either wt TAP-Zuo1$_{365-433}$ or TAP-Zuo1$_{365-433}$ containing one of the 13 alanine point mutations were plated on media containing or lacking cycloheximide (Figure 3-1D). Cells expressing the Leu428, Leu429, Tyr431 or Val433 substitutions did not grow on cycloheximide-containing plates. Those expressing the Pro425 or Phe432 substitutions grew much more slowly than those expressing the wt fusion, even though all fusions were expressed at similar levels (data not shown). Alteration of only one hydrophobic residue, Leu424, was tolerated and alteration of the six other residues had no obvious affect on PDR activation. We, thus, conclude that hydrophobic residues within the extreme C-terminus play critical roles in PDR induction (Figure 3-1E).

Specificity of Zuo1's hydrophobic C-terminus in Pdr1-dependent transcription

The sufficiency of a short peptide at Zuo1's C-terminus and importance of hydrophobic residues in activation of PDR raised the question as to the specificity of activation, as short hydrophobic peptides have been found to act as general transcriptional activators when tethered to DNA. As an initial test of specificity, we asked whether the observed activation of PDR by $Zuo1_{421-433}$ occurred in a Pdr1-dependent manner, as we had previously reported for the longer $Zuo1_{365-433}$ construct (Prunuske et al., 2012). We found that Δ*pdr1* cells expressing TAP-$Zuo1_{421-433}$ showed similar activation of the *PDR5-lacZ* reporter as cells expressing the TAP tag alone (Figure 3-2A), even though the fusion was expressed at similar levels in both wt and Δ*pdr1* strains (data not shown). Next, we compared the transcription activation potential of the C-terminal Zuo1 peptide and two peptides, referred to as P201 (YLLPTCIP) and P223 (YLLPFLPY). These peptides, which have similar sequence composition to $Zuo1_{421-433}$ (SGKLPSSLLSYFV), were originally selected in a screen based on their ability to activate transcription when fused to the DNA binding domain of the TF Gal4 (GBD) (Lu et al., 2000). We, thus, constructed an analogous fusion of GBD to $Zuo1_{421-433}$ and compared its ability to activate the *GAL1* promoter to that of GBD-P201 and GBD-P233. These experiments were carried out in a strain containing a fusion between the *GAL1* promoter and the *HIS3* gene (*Gal1-HIS3*), allowing growth in the absence of histidine as a read-out of transcriptional activation. Unlike cells expressing only GBD, cells expressing any one of the three peptide fusions grew on plates lacking histidine (Figure 3-2B, left panel). We next tested the ability of the fusions to activate transcription in the absence of Pdr1. As we had previously observed with a larger Zuo1 fusion, GBD-$Zuo1_{365-433}$, *pdr1*Δ cells expressing GBD-$Zuo1_{421-433}$ did not grow in the absence of

histidine. GBD-P201 and GBD-P223, on the other hand, activated *Gal1-HIS3* even in the absence of Pdr1 (Figure 3-2B, center panel). This indicates that the transcriptional activation by GBD-Zuo1$_{421-433}$ is Pdr1 dependent, while activation by GBD-P201 and GBD-P233 is not (Figure 3-2C).

Since Zuo1$_{421-433}$ can activate transcription of the PDR regulon when expressed as a TAP tag fusion and not tethered to DNA, as another test of specificity we asked whether cells expressing TAP tag fusions of the hydrophobic P201 and P223 peptides could similarly activate PDR. However, while expression of TAP-Zuo1$_{421-433}$ enabled cells to grow in the presence of cycloheximide, no detectable drug resistance was observed for cells expressing TAP-P201 or TAP-P223 (Figure 3-2B, right panel) even though all fusions were expressed at similar levels (data not shown). Together these data indicate that although activation of Pdr1 by Zuo1 requires a short, hydrophobic peptide, the observed transcriptional activation is distinct from the general transcriptional properties observed previously by hydrophobic peptides tethered to DNA.

Residues 348 to 364 inhibit the ability of Zuo1's C-terminus to activate Pdr1

Since overexpression of full-length Zuo1 does not activate PDR (Eisenman and Craig, 2004), we next carried out experiments to define the minimal sequence sufficient to inhibit the activity of the C-terminus. We began our analysis by creating TAP-tag fusions analogous to those described above extending the N-terminus of the largest known active fragment, TAP-Zuo1$_{365-433}$, by 7 or 17 residues, generating TAP-Zuo1$_{358-433}$ and TAP-Zuo1$_{348-433}$. We then tested the ability of these new constructs to induce drug resistance. While cells expressing TAP-Zuo1$_{365-433}$ grew well on cycloheximide-containing plates, those expressing TAP-Zuo1$_{358-433}$

grew more slowly in the presence of drug (Figure 3-3A). Cells expressing TAP-Zuo1$_{348-433}$, on the other hand, showed no observable drug resistance. We also compared the activity of these three C-terminal fragments using the *PDR5-lacZ* reporter. Results were consistent with the drug resistance assay. Cells expressing TAP-Zuo1$_{365-433}$ had 3.5-fold higher levels of ß-galactosidase than control cells expressing only the TAP tag. However, TAP-Zuo1$_{358-433}$ activated the *PDR5-lacZ* reporter only 2.5-fold and the longer TAP-Zuo1$_{348-433}$ fusion showed no activity over the basal level reported for the TAP tag alone (Figure 3-3A), even though all the fusions were expressed at similar levels (data not shown). This indicates that the presence of residues 348-364 is sufficient to prevent activation of Pdr1 by Zuo1's C-terminus and that both the transcription-activating and predicted autoinhibitory regions of Zuo1 are contained within the last 86 residues of the protein.

Dissociation of Zuo1 from the ribosome is not sufficient for Pdr1 activation

Our previous investigations suggested that activation of Pdr1 occurs by Zuo1 free from its association with ribosomes and that deletion of Zuo1's charged ribosome-binding domain (residues 285-364) is sufficient to activate transcription (Eisenman and Craig, 2004). As the identified inhibitory region (residues 348-364) contains a large proportion of positively charged residues that may contribute to ribosome association, we next tested whether the 348-433 fragment is unable to activate Pdr1 due to an association with the ribosome. To determine the amount of protein free from ribosomes, lysates from cells expressing TAP, TAP-Zuo1$_{365-433}$, TAP-Zuo1$_{358-433}$, or TAP-Zuo1$_{348-433}$ were subjected to ultracentrifugation through sucrose cushions to separate ribosome-bound and unbound populations. Levels of the inactive TAP-

Zuo1$_{348-433}$ fragment in the supernatant (unbound) fraction were comparable to those of the partially active TAP-Zuo1$_{358-433}$ and the active TAP-Zuo1$_{365-433}$ fragments (Figure 3-3B). No binding over background was observed for any of the three fragments in the pellet (ribosome-bound) fraction. This suggests that ribosome association is unlikely to account for the inactivity of Zuo1$_{348-433}$ and that dissociation of Zuo1 from the ribosome is not sufficient for activation. To further test the relationship between ribosome association and the ability of Zuo1 to activate Pdr1, we created a construct of Zuo1 lacking the majority of the charged region but maintaining the residues identified as inhibitory, generating Zuo1$_{\Delta 285-347}$. We then tested this construct both for ribosome association via sucrose gradient centrifugation and for its ability to induce PDR by plating on media containing the drug cycloheximide. As expected, cells expressing full-length Zuo1, the vast majority of which co-migrated with ribosomes, did not grow in the presence of the drug, while cells expressing Zuo1$_{\Delta 285-364}$, which was not ribosome-associated, grew on the drug-containing plates (Figure 3-3C,D). Like Zuo1$_{\Delta 285-364}$, the vast majority of Zuo1$_{\Delta 285-347}$, which maintains the inhibitory residues, did not co-migrate with ribosomes; however, Zuo1$_{\Delta 285-347}$ was not competent to induce PDR, as growth was not observed for cells expressing this construct on plates containing cycloheximide. These data suggest that dissociation of Zuo1 from the ribosome is not sufficient for PDR activation and suggests that an alternative autoinhibitory mechanism may be used to regulate Zuo1's function.

Inactive and active C-terminal fragments differ in both stability and fold

As an initial effort to understand the potential autoinhibition of Zuo1, we initiated biochemical characterization of the inactive and active C-terminal fragments we identified. Since

we were unable to obtain sufficient quantities of $Zuo1_{365-433}$, we compared the partially active $Zuo1_{358-433}$ and the inactive $Zuo1_{348-433}$ fragments. The melting temperatures of $Zuo1_{348-433}$ and $Zuo1_{358-433}$, determined using circular dichroism, were substantially different, 43.5 ºC and 35.5 ºC, respectively (Figure 3-3E), suggesting that truncation of N-terminal residues, which confers partial activity to the C-terminus, also results in a decrease in thermal stability. Analysis of the ^{15}N-^{1}H heteronuclear single quantum coherence (HSQC) NMR spectra of $Zuo1_{348-433}$ revealed chemical shift dispersion and uniform peak intensity consistent with a single folded domain (Figure 3-3F). The ^{15}N-^{1}H HSQC of $Zuo1_{358-433}$, on the other hand, contained approximately twice the number of expected peaks, suggesting the presence of multiple structural populations in this sample. These data indicate that C-terminal fragments of Zuo1 that differ in their *in vivo* activity also show differences in both stability and fold and suggest that a structural transition in Zuo1's C-terminus may be responsible for activation of the protein's transcriptional activity.

Autoinhibited C-terminus is a four-helix bundle

To better understand the proposed structural basis for Zuo1 autoinhibition, we decided to characterize the C-terminal region of Zuo1 at a structural level. To identify the optimal construct for structure determination, we screened a series of additional C-terminal fragments by NMR. Knowing that a fragment shorter than $Zuo1_{348-433}$ was only marginally stable, we generated two longer constructs encoding N-termini extended by 13 or 32 residues compared to that of $Zuo1_{348-433}$. An overlay of the ^{15}N-^{1}H HSQC spectra of these new fragments, $Zuo1_{335-433}$ and $Zuo1_{306-433}$, with that of $Zuo1_{348-433}$ revealed the addition of predominantly random coil peaks (Figure 3-4A), suggesting that these N-terminal extensions do not add any significant structural elements to the

C-terminal domain. Furthermore, no significant chemical shift perturbations were observed between these fragments, suggesting that the structure present in $Zuo1_{348-433}$ is retained upon addition of more native residues. We, thus, chose residues 348-433 as the optimal domain boundaries and determined the solution structure of this domain using an automated procedure for iterative NOE assignment (Table 3-1). This analysis revealed that the autoinhibited C-terminal domain of Zuo1 folds into a left-handed four-helix bundle (Figure 3-4B,C). Residues 348-364, which we identified as being inhibitory to Zuo1's transcriptional activity, form the first helix of the bundle (Figure 3-4B, green) and thus appear to be critical in maintaining C-terminal fold. Residue 358, a buried Ile, is contained in the center of helix I. The fact that truncation of residues N-terminal to Ile358 results in decreased thermal stability highlights the importance of this helix in stability of the domain. The extreme C-terminal peptide, which we identified as both necessary and sufficient for transcriptional activation (Figure 3-4B, purple), is tucked back into the hydrophobic core of the domain. The three most C-terminal residues, Tyr431, Phe432, and Val433, are deeply buried and particularly well constrained, as ^{15}N NOESY data indicated strong NOEs between these residues and a large number of hydrophobic residues in the domain's interior (Figure 3-4D). The importance of these extreme C-terminal residues in maintaining domain structure was confirmed by the observation that the ^{15}N-^{1}H HSQC of a construct lacking the most C-terminal three residues, $Zuo1_{348-430}$, showed poor peak dispersion with the majority of peaks centered around the random coil chemical shift value of ~8.2 ppm, consistent with the protein being in an unfolded conformation (Figure 3-4E). These data suggest that these residues form a C-terminal "plug" that is critical to the fold of the C-terminal helical bundle. The fact that alteration of any of these three terminal residues to alanine also results in either loss of or greatly

diminished PDR activation suggests that residues required for the structural integrity of the domain are also important for activity.

Unfolding of Zuo1's C-terminal domain releases autoinhibition

Since our *in vivo* data indicate that Zuo1 is only fully active in the absence of helix I, which appears to be integral to the fold of the C-terminal domain, we hypothesized that the C-terminus of Zuo1 activates Pdr1 in an unfolded conformation and that C-terminal structure may be the cause of autoinhibition. To test this idea, we first compared the ^{15}N-^{1}H HSQC spectra of the inactive $Zuo1_{348-433}$ and the partially active $Zuo1_{358-433}$ fragments to look for any indication of differences in protein conformation that might explain their difference in activity. An overlay of these two spectra revealed that the two samples show a very similar pattern of dispersed peaks (Figure 3-5A), suggesting that the structured protein present in the partially active $Zuo1_{358-433}$ sample is similar in conformation to that of the inactive $Zuo1_{348-433}$ fragment. The additional peaks observed in the $Zuo1_{358-433}$ sample appear to be predominantly clustered around the random coil chemical shift value, suggesting that a significant population of unfolded protein is present in the sample. The few significant perturbations in chemical shifts observed in the dispersed regions of the ^{15}N-^{1}H HSQC spectra map to the loop region in direct contact with helix I (data not shown), suggesting that these differences are likely attributable to the presence/absence of the N-terminal ten residues rather than to a global conformational change in protein structure. We, thus, conclude that the difference in activity observed between these fragments is likely due to differences in the amount of the folded form of the protein present and

suggest that activation of Zuo1 may represent a transition between the folded and unfolded conformation of the C-terminal domain.

Secondly, we reasoned that if residues important for activity are also required to maintain C-terminal fold, then unfolding of Zuo1's C-terminal domain might be sufficient to cause activation of Pdr1 *in vivo*. To test this, we designed two constructs encoding amino acid alterations in the inactive TAP-Zuo1$_{348\text{-}433}$ construct aimed at destabilizing the fold of the domain (Figure 3-5B): (1) the buried hydrophobic residue, Leu411, was replaced with the charged residue Arg, generating TAP-Zuo1$_{348\text{-}433\ L/R,}$ and (2) Lys351 and Lys355 were replaced with Pro, with the goal of preventing helix I from folding properly, generating TAP-Zuo1$_{348\text{-}433\ K/P.}$ To experimentally determine whether these alterations disrupted protein fold, we analyzed the ^{15}N-^{1}H HSQC spectra of these variants. The spectra of both Zuo1$_{348\text{-}433\ L/R}$ and Zuo1$_{348\text{-}433\ K/P}$ showed poor peak dispersion, with the majority of peaks clustered around the random coil chemical shift value (Figure 3-5C), indicating that these amino acid alterations were sufficient to prevent folding of the C-terminal domain. The activity of these two variants was then tested *in vivo* for their ability to induce PDR. Both were competent to render cells resistant to cycloheximide (Figure 3-5D). We next wanted to determine if the autoinhibition of full-length Zuo1 could similarly be alleviated by unfolding of its C-terminus. To test this, we generated a construct to overexpress full-length Zuo1 containing the L/R alteration (Zuo1$_{L/R}$) and tested the ability of cells expressing this variant to induce PDR. Cells expressing Zuo1$_{L/R}$ were able to grow in the presence of cycloheximide, while cells expressing Zuo1 without the alteration did not (Figure 3-5D) even though both were expressed at similar levels (Figure 3-5E). Together these data

support the idea that access to the unfolded state of Zuo1's C-terminus is required for activation of its Pdr1-stimulatory ability.

Residues required for interaction with Pdr1 are sequestered in the structured C-terminus

Having identified this correlation between protein unfolding and activity, we next wanted to determine if unfolding of Zuo1's C-terminal domain was necessary for its ability to interact with Pdr1. To test this, we made use of our modified yeast two-hybrid assay with which we previously demonstrated that a fusion between GBD and $Zuo1_{365-433}$ auto-activated *GAL* promoters in a Pdr1-dependent manner (Prunuske et al., 2012). To test whether a correlation existed between the unfolding we observed *in vitro* and interaction with Pdr1 based on this *in vivo* assay, we generated constructs to express GBD fusions of the longer C-terminal fragments, $Zuo1_{348-433}$ and $Zuo1_{358-433}$, analogous to those described above. The ability of the fragments to auto-activate the *GAL1-HIS3* reporter was compared to GBD-$Zuo1_{365-433}$ by monitoring the ability of cells expressing the GBD fusions to grow in the absence of histidine. Cells expressing GBD-$Zuo1_{365-433}$ showed the most robust growth of the three constructs in the absence of histidine (Figure 3-6A). On the other hand, cells expressing GBD fused to $Zuo1_{348-433}$, the fragment that showed stable fold *in vitro* and no induction of PDR, similarly did not form colonies on media lacking histidine, though expressed at expected levels (data not shown). Cells expressing the fusion of GBD to $Zuo1_{358-433,}$ the fragment that showed a mixture of folded and unfolded conformations *in vitro* and an intermediate growth phenotype on drug-containing plates, also formed colonies, but grew more poorly than cells expressing the shorter GBD-$Zuo1_{365-433}$ fusion. Thus, the ability of these GBD-Zuo1 C-terminal fusions to interact with Pdr1,

based on this *in vivo* assay, occurred in a manner consistent with their ability to activate PDR and with the degree of the unfolded form of the protein present in *in vitro* preparations. To further test the idea that C-terminal unfolding is required for this interaction, we generated a GBD-Zuo1$_{348-433}$ fusion containing the destabilizing L/R mutation. Cells expressing this variant grew as well as those expressing GBD-Zuo1$_{365-433}$ on media lacking histidine (Figure 3-6A). These data suggest that unfolding of Zuo1's C-terminal domain is required for interaction with Pdr1.

We next wanted to determine which of the hydrophobic residues in the extreme C-terminus we identified as important for activation of PDR by Zuo1 were specifically required for interaction with Pdr1. To test this, we performed an alanine scan of the 13 most C-terminal residues using the GBD-Zuo1$_{365-433}$ fusion. Cells expressing the altered C-terminal fusions were tested for their ability to grow in the absence of histidine and adenine in the media to test for activation of the *Gal1-HIS3* and *Gal2-ADE2* reporters, respectively. Cells expressing GBD-Zuo1$_{365-433}$ in which any of the seven hydrophobic residues in the extreme C-terminus (Leu424, Pro425, Leu428, Leu429, Tyr431, Phe432, or Val433) were altered showed no growth in the absence of histidine or adenine (Figure 3-6B), even though all fusions were expressed at similar levels (Figure 3-6C). Alteration of any of the polar or charged residues, on the other hand, showed no difference in activity. The importance of the extreme C-terminal 13 residues of Zuo1 for interaction with Pdr1 were further confirmed by the observation that a construct lacking codons for the most C-terminal 13 residues (GBD-Zuo1$_{365-420}$) was unable to activate the *GAL* reporters (Figure 3-6B). This analysis suggests that Zuo1 utilizes hydrophobic residues, which are sequestered in the folded C-terminal helical bundle, to interact with the transcription factor Pdr1 upon unfolding of this domain (Figure 3-6D, orange).

Discussion

Our *in vivo* and *in vitro* data reported here are consistent with a pathway of activation of Pdr1 by residues in the extreme C-terminus of Zuo1 that are normally sequestered within a folded domain, with their transcriptional activation potential unleashed upon unfolding. Several lines of evidence indicate that the structured four-helix bundle formed by the C-terminal 86 residues transitions to an open, unfolded state rendering Zuo1 competent to activate Pdr1. Only constructs of Zuo1's C-terminus that lack part or all of the first helix of the bundle, which structural and biochemical analyses indicate is integral to the domain's structure, are competent to activate the PDR pathway *in vivo.* Residues in the extreme C-terminus identified as critical for both activation of and interaction with Pdr1 are predominantly buried in the hydrophobic core of the domain and thus inaccessible in the folded conformation. As deletion of three of these critical residues at the extreme C-terminus resulted in global unfolding of the helical bundle, it is likely that exposure of these key residues would require unfolding of the C-terminal domain. Although, to our knowledge there are few, if any, analogous examples of an unfolding requirement of a protein to activate a transcription factor, unfolding as a mode of positive regulation certainly has precedents. Perhaps best known is the case of N-WASP, which, in its structured form, sequesters key hydrophobic residues required for binding to the Arp2/3 complex (Panchal et al., 2003).

While the C-terminal 86 residues of Zuo1 are required for formation of the four-helix bundle, the C-terminal 13 residues are sufficient for activation, with the hydrophobic amino acids being critical for activity. Although short, hydrophobic peptides have been identified as recruiters of the general transcription machinery (Lu et al., 2002; Wu et al., 2003), Zuo1's C-terminus appears to activate transcription specifically through Pdr1. This dependence on Pdr1 for

Zuo1's transcriptional activation occurs whether activating native Pdr1-dependent promoters or activating other genes when tethered there by a DNA-binding domain. This specificity is consistent with previously reported microarray data indicating that the PDR regulon is the major class of genes upregulated by the C-terminus of Zuo1 (Prunuske et al., 2012). Together these data support a model in which Zuo1's C-terminal hydrophobic peptide interacts directly with Pdr1, leading to mobilization of its activation domain thought to be sequestered by its central inhibitory region. Such a mode of activation is analogous to the direct binding of xenobiotics observed for both yeast and mammalian transcription factors in pleiotropic drug resistance (Kliewer et al., 2002; Thakur et al., 2008; Willson and Kliewer, 2002).

Overall, the data presented here point to a pathway, rather than a single event, required for activation of Zuo1's function in transcriptional regulation. Limited earlier analyses suggested that Zuo1 dissociating from the ribosome might be sufficient for PDR activation, as deletion of the RNA-binding domain necessary for Zuo1's association with the ribosome resulted in induction of the PDR regulon (Eisenman and Craig, 2004). The studies presented here, however, reveal that this deletion removed not only sequences necessary for ribosome binding, but also sequences comprising one of the alpha helices critical for formation of the autoinhibitory four-helix bundle. As all data collected thus far point to a model in which Zuo1 activates Pdr1 via a direct mechanism, it is likely that dissociation from the ribosome is one step in this activation process. However, these data indicate that this is not sufficient for activation of Pdr1 by Zuo1.

The data presented here raise the critical question of what triggers the unfolding of Zuo1's C-terminal domain. Though our results do not directly address this question, it is interesting that even the most stable C-terminal fragment of Zuo1 tested showed low thermally

stability, suggesting that little energy may be required to shift the domain to an unfolded state and expose these critical residues. However, the fact that full-length Zuo1, even when overexpressed, does not activate Pdr1 suggests that active unfolding of this domain may be necessary. It is conceivable that Zuo1 is bound by a yet to be identified adapter protein that stabilizes the unfolded form of the protein or displaces its extreme C-terminal peptide. A potential candidate for this type of binding might be a PDZ domain-containing protein, as ligands of PDZ domains are often short peptides of bulky hydrophobic residues located at the extreme C-termini of proteins. Proteins containing these domains often function as adapter proteins that mediate the assembly of cell signaling complexes (Harris and Lim, 2001). The fact that global unfolding of the C-terminal domain, rather than a more subtle conformational change, appears to be required to expose its critical residues, binding or modification of the helical bundle in a region other than the extreme C-terminus could also facilitate activation by destabilizing overall domain structure. This type of mechanism is illustrated by the activation of N-WASP, in which binding of Cdc42 to the GTPase-binding domain releases autoinhibition by destabilizing domain structure and displacing the hydrophobic VCA peptide required for binding and activation of the Arp2/3 complex (Panchal et al., 2003).

A hyperactive allele of Zuo1's C-terminus has been identified, S427G. Although one might hypothesize that such an allele destabilizes the four-helix bundle, this residue is surface exposed and alteration to glycine does not affect the folding:unfolding dynamics (Appendix Figure A-6). We think it is more likely that this alteration plays either an indirect role in unfolding by affecting interaction with an adaptor protein or affecting the potency of the interaction with Pdr1. The latter idea is supported by the observation that Zuo1's C-terminus

with this alteration interacts more strongly with Pdr1 in the yeast two-hybrid system (Prunuske et al., 2012).

It also must be remembered that Zuo1 is in a complex with the atypical Hsp70 Ssz1. Ssz1, when not ribosome associated, is also capable of activating PDR and, like Zuo1, interacts with Pdr1 in the two-hybrid system (Eisenman and Craig, 2004; Prunuske et al., 2012). Thus, it is likely that these two proteins act in concert as a heterodimer to activate Pdr1. Further work will be necessary to understand the dynamics of this heterodimer and the balance between its ribosomal function in protein folding and its role in extra-ribosomal cellular signaling. The data shown here provide initial structural insights into this regulation, presenting a model in which Zuo1's activity in Pdr1-dependent transcriptional activation is regulated by autoinhibition conferred by C-terminal structure with activity being induced upon a folding:unfolding transition of its helical bundle domain.

Figures, Tables, and Legends

Figure 3-1. A hydrophobic peptide at the extreme C-terminus of Zuo1 is necessary and sufficient for PDR activation. (A-C) Residues 421-433 are necessary and sufficient for activity. Cells were transformed with vector containing DNA encoding a tandem affinity purification tag (TAP) alone (-) or TAP fused to the indicated fragments of the C-terminus of Zuo1. (A) Serial dilutions of wild-type (wt) cells transformed with the indicated plasmids were spotted onto media without (-) or with (+) cycloheximide. Cells containing an integrated *PDR5-lacZ* reporter were transformed with the indicated plasmids and ß-galactosidase activity was measured. The average activity of 3 transformants of each was quantified and reported in Miller units with error bars indicating standard error. (B) Serial dilutions of wt cells harboring the indicted plasmids were performed as described in A. (C) Cell extracts were prepared from cultures used for serial dilutions in A and B and subjected to immunoblot analysis using rabbit IgG to detect the TAP-tagged Zuo1 fusions. (D) Hydrophobic residues are critical for activity. Cells were transformed with vector containing DNA encoding TAP (-) or TAP fused to wt $Zuo1_{365-433}$ (wt) or $Zuo1_{365-433}$ containing one of the 13 alanine point mutations and plated onto media without (-) or with (+) cycloheximide. (E) Sequence of the C-terminal 69 residues of Zuo1 with arrows indicating the starting residue for each of the truncated constructs tested in A and B. Residues sufficient for activation are boxed and residues important for activity as determined by loss of activity upon substitution with alanine are colored in red.

Figure 3-1

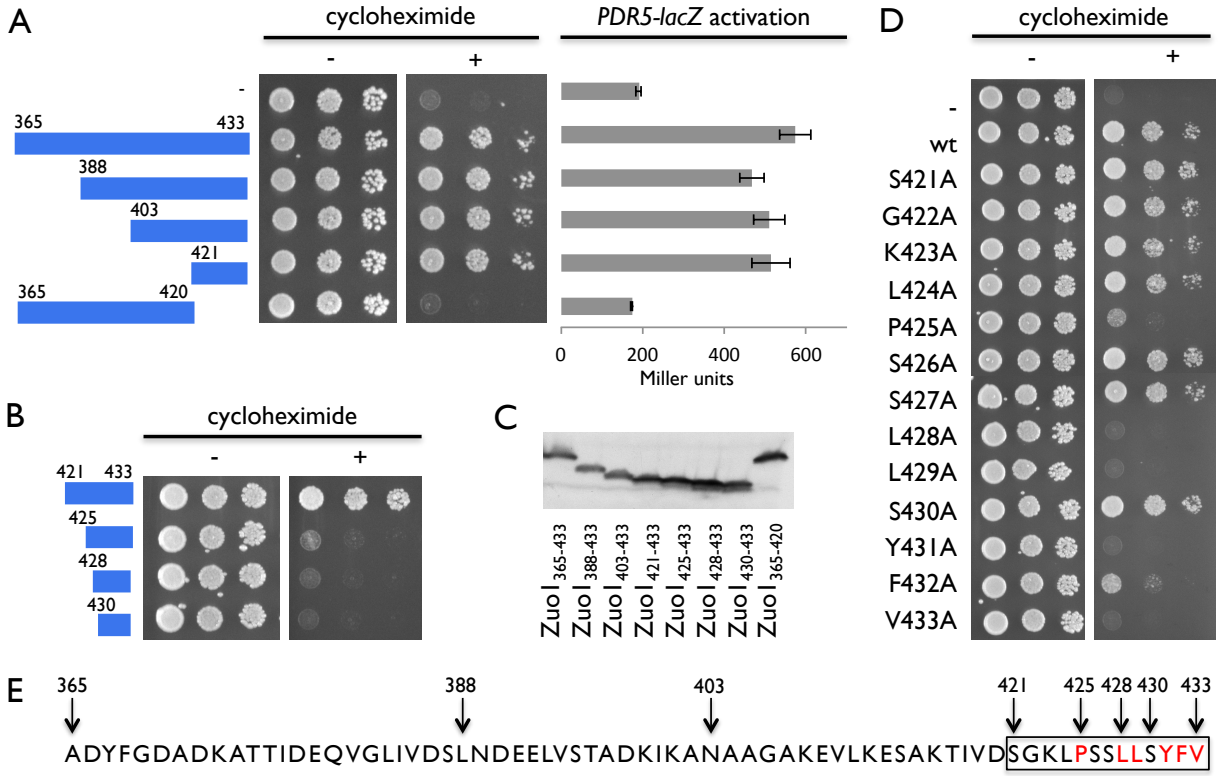
A
cycloheximide
PDR5-lacZ activation
-
+
365
433
388
403
421
365
420
0
200
400
600
Miller units
B
cycloheximide
421
433
425
428
430
C
Zuo 365-433
Zuo 388-433
Zuo 403-433
Zuo 421-433
Zuo 425-433
Zuo 428-433
Zuo 430-433
Zuo 365-420
D
cycloheximide
wt
S421A
G422A
K423A
L424A
P425A
S426A
S427A
L428A
L429A
S430A
Y431A
F432A
V433A
E
365
388
403
421
425
428
430
433
ADYFGDADKATTIDEQVGLIVDSLNDEELVSTADKIKANAAGAKEVLKESAKTIVDSGKLPSSLLSYFV

Figure 3-2. Specificity of Zuo1's hydrophobic C-terminus in Pdr1-dependent transcriptional activation. (A) Wt or Δ*pdr1* cells containing an integrated *PDR5-lacZ* reporter were transformed with vector DNA encoding TAP or TAP fused to Zuo1's C-terminal 13 residues ($Zuo1_{421-433}$). The ß-galactosidase activity of 3 transformants of each was quantified and reported in Miller units with error bars indicating standard error. (B) Comparison of the requirement for Pdr1 for transcriptional activation by hydrophobic peptides. (left and center panels) Wt or Δ*pdr1* cells containing an integrated *Gal1-HIS3* reporter were transformed with DNA encoding the Gal4 DNA binding domain (GBD) alone (-) or GBD fused to either $Zuo1_{421-433}$ or the indicated peptides. Cells containing the indicated plasmids were spotted in serial dilutions onto media with (+) or without (-) histidine. (right panel) Wt cells were transformed with DNA encoding TAP (-) or TAP fused to the indicated peptides and spotted in serial dilutions onto media without (-) or with (+) cycloheximide. (C) Model of Pdr1-dependent transcriptional activation by GBD-$Zuo1_{421-433}$ and Pdr1-independent activation by GBD-P201/P223.

Figure 3-2

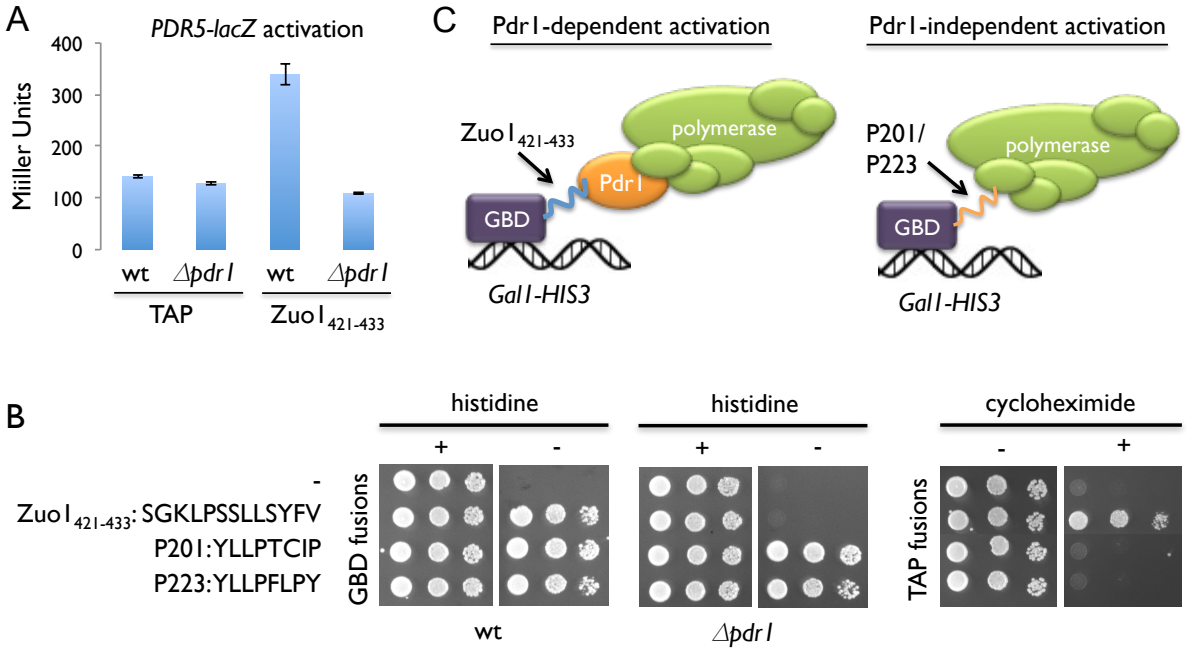
A
PDR5-lacZ activation
Miiller Units
400
300
200
100
0
wt
Δpdr1
wt
Δpdr1
TAP
Zuo1 421-433
C
Pdr1-dependent activation
Zuo1 421-433
polymerase
Pdr1
GBD
Gal1-HIS3
Pdr1-independent activation
P201/
P223
polymerase
GBD
Gal1-HIS3
B
histidine
histidine
cycloheximide
+
-
+
-
-
+
-
Zuo1 421-433: SGKLPSSLLSYFV
P201:YLLPTCIP
P223:YLLPFLPY
GBD fusions
TAP fusions
wt
Δpdr1

Figure 3-3. The last 86 residues of Zuo1 are sufficient for autoinhibition. (A) Residues 348-433 are sufficient for autoinhibition. Cells were transformed with vector containing DNA encoding TAP (-) or TAP fused to the indicated fragments of the C-terminus of Zuo1. Serial dilutions of wt cells harboring the indicated plasmids were spotted onto media without (-) or with (+) cycloheximide. ß-galactosidase activity was measured for cells containing an integrated *PDR5-lacZ* reporter and transformed with the indicated plasmids. The average activity of 3 transformants of each was quantified and reported as fold activation of cells expressing TAP alone (TAP fusion/TAP). (B-D) Ribosome disassociation is not sufficient for activation. (B) Lysates of Δ*zuo1* cells expressing either TAP (-) or TAP fused to the indicated Zuo1 C-terminal fragments were centrifuged through a sucrose cushion to separate the ribosome-containing fraction (pellet) from the unbound fraction (sup). Equivalent amounts of each fraction were subjected to immunoblot analysis using rabbit IgG to detect the TAP-tagged fusions. (C-D) Wt or Δ*zuo1* cells were transformed with plasmid DNA encoding Zuo1 or the indicated Zuo1 variants under control of the endogenous *ZUO1* promoter. (C) Lysates of Δ*zuo1* cells harboring the indicated plasmids were separated on a 5-50% sucrose gradient and fractions were collected and subjected to immunoblot analysis using an antibody specific to Zuo1. The migration of ribosomal subunits was monitored by absorbance at 254 nm and plotted versus the time course of fraction collection. (D) Serial dilutions of wt cells harboring the indicated plasmids were spotted onto media without (-) or with (+) cycloheximide. (E-F) Inactive and active C-terminal fragments differ in fold and stability. (E) Circular dichroism thermal melting curves of the inactive $Zuo1_{348-433}$ fragment (blue) and the partially active $Zuo1_{358-433}$ fragment (red) collected at 222nm. (F) Two-dimensional ^{15}N–^{1}H HSQC spectra of $Zuo1_{348-433}$ and $Zuo1_{358-433}$.

Figure 3-3

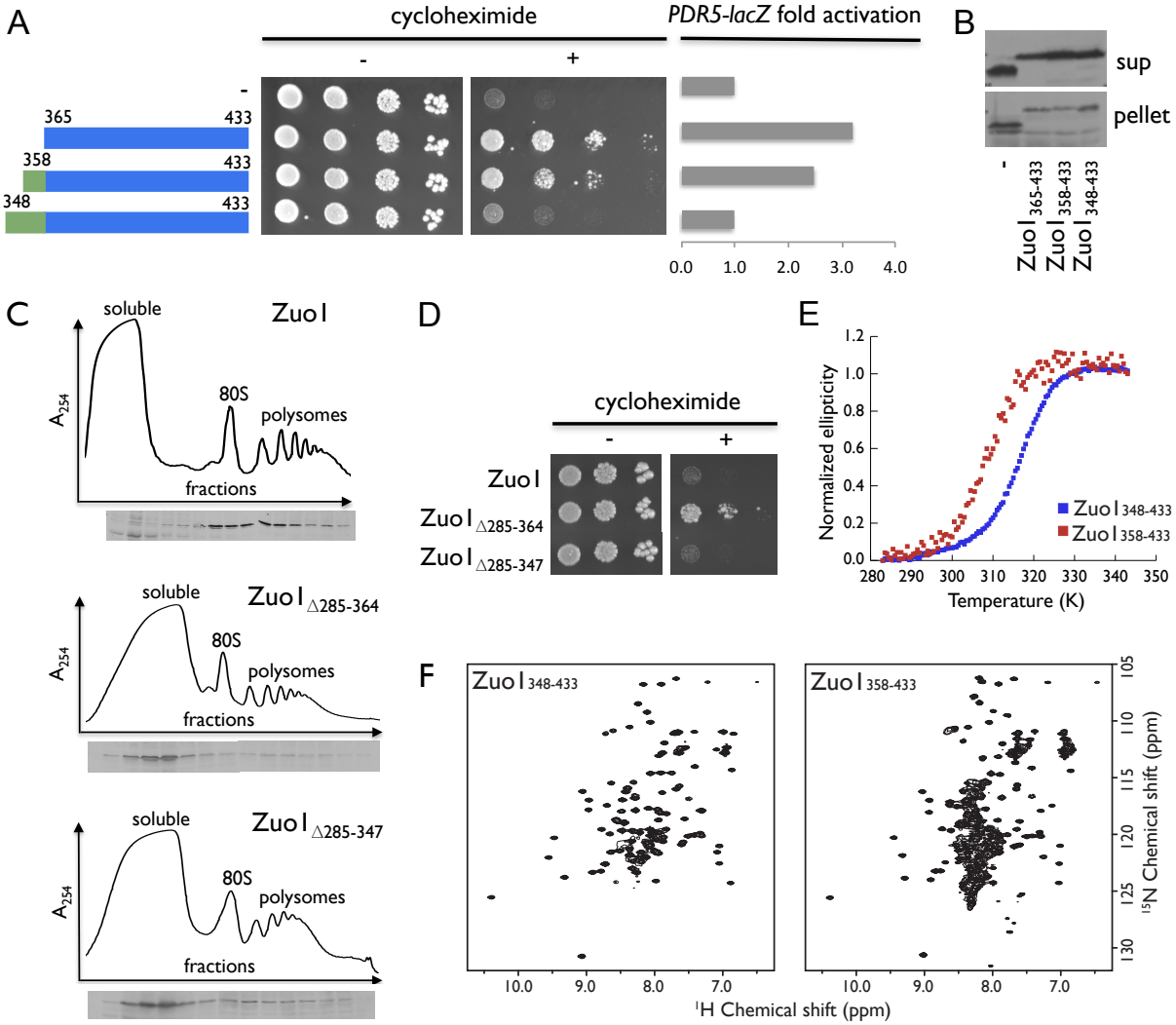
A
cycloheximide
PDR5-lacZ fold activation
-
+
365
433
358
433
348
433
0.0
1.0
2.0
3.0
4.0
B
sup
pellet
-
Zuo1 365-433
Zuo1 358-433
Zuo1 348-433
C
soluble
Zuo1
80S
polysomes
fractions
A254
Zuo1 △285-364
Zuo1 △285-347
D
cycloheximide
Zuo1
Zuo1 △285-364
Zuo1 △285-347
E
Normalized ellipticity
Temperature (K)
Zuo1 348-433
Zuo1 358-433
F
Zuo1 348-433
Zuo1 358-433
1H Chemical shift (ppm)
15N Chemical shift (ppm)

Figure 3-4. Structure of the autoinhibited C-terminal domain of Zuo1. (A) Overlay of the $^{15}N–^{1}H$ HSQC spectra of Zuo1 residues 348-433 (black), 335-433 (magenta), and 306-433 (orange). (B) Ribbon diagram of the solution structure of the four-helix bundle formed by the C-terminal 86 residues (348-433) of Zuo1. Residues 348-364, which inhibit C-terminal activity, are shown in green and residues 421-433, which are necessary and sufficient for activity, are shown in purple. (C) Stereo diagram of the Cα trace of the ensemble of the final 20 NMR structures. (D-E). The extreme C-terminal three residues are required for domain structure. (D) The three most C-terminal residues, Tyr431, Phe432, and Val433 (cyan), are well constrained in the hydrophobic core of the domain, as indicated by the large number of NOEs observed between these and surrounding residues, which are shown in orange. (E) Two-dimensional $^{15}N–^{1}H$ HSQC spectra of Zuo1 lacking the three most C-terminal residues ($Zuo1_{348-430}$).

Figure 3-4

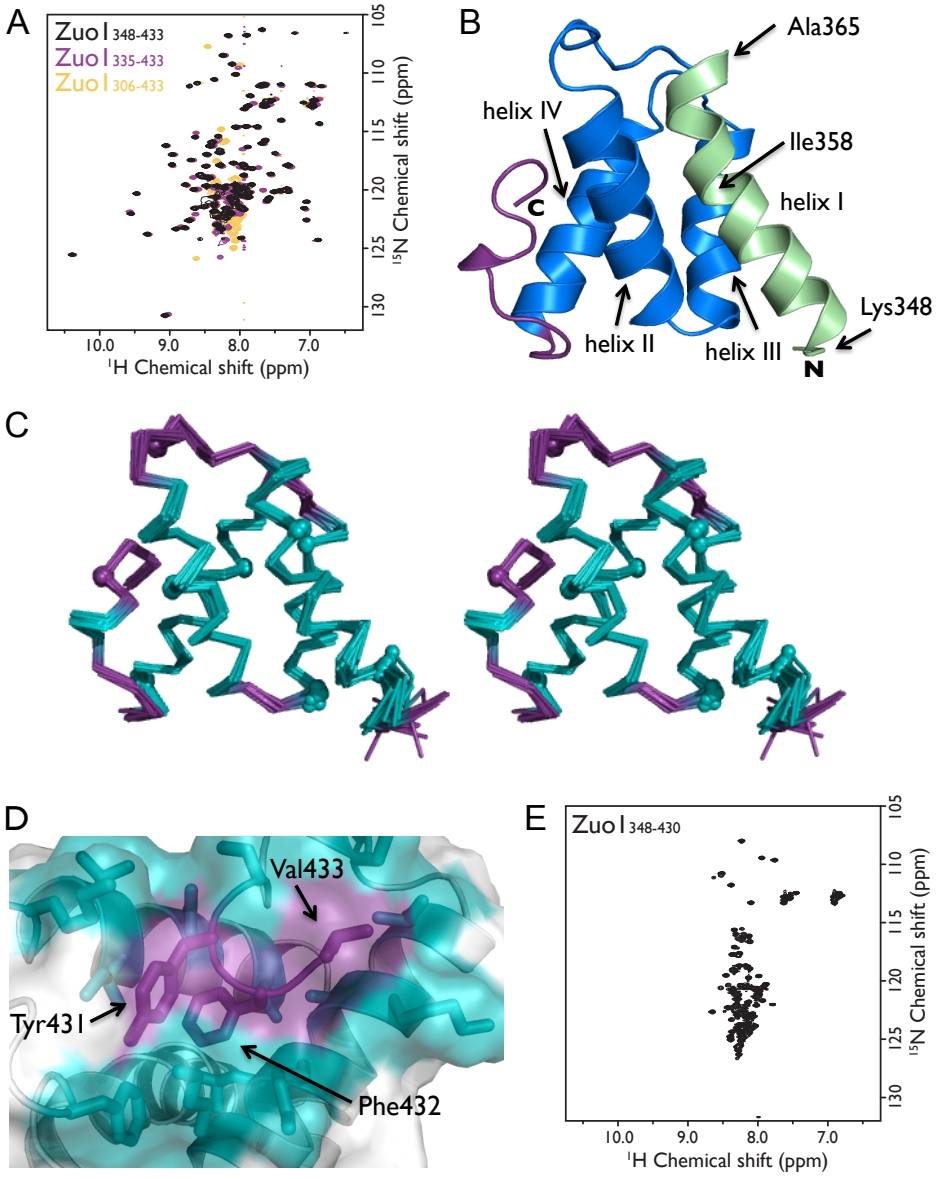
A
Zuo1 348-433
Zuo1 335-433
Zuo1 306-433
105
110
115
120
125
130
15N Chemical shift (ppm)
10.0
9.0
8.0
7.0
1H Chemical shift (ppm)
B
Ala365
helix IV
Ile358
helix I
C
helix II
helix III
Lys348
N
C
D
Val433
Tyr431
Phe432
E
Zuo1 348-430
105
110
115
120
125
130
15N Chemical shift (ppm)
10.0
9.0
8.0
7.0
1H Chemical shift (ppm)

Figure 3-5. Unfolding of Zuo1's C-terminal domain releases autoinhibition. (A) Overlay of the ^{15}N–^{1}H HSQC spectra of the inactive $Zuo1_{348-433}$ (cyan) and partially active $Zuo1_{358-433}$ (orange) C-terminal fragments. (B) Ribbon diagram of a portion of the C-terminal domain with side chains of residues predicted to disrupt domain structure indicated. (C) ^{15}N–^{1}H HSQC spectra of $Zuo1_{348-433}$ containing a Leu411 to Arg (L/R) alteration or an alteration of Lys351 and Lys355 to Pro (K/P). (D) Wt cells were transformed with DNA encoding TAP tag fusions of $Zuo1_{348-433}$ or $Zuo1_{348-433}$ with the indicated mutations or full-length Zuo1 or Zuo1 with the L/R mutation under control of the *GPD* promoter. Serial dilutions of cells containing the indicated plasmids were spotted onto media without (-) or with (+) cycloheximide. (E) Cell extracts were prepared from cultures used for serial dilutions in D and subjected to immunoblot analysis using rabbit IgG to detect TAP-tagged Zuo1 fusions, an antibody specific to Zuo1 to recognize full-length Zuo1, or an antibody specific to Ssc1 as a loading control.

Figure 3-5

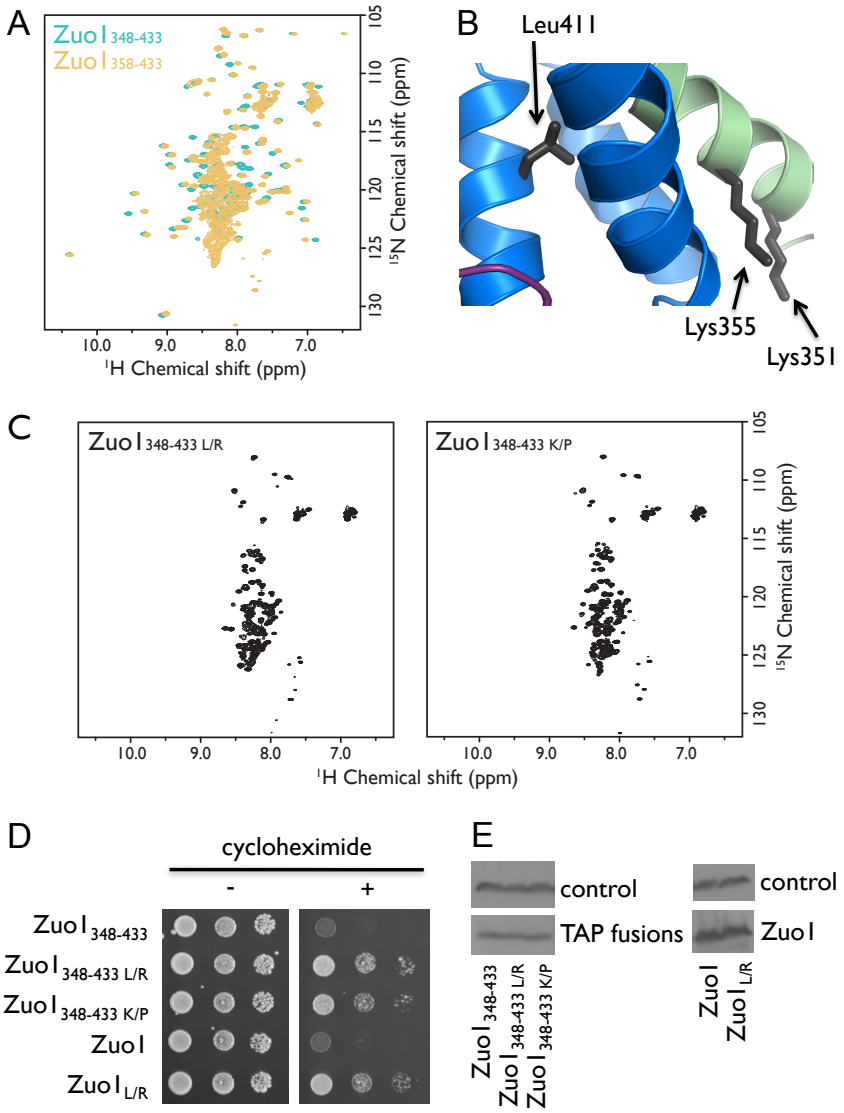
A
Zuo1 348-433
Zuo1 358-433
105
110
115
120
125
130
15N Chemical shift (ppm)
10.0
9.0
8.0
7.0
1H Chemical shift (ppm)
B
Leu411
Lys355
Lys351
C
Zuo1 348-433 L/R
Zuo1 348-433 K/P
105
110
115
120
125
130
15N Chemical shift (ppm)
10.0
9.0
8.0
7.0
1H Chemical shift (ppm)
D
cycloheximide
-
+
Zuo1 348-433
Zuo1 348-433 L/R
Zuo1 348-433 K/P
Zuo1
Zuo1 L/R
E
control
TAP fusions
Zuo1 348-433
Zuo1 348-433 L/R
Zuo1 348-433 K/P
control
Zuo1
Zuo1
Zuo1 L/R

Figure 3-6. Residues required for interaction with Pdr1 are sequestered in the structured C-terminal domain. (A-C) Modified yeast two-hybrid. Cells containing an integrated *Gal1-HIS3* and *Gal2-ADE2* reporter were transformed with DNA encoding GBD (-) or GBD fused to the indicated fragments of the C-terminus of Zuo1. (A) Correlation between protein fold, PDR induction, and interaction with Pdr1. Cells containing the indicated plasmids were spotted in serial dilutions onto media with (+) or without (-) histidine to detect auto-activation of the *Gal1-HIS3* reporter. The chart refers to PDR induction data shown in Figures 3-3A and 3-5D and *in vitro* folding data shown in Figures 3-3F and 3-5C. (B) Alanine scan. Cells containing the indicated plasmids were spotted in serial dilutions onto media with (+) or without (-) histidine and adenine to detect auto-activation of *Gal1-HIS3* and *Gal2-ADE2* reporters. (C) Cell extracts were prepared from cultures used for serial dilutions in B and subjected to immunoblot analysis using an antibody specific to GBD (Millipore) or an antibody specific to Ssc1 as a loading control. (D) Residues important for interaction with Pdr1 are buried in the folded C-terminal domain. Residues important for interaction, as determined by loss of activity upon alteration to alanine as described in B, are indicated in orange. Residues that had no effect on activity when changed to alanine are shown in magenta.

Figure 3-6

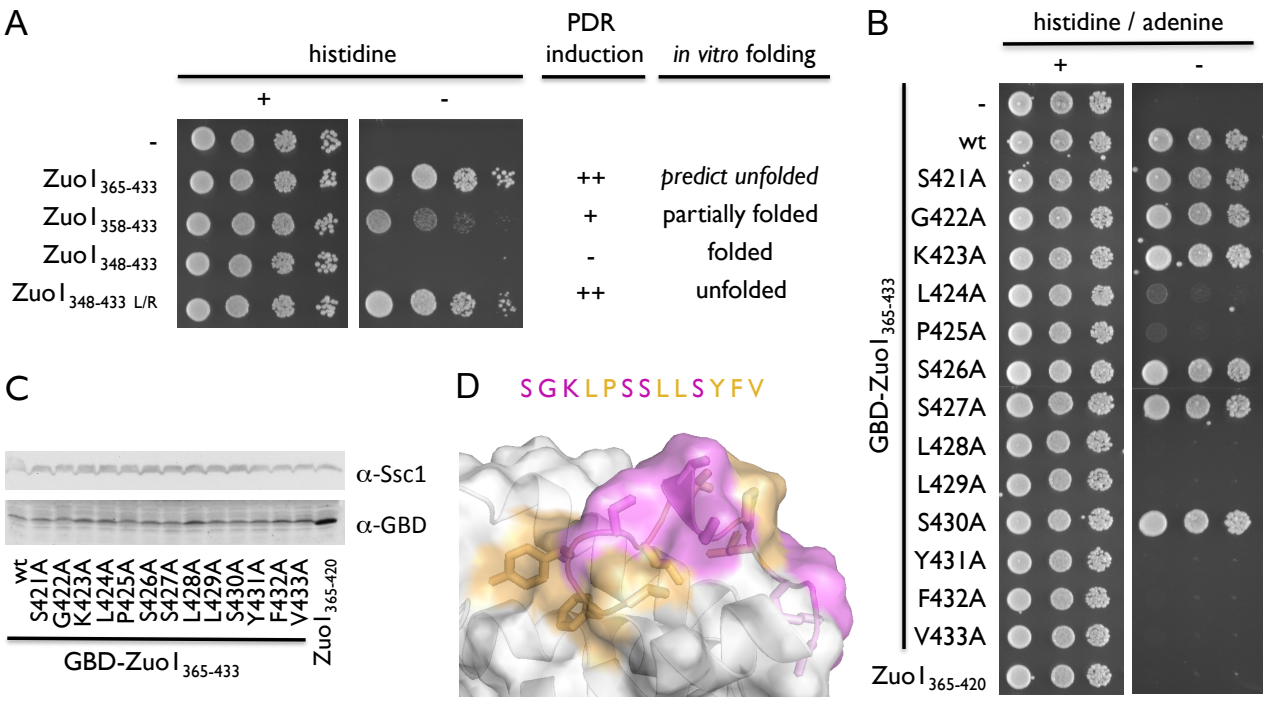
A
histidine
+
-
PDR induction
in vitro folding
-
Zuo1 365-433
Zuo1 358-433
Zuo1 348-433
Zuo1 348-433 L/R
++
predict unfolded
+
partially folded
-
folded
++
unfolded
B
histidine / adenine
+
-
GBD-Zuo1 365-433
-
wt
S421A
G422A
K423A
L424A
P425A
S426A
S427A
L428A
L429A
S430A
Y431A
F432A
V433A
Zuo1 365-420
C
α-Ssc1
α-GBD
wt
S421A
G422A
K423A
L424A
P425A
S426A
S427A
L428A
L429A
S430A
Y431A
F432A
V433A
Zuo1 365-420
GBD-Zuo1 365-433
D
S G K L P S S L L S Y F V

Table 3-1. NMR and refinement statistics for the 20 Zuo1 conformers

Experimental constraints		
Distance constraints		
Long		318
Medium [1<(i–j)≤5]		463
Sequential [(i–j)=1]		272
Intraresidue [i=j]		418
Total		1471
Dihedral angle constraints (ϕ and ψ)		148
Average atomic RMSD to the mean structure (Å)		
Residues 349-433		
Backbone (C^{α}, C′, N)		0.44 ± 0.08
Heavy atoms		0.87 ± 0.06
Deviations from idealized covalent geometry		
Bond lengths (Å)		0.014
Torsion angles (°)		1.2
Constraint violations		
NOE distance	Number > 0.3 Å	0.00 ± 0.00
NOE distance	RMSD (Å)	0.021 ± 0.001
Torsion-angle violations	Number > 5 °	0.00 ± 0.00
Torsion-angle violations	RMSD (°)	0.456 ± 0.062
WHATCHECK quality indicators		
Z-score		2.90 ± 0.14
RMS Z-score		
Bond lengths		0.62 ± 0.02
Bond angles		0.58 ± 0.03
Bumps		0.00 ± 0.00
Lennard-Jones energy[c] (kJ mol^{-1})		-1,694 ± 72
Ramachandran statistics (% of all residues)		
Most favored		91.9 ± 1.5
Additionally allowed		6.6 ± 1.5
Generously allowed		0 ± 0
Disallowed		1.5 ± 0.6

Materials and Methods

Yeast strains and plasmids

Yeast strains used were isogenic with DS10 and contain the following mutations: *his3-11,15 leu2-3,112 lys1 lys2 trp1*Δ *ura3-52*. Δ*zuo1::HIS3* (Hundley et al., 2002) and Δ*pdr1::TRP1* (Prunuske et al., 2012) have been described previously. A strain containing an integrated *PDR5-lacZ* reporter was created by digesting the pTH120 plasmid containing *PDR5-lacZ::HIS3* (Hallstrom et al., 1998) with StuI and transforming the resulting fragment into DS10 wt or Δ*pdr1::TRP1* to direct integration at the *PDR5* locus.

TAP and TAP-Zuo1$_{365-433}$ (TAP-ZuoC) plasmids were described previously (Prunuske et al., 2012). TAP-Zuo1$_{348-433}$ and TAP-Zuo1$_{358-433}$ were created by amplifying codons for the corresponding residues by PCR and cloning into pRS415-GPD using BamHI and PstI. TAP-Zuo1$_{388-433}$, TAP-Zuo1$_{403-433}$, and TAP-Zuo1$_{421-433}$ were created using QuickChange to delete the codons for the truncated residues from TAP-Zuo1$_{365-433}$. A similar approach was used to create TAP-Zuo1$_{425-433}$, TAP-Zuo1$_{428-433}$ and TAP-Zuo1$_{430-433}$ using TAP-Zuo1$_{421-433}$ as a template. GST-Zuo1$_{421-433}$ was created by deleting the codons for residues 365-420 from 316-GAL1-GST-Zuo1$_{365-433}$ (Eisenman and Craig, 2004) using QuickChange. TAP-Zuo1$_{365-420}$ was created using QuickChange to introduce a stop codon after the codon for residue 420. Alanine point mutants were introduced into TAP-Zuo1$_{365-433}$ using QuickChange. The L/R and K/P mutations were introduced into TAP-Zuo1$_{348-433}$ or pRS416-GPD-Zuo1 using QuickChange to mutate the codon for Leu411 to code for Arg (L/R) or the codons for Lys351 and Lys355 to code for Pro (K/P). Zuo1$_{\Delta 285-347}$ and Zuo1$_{\Delta 285-364}$ were created using QuickChange to delete the codons for the corresponding residues from pRS316-Zuo1 (Yan et al., 1998a).

Assays for PDR induction

To assay drug resistance, approximately equal numbers of cells were subjected to 10-fold serial dilutions and spotted on selective minimal glucose media containing 0, 0.7 or 1 µg/ml cycloheximide. Plates were incubated at 30°C for 2-3 days before photographing. β-galactosidase assays were performed as previously described (Eisenman and Craig, 2004) using cells containing an integrated *PDR5-lacZ* reporter. A minimum of three independent transformants was tested and the average activity determined.

Analysis of ribosome association

Δ*zuo1* cells containing the indicated plasmids were grown to an OD_{600} between 0.5 and 1.0 in selective minimal media, treated with 100 µg/ml cycloheximide, and harvested by centrifugation at 4 °C. Cells were resuspended in CB buffer (20 mM HEPES pH 7.5, 1 mM EGTA, 5 mM $MgCl_2$, 10 mM KCl, 10% glycerol and 2 mM ß-mercaptoethanol) containing 300 mM D-sorbitol and treated with rNAsin (Promega) at a dilution of 1:1,000. Yeast lysates were prepared by bead beating for 5 min and clarified by centrifugation at 14,000 rpm for 10 min. To pellet the ribosomal fraction, approximately 10 OD_{260} units of lysate were applied to the top of a 2-ml sucrose cushion containing 0.5 M sucrose in CB buffer and centrifuged at 50,000 rpm for 3 hours in a TLA 100.3 rotor (Beckman) at 4 ºC. To fractionate polysomes, approximately 10 OD_{260} units of lysate were applied to the top of a 4-ml 5-50% sucrose gradient in CB buffer and centrifuged for 80 min at 45,000 rpm at 4 °C in a SW50.1 Ti rotor (Beckman). Gradients were monitored for absorbance at 254 nm to detect monosomes and polysomes. Fractions were precipitated with 10% TCA, separated by SDS-PAGE, and subjected to immunoblotting.

Modified yeast two-hybrid

Strains PJ69 and PJ69 Δ*pdr1::TRP1*, the GBD and GBD-Zuo1$_{365-433}$ plasmids, and yeast two-hybrid methods were described previously (James et al., 1996; Prunuske et al., 2012). GBD-Zuo1$_{348-433}$ and GBD-Zuo1$_{358-433}$ were created by amplifying codons for the corresponding residues by PCR and cloning into pGBDU-C1 using BamHI and PstI. QuickChange was used to create GBD-Zuo1$_{348-433\ L/R}$, GBD-Zuo1$_{365-420}$, and GBD-Zuo1$_{365-433}$ alanine point mutants, as described above for the TAP plasmids. To create peptide fusions identical to those previously published in (Lu et al., 2000), a modified GBD plasmid was created by deleting the codons for residues 101-147 of GBD using QuickChange. The sequences coding for the P201 and P223 peptides were inserted into the modified GBD$_{1-100}$ plasmid using QuickChange. Modified yeast two-hybrid was carried out by detecting auto-activation of *Gal1–HIS3* and/or *Gal2-ADE2* reporters of PJ69 wt or Δ*pdr1* cells by monitoring growth on minimal media lacking uracil for plasmid selection and either histidine and adenine or histidine and containing 2 mM 3-aminotriazole, as described previously (Prunuske et al., 2012). Plates were incubated for 2-3 days at 30°C before photographing.

Protein expression and purification

8xHis-tagged Zuo1$_{348-433}$, Zuo1$_{358-433}$, Zuo1$_{335-433}$, and Zuo1$_{306-433}$ were created by amplifying codons for the corresponding residues by PCR and cloning into the BamHI and PstI sites of pQE308HT (Waltner et al., 2005). 8HT-Zuo1$_{348-430}$, -Zuo1$_{348-433\ L/R}$, and -Zuo1$_{348-433\ K/P}$ were created using QuickChange, as described above. Proteins were expressed in *E. coli* BL21[pREP4]. Cells were grown at 37 ºC to an $OD_{600} \approx 0.8$ in LB media containing 150 µg/ml

ampicillin and 50 µg/ml kanamycin, expression was induced by the addition of isopropyl β-D-thiogalactopyranoside to a final concentration of 1 mM, and cells were grown for an additional 3 hours at 15°C following induction. Isotopically labeled proteins were prepared for NMR by growing cultures in M9 media containing ^{15}N-ammonium chloride and/or ^{13}C-glucose as the sole nitrogen and carbon sources, respectively. Cells harvested from a 1-L culture were resuspended in 50 mM sodium phosphate at pH 7.4, 300 mM NaCl, 40 mM imidazole, 0.1% (w/v) 2-mercaptoethanol buffer containing an EDTA-free Complete Protease Inhibitor Cocktail tablet (Roche). Cells were lysed using a French pressure cell and protein was purified at 4 ºC by immobilized metal-ion affinity chromatography using Ni-sepharose 6 Fast Flow resin (GE Healthcare) according to a previously published protocol (Lytle et al., 2004). Following purification, the protein solutions were dialyzed 2x into 2 L of 20 mM sodium phosphate at pH 6.5, 50 mM NaCl, 1 mM dithiothreitol. Dialyzed protein was concentrated to 500µl for analysis by NMR and the purity and identity was verified by SDS-PAGE and mass spectrometry.

NMR spectroscopy

NMR samples were prepared in buffer containing 20 mM sodium phosphate at pH 6.5, 50 mM sodium chloride, 1 mM dithiothreitol, and 5-10% $^{2}H_2O$. All 2D ^{15}N-^{1}H HSQC spectra were acquired at 20 or 25 °C on a Bruker 500 or 600 MHz spectrometer equipped with a triple-resonance CryoProbe™ and processed with NMRPipe software (Delaglio et al., 1995). The $Zuo1_{348-433}$ sample used for structure determination was prepared in the identical buffer at a concentration of 1.2 mM. All structural data were acquired at 10 °C using a field strength of 600 MHz. Backbone ^{1}H, ^{15}N, and ^{13}C chemical shift assignments for $Zuo1_{348-433}$ were obtained

automatically as previously described using peak lists from ^{15}N-^{1}H HSQC, HNCO, HN(CO)CA, HN(CO)CACB, HNCA, HNCACB, HN(CA)CO, and CC(CO)NH (Markley et al., 2009). Sidechain assignments were completed manually from 3D HBHACONH, HCCONH, HCCH total correlation spectroscopy, and ^{13}C(aromatic)-edited NOESY-HSQC spectra. Chemical shift assignments were >99% complete for Zuo1$_{348-433}$. Heteronuclear NOE values were measured from an interleaved pair of 2D ^{15}N-^{1}H sensitivity enhanced correlation spectra recorded with and without a 5s proton saturation period.

Structure calculation and analysis

The Zuo1$_{348-433}$ structure was calculated using distance constraints obtained from 3D ^{15}N-edited NOESY-HSQC and ^{13}C-edited NOESY-HSQC (τ_{mix} = 80 ms). Backbone ϕ and ψ dihedral angle constraints were generated from secondary shifts of the ^{1}H, $^{13}C^{\alpha}$, $^{13}C^{\beta}$, ^{13}C' and ^{15}N nuclei using the program TALOS (Cornilescu et al., 1999). Structure calculations were performed using the torsion angle dynamics program CYANA (Guntert, 2004) followed by iterative rounds of manual refinement to eliminate constraint violations. Of the 100 CYANA structures calculated, the 20 conformers with the lowest target function were subjected to a molecular dynamics protocol in explicit solvent (Linge et al., 2003) using XPLOR-NIH (Schwieters et al., 2003).

Circular dichroism spectroscopy

Samples of Zuo1$_{348-433}$ and Zuo1$_{358-433}$ were prepared at a concentration of 20 μM in buffer containing 20 mM sodium phosphate at pH 6.5 and 50 mM NaCl. Thermal denaturation experiments were performed in a 1 mm cuvette and the ellipticity was monitored at 222 nm over

a temperature range of 10-70 °C. Thermal denaturation curves were analyzed by nonlinear least-squares fitting as previously described to determine the melting temperature (Allen and Pielak, 1998).

Acknowledgements

We thank Scott Moye-Rowley (University of Iowa, Iowa City) for sharing plasmids and Peter Kuhn, Lindsey Hoover, and Davin Jenson for assistance with data collection and helpful advice. This work was supported by National Institutes of Health Grant GM31107 (E.A.C.).

CHAPTER FOUR:

Conclusions and Future Directions

Conclusions

The goal of this project was to better understand the role of Ssz1 and Zuo1 in activation of the pleiotropic drug resistance regulon in *Saccharomyces cerevisiae.* The research presented in this thesis provides new insights into the mechanism of PDR activation by Ssz1 and Zuo1 and presents a possible model for the physiological basis of this signaling.

The research presented in chapter two indicates that Zuo1 requires the TF Pdr1 to activate the PDR regulon, as had previously been reported for Ssz1. Activation of Pdr1 by either Ssz1 or Zuo1 appears to be highly specific, as microarray analysis indicates that genes of the PDR regulon are the primary target of upregulation by either of these proteins. Using a yeast two-hybrid system, I was able to detect an interaction between Pdr1 and the domains of either Ssz1 or Zuo1 required for PDR activation. Furthermore, ChIP analysis showed enrichment of Ssz1 at the promoter of the ABC transporter-encoding gene *PDR5.* These results are consistent with a model in which activation of the PDR regulon by Ssz1 or Zuo1 occurs via direct regulation of the activity of the TF Pdr1. Activation of Pdr1 by either Ssz1 or Zuo1 also results in the early growth arrest of cells at the diauxic shift, a point during which cells must respond to limiting nutrient conditions. Cells lacking Ssz1 and Zuo1, on the other hand, overgrow at the diauxic shift, reaching higher culture densities than wt cells. This overgrowth was abrogated by the addition of media harvested from wt cells, suggesting the presence of a molecule(s) secreted from wt cells that is involved regulating cellular growth. These data support a role for Ssz1 and Zuo1 in quorum sensing, which likely occurs through Pdr1-dependent upregulation of plasma membrane transporters that export molecules involved in cell:cell communication.

In chapter three, I presented results related to understanding the mechanism of Pdr1 activation by Zuo1. Previous research indicated that the last 69 residues of Zuo1 were necessary and sufficient for activation of the PDR regulon (Eisenman and Craig, 2004). In this work, I further narrowed the region responsible for this activation to a 13-residue peptide at Zuo1's extreme C-terminus and found that expression of this highly hydrophobic peptide is sufficient to drive Pdr1-dependent transcription. As full-length Zuo1 had previously been shown to be unable to activate transcription, I investigated the possibility that Zuo1's C-terminal activity is regulated by autoinhibition. Though previous research indicated that Zuo1 is capable of activating PDR when not bound to ribosomes, I found that dissociation of Zuo1 from the ribosome was not sufficient to activate Pdr1-dependent transcription. Instead, structural analysis revealed that the C-terminal 86 residues of Zuo1 form an autoinhibitory four-helix bundle with the critical 13-residue peptide forming a C-terminal plug that is essential to the structural integrity of the domain. Residues required for activation of Pdr1 are thus buried in the hydrophobic core of the domain and necessary for its stability. I found that unfolding of this helical bundle enables Zuo1 to interact with and activate Pdr1. These data support a model in which Zuo1's transcriptional activity is regulated by autoinhibition conferred by the sequestering of key residues and that the C-terminal domain must undergo a structural transition to an unfolded conformation in order to release this inhibition.

Discussion and Future Directions

Mechanism of Pdr1 activation by Ssz1 and Zuo1

The data presented in this thesis are consistent with a model in which Ssz1 and Zuo1 regulate the activity of the TF Pdr1 via a direct mechanism. In Zuo1, this regulation appears to require the release of a hydrophobic peptide from a folded C-terminal domain. However, the details of how these proteins interact are still unknown. To gain a better understanding of the mechanism of activation of the PDR regulon by Ssz1/Zuo1, it would be important to determine if Ssz1/Zuo1 interact directly with Pdr1 and to identify the domain of Pdr1 responsible for activation by these proteins. Furthermore, the identification of additional factors that interact with Zuo1's C-terminus could aid in elucidating the mechanism by which unfolding occurs.

1) Do Ssz1/Zuo1 interact directly with Pdr1?

Yeast two-hybrid results presented in chapter two of this thesis suggest that Ssz1 and Zuo1 interact with the TF Pdr1. Either the N-terminus of Ssz1 or the C-terminus of Zuo1, when expressed as a fusion to GBD, was able to auto-activate reporters of the two-hybrid system in a Pdr1-dependent manner. Furthermore, in a classic yeast two-hybrid experiment, reporter activation was observed when GBD-Pdr1 was co-expressed with GAD fusions of either the N-terminus of Ssz1 or the C-terminus of Zuo1. These results suggest the possibility that Ssz1 and Zuo1 bind directly to the TF Pdr1 to regulate its activity. This type of direct activation of Pdr1 has been observed previously by xenobiotics (Thakur et al., 2008). However, based on these results, it is also possible that other factors are involved in the formation of a stable complex that includes both Pdr1 and Ssz1/Zuo1. Thus, it will be important to determine if the interaction

between Ssz1/Zuo1 and Pdr1 is direct and/or to identify other factors involved in interactions with these proteins.

The ability to detect an interaction between Pdr1 and Ssz1/Zuo1, however, is not trivial. My preliminary efforts to co-IP Ssz1/Zuo1 and Pdr1 from yeast lysates have been unsuccessful. Furthermore, my initial attempts to express Pdr1 in *E. coli* for *in vitro* binding experiments have yielded no protein. Several factors likely contribute to the difficulty of these experiments. The large size of Pdr1 (>100 kDa) presents a challenge for recombinant expression. This protein is also present at only approximately 1300 molecules/cell in yeast (Ghaemmaghami et al., 2003) and thus may elude detection *in vivo* due to its low abundance. The proposed interaction between Ssz1/Zuo1 and Pdr1 may also occur in a transient nature, making it more difficult to detect. Furthermore, I have shown that the C-terminus of Zuo1 activates Pdr1 in an unfolded conformation. Thus, pulldowns with extended purification steps have resulted in the degradation of Zuo1 protein. Therefore, a number of different methods must be employed to observe this potential interaction, taking steps to combat these various difficulties.

Although my initial efforts to express full-length Pdr1 in *E. coli* have been unsuccessful, truncated forms of Pdr1 have recently been expressed and purified for use in *in vitro* drug binding experiments (Thakur et al., 2008). Our lab has obtained these plasmids and preliminary expression testing indicates that we are able to express significant enough quantities of soluble Pdr1 fragments for use in *in vitro* binding experiments. These GST-tagged Pdr1 fusions can be used to detect interaction with PDR-inducing TAP-tagged constructs of Ssz1 and Zuo1 from yeast lysates. Furthermore, the domains of Ssz1 and Zuo1 responsible for PDR induction have been expressed in *E. coli* and could be used to determine if a direct interaction occurs between

Ssz1/Zuo1 and these Pdr1 fragments *in vitro*. Although the instability of Zuo1's C-terminus presents a challenge in these assays, I have been able to purify a number of C-terminal truncations and mutants with varying degrees of fold and stability that can be tested in these assays.

If significant enough quantities of purified Pdr1 truncations can be produced, they could also be used in NMR experiments to detect binding to the C-terminal domain of Zuo1. If this domain interacts directly with Pdr1, titration of Pdr1 constructs with ^{15}N-labeled Zuo1 C-terminal fragments should result in significant chemical shift perturbations detectable in a ^{1}H-^{15}N HSQC experiment. If an interaction is detected, identification of the most significant perturbations of the fully assigned HSQC of Zuo1's C-terminal domain upon interaction could be further used to identify residues important for this interaction. As Zuo1 has been shown to activate Pdr1 in an unfolded conformation, it is also possible that Pdr1 interacts with the unfolded form of Zuo1's C-terminal domain. Furthermore, folding or unfolding of Zuo1's C-terminal domain might be induced upon binding to Pdr1. A number of transcription factor ADs, for instance, have been shown to be active in an unfolded conformation, but become structured upon binding to their coactivators (Ferreira et al., 2005; Uesugi et al., 1997). Similarly, in the case of N-WASP autoinhibition, a hydrophobic peptide required for activity is involved in intramolecular domain interactions, but upon domain destabilization, this peptide is displaced and forms a new amphipathic helix upon binding to the Arp2/3 complex (Panchal et al., 2003). Thus, titrations with Pdr1 should be carried out using constructs and mutants of Zuo1's C-terminus that differ in fold, as described in chapter three. Thermal denaturation may also be used

to induce these different states in the full C-terminal domain, which would allow the possibility of refolding to occur.

Another possible method to detect an interaction between Ssz1/Zuo1 and Pdr1 is to perform photo-crosslinking using the amino acid derivative *p*-benzoyl-L-phenylalanine (pBpa). In addition to its ability to detect low abundance binding partners and transient interactions, pBpa crosslinking shows more specificity than many available crosslinkers and has been successfully used in live yeast cells (Lee et al., 2009; Majmudar et al., 2009). Therefore, this technique may be useful for detecting functionally relevant interactions *in vivo*. Since I have narrowed the region responsible for Zuo1's interaction with Pdr1 to only 13 residues, I have been able to create mutants to incorporate pBpa at each site within this peptide. Working with this limited number of mutants will hopefully provide a good chance of finding a mutant that is functional in the presence of the non-natural amino acid as well as one that incorporates a crosslink close enough to the interaction site that it is possible to detect an interaction with Pdr1. A similar approach could be taken with Ssz1 by incorporating pBpa at sites near Ser295, as alteration of this and surrounding residues has been shown to effect PDR activation by Ssz1 (A. Prunuske, unpublished data, (Hallstrom et al., 1998)). Crosslinked products of Ssz1/Zuo1 could then be tested for the presence of Pdr1 by immunoblotting.

2) What proteins interact with Zuo1's C-terminal domain in its folded/unfolded conformations?

Whether or not Zuo1 binds directly to Pdr1, it is likely that other factors are involved in interactions with this protein. Although the results presented in chapter three indicate that Zuo1's C-terminal domain must undergo a structural transition to its unfolded state in order to activate

Pdr1, it is not clear how this occurs. The fact that overexpression of full-length Zuo1 does not activate Pdr1 suggests that thermodynamic instability of the C-terminal domain does not provide a simple explanation for this activation. Thus, it is possible that an active unfolding process may be necessary to activate the transcriptional properties of this domain. One possibility is that binding of an adapter protein somewhere in the C-terminal domain causes disruption of domain structure and thus releases the critical peptide at the extreme C-terminus. It is also conceivable that binding of an adapter protein is necessary to stabilize the unfolded conformation of the domain as it is in equilibrium between folded and unfolded states. Thus, identification of additional binding partners of Zuo1's C-terminus could aid in elucidating this mechanism of unfolding. Identification of novel binding partners could be carried out using tandem affinity purification pulldowns, as I have created a number of TAP-tagged fusions of C-terminal truncations and mutants that vary in their fold, stability, and ability to induce PDR in yeast. TAP pulldowns with these various constructs could be useful in the identification of novel interactions with both conformations of Zuo1's C-terminal domain, which could provide important clues regarding the mechanism of activation of Zuo1's transcriptional properties. If this method is unsuccessful, the pBpa crosslinking method described above could also be useful for the detection of additional binding partners of Zuo1's C-terminal domain. In addition to immunoblotting for specific binding partners, crosslinked products of Zuo1's C-terminal domain could potentially be identified using mass spectrometry. The downside to this method is the low incorporation of pBpa, which requires the use of large amounts of cells. However, this method is currently being employed successfully in Anna Mapp's lab at the University of Michigan to

identify novel interactions of low abundance, unstable proteins that are transient in nature (C. Majmudar, personal communication).

3) Do Ssz1/Zuo1 activate Pdr1 through its XBD similar to xenobiotics?

Pdr1 is directly activated by the binding of small hydrophobic molecules to a xenobiotic binding domain (XBD) within its central regulatory region (Thakur et al., 2008). Results presented in chapter three of this thesis reveal that Zuo1 utilizes a short, hydrophobic peptide at its extreme C-terminus to interact with Pdr1 and activate transcription. These data present the possibility that Zuo1's C-terminal peptide binds to Pdr1's XBD and mimics the binding of xenobiotics. Alternatively, it is possible that this activation is not direct, as discussed above, or that Zuo1 uses a different region of Pdr1 for activation. Furthermore, it is not known if Ssz1 and Zuo1 activate Pdr1 through the same domain.

Initial attempts in the lab to identify the domain of Pdr1 responsible for activation by Ssz1/Zuo1 have been inconclusive. This is primarily due to the fact that deletions of various regions of Pdr1's central regulatory region have been shown to render the protein hyperactive (Kolaczkowska et al., 2002). The large differences in activity observed between different Pdr1 truncations makes their responsiveness to inducing signals difficult to interpret. Thus, identification of the domain of Pdr1 responsible for interaction with Ssz1/Zuo1 might be a more suitable approach and eliminate the issue of differential activity between constructs. *In vitro* binding experiments with Pdr1 truncations, if successful, would be optimal for this experiment. Since a number of Pdr1 truncations were used to identify the XBD as the region responsible for drug binding, these fragments should provide a good starting place for identifying the domain of

Pdr1 required for binding to Ssz1/Zuo1. However, if direct interactions are not detected *in vitro*, an alternative approach would be to use the yeast two-hybrid system. As presented in chapter two, interactions between Ssz1 and Zuo1 and Pdr1 lacking both its DBD and AD have been identified. This suggests that both Ssz1 and Zuo1 require Pdr1's large central regulatory region for interaction. It would be interesting to narrow this region further by testing Pdr1 lacking its XBD or a Pdr1 fragment containing only the XBD for interaction with Ssz1 and Zuo1. It must be noted, however, that the large differences in activity observed between different Pdr1 truncations suggest that alteration of one region of Pdr1 may have large structural effects on the rest of the protein that could preclude interaction. Therefore, it would be important to test a variety of different Pdr1 constructs in these assays.

To avoid the issue of creating truncations of Pdr1 with varying levels of activity or conformational differences, an alternative might be to create Pdr1-Pdr3 chimeras. Despite the high homology of Pdr1 and Pdr3, Ssz1 and Zuo1 require only Pdr1 for activation of the PDR regulon (chapter two of this thesis, (Hallstrom et al., 1998)), while drugs can utilize both of these TFs. A variety of Pdr1-Pdr3 chimeras, with different regions of these proteins swapped, could be tested for their ability to interact with and become activated by Ssz1/Zuo1 and, as a control, xenobiotics. These experiments might not only provide insight into which domain of Pdr1 is required for signaling by Ssz1/Zuo1, but also clues as to how specificity for Pdr1 is achieved by these proteins.

We have also attempted to determine if Ssz1/Zuo1 activate Pdr1 using a similar mechanism to drugs by performing *in vivo* competition assays. However, the results of these assays have been inconclusive. This is likely due in part to *in vivo* complexities of the PDR

regulon, including the ability of drugs to activate other TFs, such as Pdr3. Also, it is not known to what extent Pdr1, once activated, can be further activated by binding of an inducing factor to a different region of the protein. Therefore, if binding of Pdr1 and Ssz1/Zuo1 is observed *in vitro,* it would be interesting to perform binding competition assays between Ssz1, Zuo1, and drugs *in vitro*, as this might provide a better understanding of the similarities or differences in the mechanisms of Pdr1 regulation by these factors.

Role of the RAC heterodimer in Pdr1 activation

Although it has been shown that both Ssz1 and Zuo1 are capable of activating Pdr1 independently (Eisenman and Craig, 2004), these proteins are known to form a stable heterodimer *in vivo* (Conz et al., 2007b; Gautschi et al., 2001a). Therefore, it is not clear whether these proteins activate Pdr1 independently under native conditions or whether they function together as a heterodimer in transcriptional activation. In addition, this heterodimer has a conserved role in protein folding in higher eukaryotes and a number of Zuo1 orthologs have also been shown to function in transcription. However, it is not known whether the signaling functions of these orthologs relate to the PDR induction observed by Zuo1 in yeast. Thus, further characterization of this unique heterodimer and its involvement in transcription is necessary to achieve a better understanding of the cellular functions of Ssz1 and Zuo1.

1) Does disruption of the RAC heterodimer cause PDR induction?

One possible model for the role of the RAC heterodimer is that while it enables Ssz1/Zuo1 to function together in nascent chain folding on the ribosome, disruption of this

complex under certain conditions frees these proteins to perform their transcriptional roles. Thus, a transition in the association of these proteins from a ribosome-associated heterodimer to extra-ribosomal monomers could provide a means of regulating these seemingly disparate functions of Ssz1 and Zuo1. It would, therefore, be interesting to determine if destabilization of the RAC heterodimer causes activation of Pdr1. This could be done by introducing mutations into the N-terminus of Zuo1 or the C-terminus of Ssz1 that would be predicted to disrupt complex formation and testing these mutants for their ability to activate PDR. Since Ssz1 is tethered to the ribosome through interaction with Zuo1, monitoring the co-migration of Ssz1 with ribosomes by sucrose cushion ultracentrifugation could be used to determine the degree of heterodimer disruption. Conservation of RAC in higher eukaryotes suggests that targeted mutations could be made by sequence alignment. Furthermore, H/D exchange data collected on Ssz1 and Zuo1 individually and in complex with one another (Fiaux et al., 2010) would provide useful starting points for mutation design.

The results presented in chapter three of this thesis suggest that unfolding of Zuo1's C-terminal domain is a requisite step for activation of its transcriptional properties. Interestingly, it has been proposed that Ssz1 has a stabilizing effect on Zuo1 structure, as described in chapter one (Fiaux et al., 2010; Gautschi et al., 2001a). Though the primary interactions in this complex appear to occur between the N-terminus of Zuo1 and the C-terminus of Ssz1, some protection of the C-terminus of Zuo1 was also observed in H/D exchange experiments in the presence of Ssz1 (Fiaux et al., 2010). Thus, it is conceivable that Ssz1 contributes to the stability or fold of Zuo1's C-terminal domain or aids in the sequestering of key residues required for activation. It would, therefore, be interesting to determine if Ssz1 contributes to Zuo1 autoinhibition by testing

whether constructs of Zuo1 that are unable to activate transcription due to the presence of a folded C-terminal domain are able to induce PDR in a strain lacking Ssz1. If the absence of Ssz1 does appear to have a positive effect on the transcriptional properties of Zuo1's C-terminal domain, further characterization of this interaction would be interesting. The possibility of a direct interaction occurring between Zuo1's C-terminal domain and Ssz1 could be tested by NMR. The HSQC spectra of ^{15}N-labeled Zuo1 C-terminal domain could be monitored for chemical shift perturbations upon titration with unlabeled Ssz1 and be used to identify residues affected by complex formation.

2) Is activation of the PDR regulon by Ssz1/Zuo1 conserved in higher eukaryotes?

Interestingly, a number of higher eukaryotic orthologs of Zuo1 have also been shown to have roles both in protein folding and transcriptional activation. The human Zuo1 ortholog, known as M-phase phosphoprotein 11 (Mpp11) or ZRF1, has been shown to co-migrate with translating ribosomes and form a heterodimer with the Ssz1 homolog Hsp70L1 that is capable of rescuing the growth defects of a yeast strain lacking functional RAC (Hundley et al., 2005; Otto et al., 2005). In addition, Mpp11 is regulated in a cell cycle dependent manner, is upregulated in a variety of cancers, and has been shown to facilitate gene activation by displacing transcriptional repressors of developmental regulators (Resto et al., 2000; Richly et al., 2010). The mouse Zuo1 homolog, MIDAI, has been shown to bind to Hsp70 through its J-domain and also bind directly to DNA through Myb domains located at its C-terminus. This protein is implicated in the regulation of cell growth and cell cycle progression and its ability to directly bind DNA suggests that it can translocate to the nucleus to perform these signaling functions

(Inoue et al., 1999; Shoji et al., 1995; Yoshida et al., 2004). The Zuo1 homologs GlsA in the blue-green algae *Volvox carteri* (Pappas and Miller, 2009) and DNJ-11 in *Caenorhabditis elegans* (Hatzold and Conradt, 2008) have also been implicated in the regulation of asymmetric cell division. Despite this apparent conservation of Zuo1's role in cellular signaling, it is not clear if these transcriptional activities are related. Work presented in chapter two of this thesis suggests that activation of the PDR regulon by Zuo1 may relate to a form of cellular growth regulation, similar to the roles observed for Zuo1's higher eukaryotic orthologs. Thus, it would be interesting to determine if these proteins function in transcription through similar mechanisms.

Since Mpp11/Hsp70L1 have been shown to be capable of rescuing the growth defects of yeast lacking functional RAC (Hundley et al., 2005; Otto et al., 2005), it would be interesting to test whether these proteins can also induce a PDR phenotype in yeast. Overexpression of Hsp70L1 or Mpp11 lacking its charged domain could be tested for resistance to a variety of drugs or for the activation of genes known to be upregulated by Ssz1/Zuo1 using the *lacZ* reporters described in this work or qPCR. Furthermore, these proteins could be tested for their ability to cause premature growth arrest of cells at the diauxic shift similar to domains of Ssz1/Zuo1 that activate Pdr1. If any of these phenotypes are observed, it could be tested whether they occur in a Pdr1-dependent manner to determine if these proteins activate the PDR regulon similarly to Ssz1/Zuo1. Similar studies could be performed in human cells to observe activation of the MDR pathway using either Mpp11/Hsp70L1 or Ssz1/Zuo1. If similar activities are observed for higher eukaryotic orthologs of Ssz1/Zuo1, it would be interesting to determine what domains are responsible for these activities, as Zuo1's C-terminus does not appear to be

conserved in higher eukaryotic species and Zuo1 lacks the DNA-binding Myb/SANT domains found in these orthologs (Braun and Grotewold, 2001a).

Physiological role of PDR regulation by Ssz1/Zuo1

The results presented in chapter two of this thesis propose a physiological role for activation of the PDR regulon by Ssz1 and Zuo1 in quorum sensing. Strains lacking Ssz1 and Zuo1 show an "overgrowth" phenotype at the diauxic shift that is reminiscent of yeast cells lacking the ABC transporters Pdr5 and Snq2 (Hlavacek et al., 2009) and bacterial cells lacking the AcrAB MDR pump (Yang et al., 2006). The higher cell densities reached by these strains is proposed to occur due to the absence of a signaling molecule(s) involved in regulating cell growth, which is normally extruded from cells via these plasma membrane transporters. Consistent with this idea, the overgrowth of a strain lacking Ssz1 and Zuo1 was mitigated by the addition of conditioned media from wt cells. Furthermore, domains of Ssz1/Zuo1 that enhance activation of the PDR regulon also cause cells to arrest at a lower cell density than wt cells, suggesting an enhanced export of signaling molecules from cells expressing these proteins. Though these data propose a role for Ssz1/Zuo1 in quorum sensing via activation of the TF Pdr1, many questions remain regarding this potential function, several of which are discussed below.

1) Do Ssz1/Zuo1 respond to known quorum sensing molecules?

Quorum sensing has been reported in fungi and results in the transition of yeast from their solitary growth form to a filamentous form. Studies on quorum sensing in yeast are limited, however, due to the fact that many lab strains contain mutations in the *FLO8* gene, which is

essential for filamentation (Liu et al., 1996). Despite this, a number of quorum sensing molecules have been identified in *S. cerevisiae,* the majority of which are fusel alcohols derived from the catabolism of aromatic and branched chain amino acids (Chen and Fink, 2006; Chen et al., 2004; Dickinson, 1996; Wuster and Babu, 2010). Interestingly, expression analysis of yeast treated with isoamyl alcohol, a fusel alcohol involved in filament formation, shows significant upregulation of *PDR5* and *GRE2* (Hauser et al., 2007), two of the genes most highly upregulated in response to Ssz1* and ZuoC*, as presented in chapter two. It would thus be interesting to determine if other fusel alcohols show similar upregulation of genes induced by Ssz1* and ZuoC* and if the ability of these catabolites to induce expression of these genes is dependent on the presence of Ssz1 and Zuo1 and/or Pdr1. Furthermore, it could be tested whether the overgrowth phenotype of Δ*ssz1* Δ*zuo1* and Δ*pdr5* Δ*snq2* cells can be overcome by supplementation of media with these fusel alcohols.

2) What signaling molecules are extruded from cells in an Ssz1/Zuo1-dependent manner?

If Ssz1 and Zuo1 mediate growth arrest at the diauxic shift via quorum sensing, it might also be possible to more directly identify the factor(s) responsible for this effect. As presented in chapter two, a preliminary assessment of the nature of the factor(s) responsible for the overgrowth of Δ*ssz1* Δ*zuo1* cells suggested that it might be a small molecule(s). While media harvested from wt cells could prevent the overgrowth phenotype of Δ*ssz1* Δ*zuo1* cells, media first exposed to dialysis could not, though boiling had no effect. To further characterize the molecules responsible for this phenotype, gas chromatography and mass spectrometry could be used to identify molecules that differ in media extracted from wt, Δ*ssz1* Δ*zuo1,* and Δ*pdr5* Δ*snq2*

cells. A lower abundance of fusel alcohols or other factors in the media of Δ*ssz1* Δ*zuo1* and/or Δ*pdr5* Δ*snq2* would support the idea that an extracellular signaling molecule is responsible for their growth phenotypes. A similar characterization of media extracted from cells overexpressing ZuoC* or Ssz1* could be used to determine if a higher abundance of this molecule is extruded from these cells. If a molecule is identified in the media extracted from these cells, it could also be determined if the abundance of this factor is dependent on the presence of Pdr1. As the growth phenotypes of cells lacking *SSZ1* and *ZUO1* occurs around the diauxic shift, it would be interesting to compare the growth media of wt, Δ*ssz1* Δ*zuo1*, and Δ*pdr5* Δ*snq2* strains as cells approach the diauxic shift. Identifying differences in the molecules extruded by these strains during the diauxic shift may be useful in the identification of the molecules responsible for this potential quorum sensing. As the effect of Ssz1/Zuo1 deletion on cell density is not as large as deletion of the plasma membrane transporters Pdr5 and Snq2, it is possible that ABC transporters play a more direct role in this signaling and that Ssz1/Zuo1 serve to modulate this signal. It is also conceivable that several pathways exist to respond to nutrient limitation, one of which is through Ssz1/Zuo1. Thus, the levels or nature of any identified signaling molecules may differ between these strains.

Factors identified in these analyses could then be tested for their ability to prevent the growth phenotype of Δ*ssz1* Δ*zuo1* and Δ*pdr5* Δ*snq2* cells by supplementing the media of these cells with the identified molecule and comparing growth to wt cells. Furthermore, identified molecules could be tested for their ability to induce similar gene expression to cells expressing ZuoC* and Ssz1* and determined whether Ssz1 and Zuo1 are required for this expression.

3) Are the transcriptional properties of Ssz1/Zuo1 activated by quorum sensing molecules or during the diauxic shift?

It has been clearly demonstrated that ectopic expression of either Ssz1 or the C-terminus of Zuo1 results in activation of the PDR regulon; however, the signal by which these proteins become activated to initiate this transcriptional response under native conditions is not known. Activation of Pdr1 by Ssz1/Zuo1 appears to occur through a direct mechanism requiring the dissociation of these proteins from the ribosome and their subsequent translocation to the nucleus. If Pdr1 activation by Ssz1/Zuo1 relates to quorum sensing, it is possible that the transcriptional properties of these proteins become activated in response to quorum sensing molecules. It would, therefore, be interesting to determine if Ssz1/Zuo1 show dissociation from the ribosome and/or localize to the nucleus in the presence of fusel alcohols or other molecules identified from the above analyses. Similarly, it could be tested whether Ssz1/Zuo1 undergo these changes as cells approach the diauxic shift. Interestingly, fusel alcohols have been shown to inhibit translation and disrupt polysomes (Taylor et al., 2010). Thus, it is conceivable that under nutrient limitation, upregulation of quorum sensing molecules leads to a disruption of polysomes, causing the release of Ssz1/Zuo1 and allowing them to activate Pdr1-dependent transcription. In this model, the subsequent upregulation of ABC transporters by Ssz1/Zuo1 would cause enhanced export of quorum sensing molecules that further slow cellular growth as cells approach stationary phase.

APPENDIX:

Additional studies of PDR activation by Zuo1 and Ssz1

This appendix includes additional unpublished data I collected pertaining to activation of the PDR regulon by Zuo1 or Ssz1 that were either preliminary in nature or did not fit into the other data chapters.

Knockout library screen for factors required for PDR induction by Zuo1's C-terminus

To identify proteins required for induction of the PDR regulon by Zuo1's C-terminal domain, I performed a screen using the homozygous diploid yeast knockout collection derived from the Saccharomyces Genome Deletion Project (Winzeler et al., 1999) and acquired from Open Biosystems. Yeast deletion strains were grown from glycerol stocks for 2 days at 30 ºC in YPD media containing 200 µg/ml G418 in deep-well microtiter plates and plated on YPD media containing 200 µg/ml G418 and grown for 2-3 days at 30 ºC. Cells were transferred from the solid media into liquid YPD media containing 200 µg/ml G418 in deep-well microtiter plates using a 96-pin tool. Strains were grown overnight at 30ºC and then diluted to an OD_{600} ~ 0.2 (based on the average density of cells from four random wells) in fresh media and allowed to grow for 4 hours. Cells were transformed with a high-copy plasmid containing DNA encoding a tandem affinity purification (TAP) tag fused to residues 365-433 of Zuo1's C-terminus (pRS425-GPD-TAP-ZuoC). Transformants were grown in selective minimal liquid media for 2 days at 30 ºC and subsequently plated on selective minimal media plates containing or lacking 0.35 µg/ml cycloheximide and grown for 3 days at 30 ºC. Growth of the transformants on media containing cycloheximide was determined for each strain by visual inspection. Strains showing reduced growth compared to wt cells were ranked as follows: 0 = no growth; 1 = extremely slow growth; 2 = slow growth; 3 = slightly slow growth (Table A-1). This screen was performed for all of the plates in the knockout collection containing strains showing growth similar to wt cells (plates 301-348), but was not performed for slow-growing strains to prevent the selection of these strains as false positives. Overall, I tested 4,491 deletion strains and identified 283 candidate strains as showing reduced growth or no growth in the presence of cycloheximide compared to

wt cells when transformed with the PDR-inducing ZuoC plasmid. An additional 161 strains also showed reduced growth in the presence of drug compared to wt cells, but also showed slow growth on either YPD media containing G418 or on selective minimal media, making it difficult to assess their sensitivity to drug. Thus, this set of strains would need to be retested to determine the importance of these genes in ZuoC-induced drug resistance. Based on these numbers, I was able to eliminate ~90% of the strains tested using this screen and as many as 94% if the slow growing strains are false positives. All candidate strains identified in this screen (ranked 0-3) were compiled into fresh microtiter plates and stored as glycerol stocks at -80 ºC for future experimentation.

To more specifically identify genes required for PDR induction by ZuoC and eliminate genes required downstream of Pdr1 and genes that render cells sensitive to cycloheximide upon deletion, a secondary screen was set up. Candidate strains from the primary screen were co-transformed with the TAP-ZuoC plasmid described above and a plasmid encoding the *PDR5-lacZ* reporter to perform ß-galactosidase assays. I first attempted to perform these ß-galactosidase assays in a 96-well format. This proved difficult as both the OD_{600} and OD_{420} of each deletion strain in the plate had to be acquired in the proper range and each strain varied significantly. With limited access to a plate reader, I was unable to optimize a protocol for the type of time-point collection required for this assay. Instead, I decided to perform individual ß-galactosidase assays from two independent colonies of each transformant grown in 5-ml cultures. After identifying a number of candidate strains based on reduced ß-galactosidase activity of the *PDR5-lacZ* reporter compared to wt cells in the presence of TAP-ZuoC, I retested several strains for fold activation of cells transformed with TAP-ZuoC compared to cells transformed with TAP

alone. I found that the basal levels of *PDR5-lacZ* activity varied significantly (>2-fold) in many of the strains tested. This difference in basal activity skewed the numbers drastically such that strains that showed lower or higher ß-galactosidase activity than wt cells could still show similar fold activation when basal levels were taken into account. Therefore, in order to carry out the remainder of this screen, each plate would need to be tested with both TAP and TAP-ZuoC and fold activation would need to be determined for each individual strain. Because of the added number of colonies required to test for basal levels of *PDR5-lacZ* activity, this screen would be better suited to a high-throughput 96-well plate format. Because of this added complexity as well as new data indicating that drugs activate Pdr1 directly (Thakur et al., 2008), this screen was not completed and ZuoC was instead tested for its ability to activate Pdr1 directly. Strains from the primary screen that were tested for ß-galactosidase activity of *PDR5-lacZ* by ZuoC are presented in Table A-2. Though the basal levels of *PDR5-lacZ* may vary between these strains, strains showing the most significant reduction in activity compared to the wt strain might still be the most useful to begin further testing. Not all candidates from the primary drug resistance screen were tested for *PDR5-lacZ* activity, however, so this list is incomplete. Although I did not complete testing of all candidate strains from the primary screen, I did test a number of strains individually for fold activation of *PDR5-lacZ* by ZuoC compared to TAP. This included strains that showed extraordinarily high or low ß-galactosidase levels of *PDR5-lacZ* compared to a wt strain upon initial testing. I also tested strains deleted for the genes encoding each of the TFs known to be involved in the PDR regulon as well as strains lacking proteins that has been identified as having either a physical or genetic interaction with Zuo1, Ssz1, or Pdr1. The results of these ß-galactosidase assays are preliminary and are presented in Figure A-1.

Although the data presented in this thesis are consistent with a model of direct activation of Pdr1 by ZuoC, it is likely that other factors are involved in this activation process. The candidates identified in this primary screen for drug resistance or tested for activation of *PDR5-lacZ* might provide a useful starting place for identification of these factors. These candidate strains could also be transformed with Ssz1 to identify factors required for PDR induction by Ssz1.

Table A-1. Candidates identified in knockout library screen for ZuoC-induced drug resistance

Plate	Row	Column	Systematic Name	Standard Name	Ranking*
303	F	7	YMR015C	ERG5	0
304	H	2	YMR263W	SAP30	0
306	F	6	YOR290C	SNF2	0
307	D	6	YOL004W	SIN3	0
307	E	4	YOL018C	TLG2	0
311	E	12	YDR432W	NPL3	0
316	G	2	YKL041W	VPS24	0
316	G	7	YKL048C	ELM1	0
318	C	2	YOR153W	PDR5	0
319	H	4	YLR360W	VPS38	0
323	E	9	YPR173C	VPS4	0
325	C	5	YGL012W	ERG4	0
325	C	12	YGL025C	PGD1	0
326	C	12	YKL213C	DOA1	0
326	E	7	YKR020W	VPS51	0
328	D	5	YFR009W	GCN20	0
328	D	6	YFR010W	UBP6	0
330	G	7	YML097C	VPS9	0
333	A	5	YJR073C	OPI3	0
338	D	1	YGR104C	SRB5	0
345	C	5	YDL006W	PTC1	0
301	C	8	YAL026C	DRS2	1
301	E	2	YAL002W	VPS8	1
302	D	8	YLR054C	OSW2	1
302	D	9	YLR055C	SPT8	1
303	D	12	YML010W-A	-	1
305	A	2	YMR283C	RIT1	1
306	D	6	YOR068C	VAM10	1
306	D	7	YOR069W	VPS5	1
307	D	3	YOL001W	PHO80	1

Plate	Row	Column	Systematic Name	Standard Name	Ranking*
310	F	12	YDR120C	TRM1	1
310	H	4	YDR136C	VPS61	1
311	C	9	YDR388W	RVS167	1
311	C	10	YDR389W	SAC7	1
312	A	3	YEL044W	IES6	1
312	G	6	YER083C	GET2	1
314	H	8	YHR167W	THP2	1
314	H	11	YHR178W	STB5	1
316	C	8	YLR204W	QRI5	1
316	E	4	YKL002W	DID4	1
316	E	6	YKL007W	CAP1	1
317	C	9	YKL113C	RAD27	1
318	B	3	YOR132W	VPS17	1
318	E	4	YOR198C	BFR1	1
319	D	10	YJL154C	VPS35	1
320	A	1	YLR373C	VID22	1
320	C	11	YLR417W	VPS36	1
320	C	12	YLR418C	CDC73	1
320	E	11	YLR261C	VPS63	1
320	F	6	YLR268W	SEC22	1
321	A	2	YLR315W	NKP2	1
322	A	9	YGL250W	-	1
322	F	9	YPL055C	LGE1	1
325	A	11	YBL079W	NUP170	1
325	C	6	YGL013C	PDR1	1
325	D	8	YGL043W	DST1	1
325	E	7	YGL066W	SGF73	1
326	A	2	YNL199C	GCR2	1
333	E	11	YLR435W	TSR2	1
334	G	7	YDL192W	ARF1	1
335	F	7	YBR290W	BSD2	1
336	A	5	YCR077C	PAT1	1
336	G	8	YDL116W	NUP84	1

Plate	Row	Column	Systematic Name	Standard Name	Ranking*
339	C	2	YNR006W	VPS27	1
341	E	11	YNL097C	PHO23	1
343	A	9	YLR370C	ARC18	1
343	F	6	YOR270C	VPH1	1
343	F	12	YOR298C-A	MBF1	1
345	E	1	YDL040C	NAT1	1
345	G	2	YDL081C	RPP1A	1
345	H	11	YDR448W	ADA2	1
346	F	12	YGL127C	SOH1	1
301	H	8	YLL039C	UBI4	2
301	H	9	YLL040C	VPS13	2
302	F	1	YLR079W	SIC1	2
302	H	6	YLR119W	SRN2	2
303	A	12	YML063W	RPS1B	2
303	B	1	YML062C	MFT1	2
303	D	8	YML013W	SEL1	2
303	E	9	YML001W	YPT7	2
304	C	3	YMR179W	SPT21	2
305	C	9	YNL324W	-	2
305	C	11	YNL323W	LEM3	2
305	C	12	YNL322C	KRE1	2
305	D	6	YNL307C	MCK1	2
305	H	8	YOR014W	RTS1	2
306	D	8	YOR070C	GYP1	2
306	E	11	YOR089C	VPS21	2
307	B	7	YOR360C	PDE2	2
308	A	4	YGR078C	PAC10	2
308	B	8	YPL265W	DIP5	2
308	C	6	YPL253C	VIK1	2
308	E	12	YPL205C	-	2
308	H	11	YPL161C	BEM4	2
309	B	2	YPL139C	UME1	2
309	C	1	YPL120W	VPS30	2

Plate	Row	Column	Systematic Name	Standard Name	Ranking*
310	G	6	YDR126W	SWF1	2
311	B	12	YDR378C	LSM6	2
311	E	1	YDR418W	RPL12B	2
311	F	5	YEL003W	GIM4	2
311	H	5	YEL031W	SPF1	2
312	B	6	YEL061C	CIN8	2
312	D	1	YER020W	GPA2	2
312	G	1	YER074W	RPS24A	2
313	B	7	YGR164W	-	2
313	E	5	YGR214W	RPS0A	2
313	F	7	YHL033C	RPL8A	2
313	H	10	YHR012W	VPS29	2
314	C	7	YHR077C	NMD2	2
314	C	9	YHR079C	IRE1	2
314	F	5	YHR129C	ARP1	2
314	G	4	YHR142W	CHS7	2
315	A	8	YHR200W	RPN10	2
317	A	7	YKL076C	PSY1	2
317	F	1	YKL149C	DBR1	2
317	F	8	YKL160W	ELF1	2
318	A	10	YOR124C	UBP2	2
318	D	5	YOR183W	FYV12	2
318	D	10	YOR191W	RIS1	2
318	G	3	YOR235W	IRC13	2
318	H	3	YOR251C	-	2
318	H	7	YOR258W	HNT3	2
319	G	10	YLR352W	-	2
319	H	11	YLR371W	ROM2	2
320	A	2	YLR374C	-	2
321	D	6	YDR200C	VPS64	2
321	H	11	YGL232W	TAN1	2
322	A	5	YGL244W	RTF1	2
322	A	10	YGL252C	RTG2	2

Plate	Row	Column	Systematic Name	Standard Name	Ranking*
323	A	3	YPL008W	CHL1	2
323	G	6	YCR094W	CDC50	2
325	A	8	YBL072C	RPS8A	2
325	G	11	YNL224C	SQS1	2
326	A	12	YNL183C	NPR1	2
326	C	9	YKL207W	-	2
326	D	9	YKR007W	MEH1	2
326	F	4	YKR042W	UTH1	2
326	H	12	YDR257C	SET7	2
327	A	9	YDR266C	-	2
327	B	3	YDR276C	PMP3	2
327	D	9	YDR318W	MCM21	2
327	G	4	YIL036W	CST6	2
327	H	3	YIL057C	-	2
328	B	1	YFL025C	BST1	2
328	E	11	YGR261C	APL6	2
328	H	9	YIR033W	MGA2	2
331	C	5	YMR116C	ASC1	2
331	G	9	YPR070W	MED1	2
331	G	12	YPR074C	TKL1	2
332	A	4	YPR101W	SNT309	2
332	A	7	YJL124C	LSM1	2
332	B	4	YJL115W	ASF1	2
332	C	10	YJL080C	SCP160	2
332	E	3	YJL053W	PEP8	2
332	G	9	YHR059W	FYV4	2
333	D	2	YKR093W	PTR2	2
333	E	1	YLR423C	ATG17	2
335	B	11	YDR005C	MAF1	2
335	F	3	YBR283C	SSH1	2
335	G	12	YCR034W	FEN1	2
335	H	11	YCR065W	HCM1	2
336	B	1	YJL004C	SYS1	2

Plate	Row	Column	Systematic Name	Standard Name	Ranking*
336	G	1	YDL106C	PHO2	2
337	E	10	YGR056W	RSC1	2
340	B	7	YBR058C	UBP14	2
340	C	12	YIL098C	FMC1	2
342	A	7	YJL129C	TRK1	2
342	B	8	YJL175W	-	2
342	E	10	YBR131W	CCZ1	2
342	H	10	YDR074W	TPS2	2
343	C	6	YOR298C-A	MBF1	2
343	F	8	YOR273C	TPO4	2
345	B	9	YBR162C	TOS1	2
345	C	12	YDL020C	RPN4	2
345	E	4	YDL048C	STP4	2
345	H	8	YDR443C	SSN2	2
346	A	4	YDR455C	-	2
346	A	5	YDR456W	NHX1	2
346	C	5	YDR495C	VPS3	2
346	F	9	YGL124C	MON1	2
347	A	7	YGL167C	PMR1	2
347	B	9	YER110C	KAP123	2
347	B	10	YER111C	SWI4	2
348	B	8	YDL074C	BRE1	2
348	B	12	YDR486C	VPS60	2
301	D	6	YAL013W	DEP1	3
301	D	12	YAL004W	-	3
302	F	7	YLR085C	ARP6	3
303	C	5	YML034W	SRC1	3
303	F	8	YMR016C	SOK2	3
303	G	9	YMR031W-A	-	3
304	D	12	YMR207C	HFA1	3
304	G	1	YMR247C	RKR1	3
305	A	9	YMR294W	JNM1	3
305	B	1	YMR299C	DYN3	3

Plate	Row	Column	Systematic Name	Standard Name	Ranking*
305	C	10	YNL325C	FIG4	3
305	F	5	YNL271C	BNI1	3
306	F	1	YOR091W	TMA46	3
306	H	5	YOR322C	LDB19	3
307	G	4	YOL050C	-	3
308	G	5	YPL181W	CTI6	3
308	G	6	YPL182C	-	3
308	G	12	YPL174C	NIP100	3
309	D	1	YPL106C	SSE1	3
309	D	12	YBR173C	UMP1	3
310	C	12	YDR069C	DOA4	3
310	D	4	YDR075W	PPH3	3
310	D	8	YDR080W	VPS41	3
310	G	3	YDR123C	INO2	3
311	B	3	YDR363W	ESC2	3
311	C	12	YDR392W	SPT3	3
311	F	1	YDR433W	-	3
311	H	8	YEL037C	RAD23	3
314	G	10	YHR154W	RTT107	3
315	B	1	YHR207C	SET5	3
315	B	7	YCL005W	LDB16	3
317	C	1	YKL101W	HSL1	3
318	B	1	YOR130C	ORT1	3
318	E	12	YOR216C	RUD3	3
319	F	9	YLR330W	CHS5	3
320	C	2	YLR404W	-	3
322	D	6	YPL089C	RLM1	3
322	G	1	YPL051W	ARL3	3
323	E	4	YPR164W	MMS1	3
323	E	11	YPR179C	HDA3	3
323	H	5	YDR525W-A	SNA2	3
324	A	8	YFR034C	PHO4	3
324	A	11	YFR038W	IRC5	3

Plate	Row	Column	Systematic Name	Standard Name	Ranking*
324	A	12	YFR040W	SAP155	3
324	B	7	YFR048W	RMD8	3
324	E	11	YBL012C	-	3
325	E	10	YGL072C	-	3
325	F	12	YNL237W	YTP1	3
326	A	9	YNL191W	DUG3	3
326	A	10	YNL190W	-	3
326	A	11	YNL187W	-	3
326	B	9	YNL157W	IGO1	3
326	B	11	YNL154C	YCK2	3
326	B	12	YNL148C	ALF1	3
326	E	2	YKR014C	YPT52	3
327	A	10	YDR270W	CCC2	3
327	D	2	YDR310C	SUM1	3
327	F	10	YIL027C	KRE27	3
328	A	3	YIL090W	ICE2	3
328	F	4	YGR270W	YTA7	3
330	D	3	YLR039C	RIC1	3
330	F	2	YNL250W	RAD50	3
330	G	5	YML095C-A	-	3
330	H	3	YML103C	NUP188	3
331	C	11	YMR123W	PKR1	3
332	A	5	YJL127C	SPT10	3
332	G	10	YHR067W	HTD2	3
333	E	2	YLR425W	TUS1	3
334	E	7	YJR126C	VPS70	3
335	C	7	YDR017C	KCS1	3
335	G	5	YCR020W-B	HTL1	3
335	H	9	YCR061W	-	3
336	D	9	YJR033C	RAV1	3
336	G	9	YDL117W	CYK3	3
337	B	1	YDL160C	DHH1	3
337	F	2	YGR064W	-	3

Plate	Row	Column	Systematic Name	Standard Name	Ranking*
337	F	6	YGR105W	VMA21	3
338	C	1	YGL042C	-	3
338	C	8	YGL076C	RPL7A	3
338	D	5	YOR141C	ARP8	3
338	E	7	YIL052C	RPL34B	3
338	F	11	YDR269C	-	3
338	H	4	YPL017C	IRC15	3
339	C	5	YNR009W	NRM1	3
340	F	2	YIL137C	TMA108	3
341	A	12	YNL133C	FYV6	3
341	E	2	YNL080C	EOS1	3
343	A	3	YLR237W	THI7	3
343	H	12	YLR110C	CCW12	3
345	A	4	YBR134W	-	3
345	B	4	YBR156C	SLI15	3
345	B	12	YBR164C	ARL1	3
346	D	1	YDR507C	GIN4	3
346	D	8	YDR516C	EMI2	3
346	H	5	YGL151W	NUT1	3
347	E	5	YER151C	UBP3	3
347	E	7	YER153C	PET122	3
347	H	4	YMR058W	FET3	3

*0 = no growth; 1 = extremely slow growth; 2 = slow growth; 3 = slightly slow growth

Table A-2. Candidates identified in knockout library screen for ZuoC-induced *PDR5-lacZ* activation

New plate ID	Original plate ID	Systematic Name	Standard Name	Fold reduction of WT	Primary Screen Ranking*
2H4	318E4	YOR198C	BFR1	15.7	1
2H9	325C6	YGL013C	PDR1	11.3	1
2A10	325C12	YGL025C	PGD1	9.3	0
1E3	303B1	YML062C	MFT1	7.3	2
2G6	320E11	YLR261C	VPS63	7.3	1
1F2	301H9	YLL040C	VPS13	7.2	2
1F5	305C11	YNL323W	LEM3	6.2	2
2G4	318D10	YOR191W	RIS1	5.5	2
1C3	302H6	YLR119W	SRN2	5.1	2
2D5	318H7	YOR258W	HNT3	5.1	2
1D12	313F7	YHL033C	RPL8A	4.5	2
1H2	302D9	YLR055C	SPT8	4.5	1
2C2	314H8	YHR167W	THP2	4.5	1
1H10	311E12	YDR432W	NPL3	4.4	0
1E12	313H10	YHR012W	VPS29	4.3	2
1H12	314F5	YHR129C	ARP1	4.2	2
1E10	311C10	YDR389W	SAC7	3.5	1
1E4	304C3	YMR179W	SPT21	3.5	2
3B5	332C10	YJL080C	SCP160	3.4	2
1C10	311B12	YDR378C	LSM6	3.4	2
2G9	325C5	YGL012W	ERG4	3.4	0
1B8	308E12	YPL205C	-	3.2	2
3F12	345C12	YDL020C	RPN4	3.2	2
2B10	325D8	YGL043W	DST1	3.1	1
1H6	306F6	YOR290C	SNF2	3.0	0
1F12	314C7	YHR077C	NMD2	3.0	2
2H7	322F9	YPL055C	LGE1	3.0	1
2A7	321A2	YLR315W	NKP2	2.9	1
2E3	317A7	YKL076C	PSY1	2.8	2

New plate ID	Original plate ID	Systematic Name	Standard Name	Fold reduction of WT	Primary Screen Ranking*
2G3	317C9	YKL113C	RAD27	2.8	1
1A12	312G6	YER083C	GET2	2.8	1
1E6	306D8	YOR070C	GYP1	2.8	2
1E11	312A3	YEL044W	IES6	2.7	1
1A10	310H4	YDR136C	VPS61	2.6	1
2C5	318H3	YOR251C	-	2.5	2
2D8	323E9	YPR173C	VPS4	2.4	0
1G10	311E1	YDR418W	RPL12B	2.3	2
2E2	315A8	YHR200W	RPN10	2.2	2
1C12	313E5	YGR214W	RPS0A	2.2	2
2E6	320C11	YLR417W	VPS36	2.1	1
2B4	318A10	YOR124C	UBP2	2.1	2
1D2	301E2	YAL002W	VPS8	2.0	1
1H3	303D12	YML010W-A	-	1.9	1
1G3	303D8	YML013W	SEL1	1.9	2
2B5	318G3	YOR235W	IRC13	1.8	2
1B2	301D6	YAL013W	DEP1	1.8	3
2C10	325E7	YGL066W	SGF73	1.8	1
1H4	304H2	YMR263W	SAP30	1.7	0
1D3	303A12	YML063W	RPS1B	1.7	2
1F3	303C5	YML034W	SRC1	1.7	3
1F10	311C12	YDR392W	SPT3	1.7	3
1B11	311F5	YEL003W	GIM4	1.7	2
2B12	326E2	YKR014C	YPT52	1.6	3
2A4	317F8	YKL160W	ELF1	1.5	2
2G10	326A2	YNL199C	GCR2	1.5	1
2G5	319G10	YLR352W	-	1.5	2
2F7	322A10	YGL252C	RTG2	1.5	2
2D10	325E10	YGL072C	-	1.5	3
1C11	311H5	YEL031W	SPF1	1.5	2
2E5	319D10	YJL154C	VPS35	1.5	1
2H5	319H4	YLR360W	VPS38	1.5	0

New plate ID	Original plate ID	Systematic Name	Standard Name	Fold reduction of WT	Primary Screen Ranking*
1G8	309B2	YPL139C	UME1	1.5	2
1F11	312B6	YEL061C	CIN8	1.4	2
1C8	308G5	YPL181W	CTI6	1.4	3
1A5	305A2	YMR283C	RIT1	1.4	1
1B3	302F7	YLR085C	ARP6	1.3	3
2C4	318B1	YOR130C	ORT1	1.3	3
1D8	308G6	YPL182C	-	1.3	3
2B7	321D6	YDR200C	VPS64	1.3	2
2A8	322G1	YPL051W	ARL3	1.3	3
2H6	320F6	YLR268W	SEC22	1.3	1
1B12	313B7	YGR164W	-	1.3	2
3C7	335H9	YCR061W	-	1.3	3
2F9	325A11	YBL079W	NUP170	1.3	1
2A2	314G4	YHR142W	CHS7	1.3	2
1A8	308C6	YPL253C	VIK1	1.2	2
1H9	310G6	YDR126W	SWF1	1.2	2
1F7	307G4	YOL050C	-	1.2	3
2F5	319F9	YLR330W	CHS5	1.2	3
2H3	317F1	YKL149C	DBR1	1.2	2
2E11	326B11	YNL154C	YCK2	1.2	3
2D7	322A9	YGL250W	-	1.2	1
2F4	318D5	YOR183W	FYV12	1.2	2
2D6	320C2	YLR404W	*SEI1*	1.2	3
2H2	316C8	YLR204W	QRI5	1.2	1
2B3	316E6	YKL007W	CAP1	1.2	1
2C7	321H11	YGL232W	TAN1	1.1	2
1A3	302F1	YLR079W	SIC1	1.1	2
2E9	325A8	YBL072C	RPS8A	1.1	2
1D7	307D6	YOL004W	SIN3	1.1	0
1G2	302D8	YLR054C	OSW2	1.1	1
1E2	301H8	YLL039C	UBI4	1.1	2
2A11	326A10	YNL190W	-	1.1	3

New plate ID	Original plate ID	Systematic Name	Standard Name	Fold reduction of WT	Primary Screen Ranking*
1H7	308B8	YPL265W	DIP5	1.1	2
1C2	301D12	YAL004W	-	1.1	3
2D4	318B3	YOR132W	VPS17	1.1	1
1D5	305C9	YNL324W	-	1.1	2
2F6	320C12	YLR418C	CDC73	1.1	1
1E7	307E4	YOL018C	TLG2	1.1	0
2A12	326D9	YKR007W	MEH1	1.0	2
1G11	312D1	YER020W	GPA2	1.0	2
2E4	318C2	YOR153W	PDR5	1.0	0
2C11	326A12	YNL183C	NPR1	1.0	2
1H11	312G1	YER074W	RPS24A	1.0	2
1F9	310F12	YDR120C	TRM1	1.0	1
1G5	305C12	YNL322C	KRE1	1.0	2
2G11	326C9	YKL207W	-	1.0	2
1F8	308H11	YPL161C	BEM4	1.0	2
1D11	311H8	YEL037C	RAD23	1.0	3
2F11	326B12	YNL148C	ALF1	0.9	3
1E9	310D8	YDR080W	VPS41	0.9	3
1F6	306E11	YOR089C	VPS21	0.9	2
2F2	315B1	YHR207C	SET5	0.9	3
2D12	326F4	YKR042W	UTH1	0.9	2
1B4	303F7	YMR015C	ERG5	0.9	0
1G12	314C9	YHR079C	IRE1	0.9	2
1D10	311C9	YDR388W	RVS167	0.9	1
1G7	308A4	YGR078C	PAC10	0.9	2
2E10	325F12	YNL237W	YTP1	0.9	3
2B6	320A1	YLR373C	VID22	0.9	1
1A2	301C8	YAL026C	DRS2	0.8	1
2B8	323A3	YPL008W	CHL1	0.8	2
1G6	306F1	YOR091W	TMA46	0.8	3
1C6	306D6	YOR068C	VAM10	0.8	1
1H8	309C1	YPL120W	VPS30	0.8	2

New plate ID	Original plate ID	Systematic Name	Standard Name	Fold reduction of WT	Primary Screen Ranking*
1E8	308G12	YPL174C	NIP100	0.7	3
1H5	305D6	YNL307C	MCK1	0.7	2
1A4	303E9	YML001W	YPT7	0.7	2
2C6	320A2	YLR374C	-	0.7	2
2F8	323G6	YCR094W	CDC50	0.7	2
1D9	310D4	YDR075W	PPH3	0.7	3
1D6	306D7	YOR069W	VPS5	0.7	1
1G9	310G3	YDR123C	INO2	0.7	3
2A6	319H11	YLR371W	ROM2	0.7	2
2H12	327B3	YDR276C	PMP3	0.7	2
2G12	327A10	YDR270W	CCC2	0.7	3
2C8	323E4	YPR164W	MMS1	0.6	3
2F10	325G11	YNL224C	SQS1	0.6	2
1C7	307D3	YOL001W	PHO80	0.6	1
1B7	307B7	YOR360C	PDE2	0.6	2
3B4	331C5	YMR116C	ASC1	0.6	2
2E12	326H12	YDR257C	SET7	0.5	2
2F12	327A9	YDR266C	-	0.5	2

*0 = no growth; 1 = extremely slow growth; 2 = slow growth; 3 = slightly slow growth

Figure A-1. Effect of individual gene deletions on *PDR5-lacZ* activation by ZuoC. Strains from the yeast deletion collection were co-transformed with vector containing DNA encoding either a tandem affinity purification tag (TAP) or TAP fused to residues 365-433 of Zuo1 along with vector containing the *PDR5-lacZ* reporter. The average ß-galactosidase activity of two transformants of each was quantified and reported as fold activation of cells expressing TAP-ZuoC to cells expressing TAP. Each panel represents an independent experiment. Wild-type (wt) and Δ*pdr1* strains were used as controls in each experiment.

Figure A-1

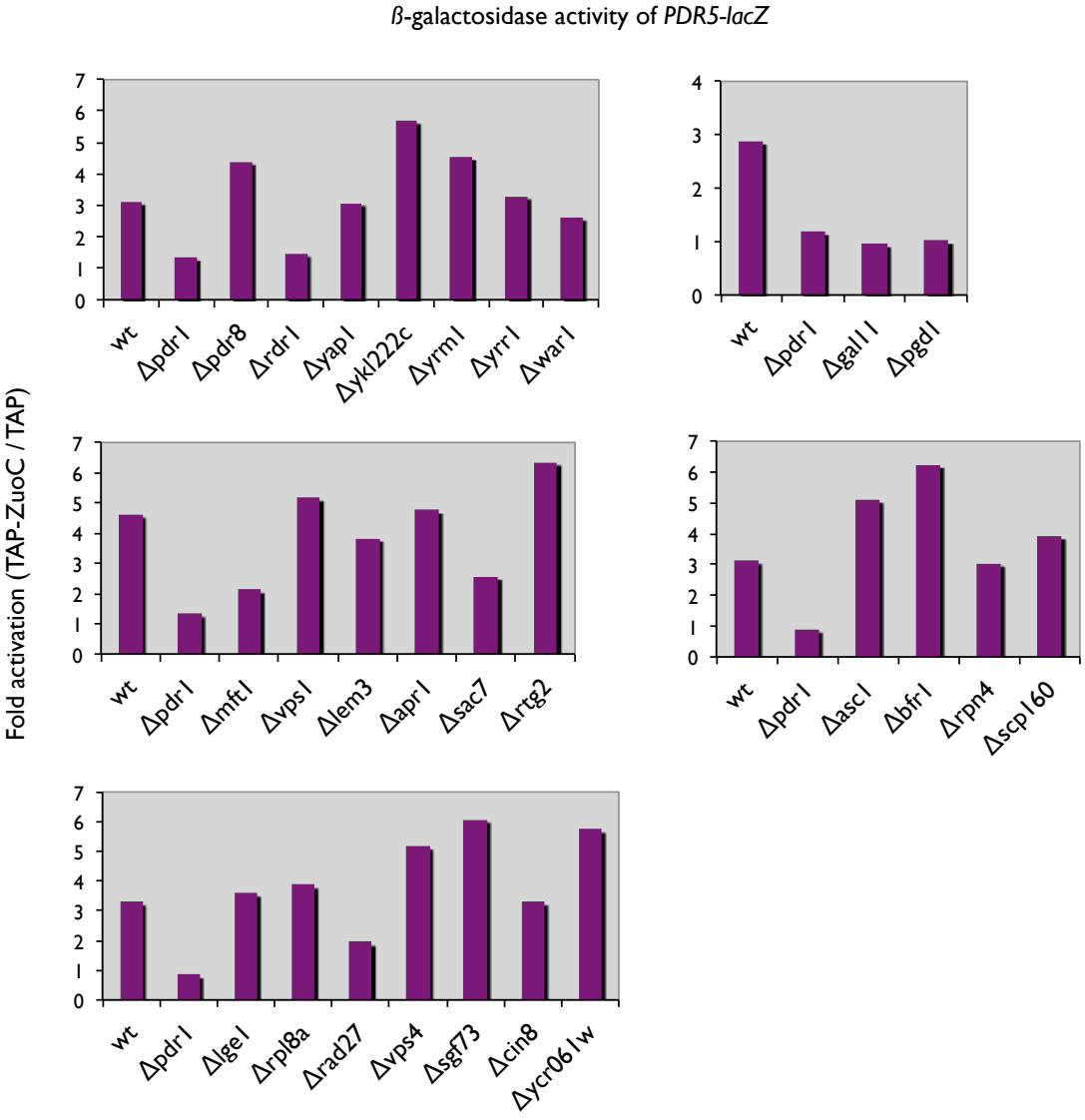
ß-galactosidase activity of PDR5-lacZ
Fold activation (TAP-ZuoC / TAP)
wt
Δpdr1
Δpdr8
Δrdr1
Δyap1
Δykl222c
Δyrm1
Δyrr1
Δwar1
wt
Δpdr1
Δgal11
Δpgd1
wt
Δpdr1
Δmft1
Δvps1
Δlem3
Δapr1
Δsac7
Δrtg2
wt
Δpdr1
Δasc1
Δbfr1
Δrpn4
Δscp160
wt
Δpdr1
Δlge1
Δrpl8a
Δrad27
Δvps4
Δsgf73
Δcin8
Δycr061w

Global analysis of the DNA binding profiles of $Ssz1_{S295F}$ and $Zuo1_{\Delta chg}$ by ChIP-chip

To determine whether Zuo1 and Ssz1 are present on the promoters of genes involved in the PDR regulon, I carried out whole-genome chromatin immunoprecipitation analysis (ChIP-chip). ChIP was performed for Zuo1 using α-Zuo1 antibody #63980 on lysates from Δ*zuo1* cells expressing $Zuo1_{\Delta chg}$ ($Zuo1_{\Delta 285-364}$) from a cen plasmid. ChIP for Ssz1 was performed using α-Ssz1 antibody #133 on lysates from Δ*zuo1* cells (to ensure Ssz1 was not ribosome associated) expressing $Ssz1_{S295F}$ from a cen plasmid. DNA was amplified and labeled using ligation-mediated PCR and sent to NimbleGen for hybridization to high-density tiling microarrays (Roche NimbleGen, Inc.). After promising results were obtained from these data, I began doing in-house hybridizations and data extraction using the same arrays.

I first analyzed these data by identifying peaks by visual observation that showed approximately two-fold enrichment in the ChIP sample over the input sample (total genomic DNA). The $Ssz1_{S295F}$ Δ*zuo1* sample showed low background across the genome with 143 peaks I identified as significant. The $Zuo1_{\Delta chg}$ sample also showed low background with 70 significant peaks. Together these strains showed an overlap of 39 peaks. To search for functional enrichments within the sets of genes bound by Ssz1 and Zuo1, I used the program FunSpec (Robinson et al., 2002). Some of the most significantly enriched groups identified included genes encoding proteins involved in cellular detoxification and lipid transport, consistent with a role in the PDR pathway. I also found that a significant number of the genes bound by $Ssz1_{S295F}$ and $Zuo1_{\Delta chg}$ overlapped with the set of genes previously identified by ChIP-chip analysis to be bound by the TF Pdr1 ((Fardeau et al., 2007), Table A-3, Figure A-2). To investigate the significance of this observed enrichment for Pdr1 target genes, I used a hypergeometric

distribution to calculate a p-value for this enrichment. Based on the identification of 30 Pdr1-bound genes in the genome, identifying 20 Pdr1 target genes out of the 143 peaks representing binding by $Ssz1_{S295F}$ corresponds to a p-value of approximately 2.19×10^{-26}. Identifying 3 Pdr1 target genes out of the 70 peaks representing $Zuo1_{\Delta chg}$ binding corresponds to a p-value of 4.6×10^{-3} (note that this construct also showed lower PDR activation than $Ssz1_{S295F}$). Finding 3 Pdr1 target genes out of the 39 peaks that represent binding of both $Ssz1_{S295F}$ and $Zuo1_{\Delta chg}$ corresponds to a p-value of approximately 8.8×10^{-4}. Thus, both $Zuo1_{\Delta chg}$ and $Ssz1_{S295F}$ showed significant enrichment for binding to genes involved in the PDR regulon and genes bound by the TF Pdr1. Furthermore, these data were extremely reproducible, as a similar binding profile was observed upon testing a number of biological and technical replicates, which included data sent from NimbleGen as well as data collected in house.

Although these data appeared very promising and highly statistically significant, these experiments were performed using polyclonal antibodies. Thus, I decided to perform two additional experiments to confirm the validity of the observed binding profiles. Since $Ssz1_{S295F}$ showed the strongest data, I performed both controls for these data. First, I expressed $Ssz1_{S295F}$ in a Δ*zuo1* Δ*pdr1* strain and found a nearly identical binding profile for $Ssz1_{S295F}$ to the one observed in the strain containing Pdr1 (Figure A-3). Though it is possible that Ssz1 can bind to PDR promoters in a Pdr1-independent manner and thus cannot be considered a true control experiment, this result was surprising to us. I next performed a background control by testing whether the α-Ssz1 antibody could IP any DNA in a Δ*ssz1* strain. Surprisingly, the binding observed in the Δ*ssz1* strain was nearly identical to the binding profile observed for $Ssz1_{S295F}$ (Figure A-3), suggesting that the majority of the binding observed for $Ssz1_{S295F}$ was background.

The only candidate that remained after subtracting this background binding was *PDR5*. This result was confirmed by qPCR and by an independent pulldown using TAP-tagged $Ssz1_{S295F}$.

As Ssz1 and Zuo1 upregulate only a small number of genes in the genome based on microarray data, it is possible that only one or a few binding sites might be identified for these proteins. However, it is unclear why such a strong statistically significant enrichment for Pdr1 target genes was identified in the control experiment as background. It is possible that there is something unique about these genes, such as abundance, propensity for amplification, or repetition, that makes them unusually prone to background signal in this type of experiment. These data were, however, subjected to computational repeat sequence masking (Tietjen et al., 2010) to help eliminate some of the concern of repetitive sequences. Furthermore, ChIP-chip analysis has previously been performed for the TF Pdr1 and binding was observed at a similar set of genes as the one I identified as background. This experiment was performed by integrating DNA encoding thirteen Myc tags upstream of *PDR1* and using an α-Myc antibody to perform ChIP. To control for nonspecifically enriched DNA, four ChIP experiments were carried out using an untagged strain (Fardeau et al., 2007). Though there may have been some background signal at these genes, this control makes it seem unlikely that this set of genes is simply unsuitable for this type of analysis. A simpler explanation is that the binding data for $Ssz1_{S295F}$ are real and that there was a problem with the control experiment. I did check the Δ*ssz1* strain to ensure that the deletion cassette could be amplified and that Ssz1 protein could not be detected by western blot. However, it is possible that samples got mixed up, that the arrays did not strip properly from previous uses, or that an equally simple issue could explain the surprisingly similar binding profiles of $Ssz1_{S295F}$ and the control. Therefore, to completely discount these data

or properly validate them, it would be important to repeat the Δ*ssz1* control ChIP and perform either qPCR on several candidate promoters or hybridize the DNA to fresh microarrays. Technical issues with amplification and labeling at the time made this difficult and some troubleshooting might be necessary. Another alternative would be to use tagged forms of Ssz1 and Zuo1 so that any antibody-specific background could be eliminated by the use of different antibodies or beads.

A proper background control experiment was never carried out for the $Zuo1_{\Delta chg}$ data. However, the genes I identified as background in the Δ*ssz1* control eliminated all genes bound by $Zuo1_{\Delta chg}$ that were associated with PDR. Though different antibodies were used for the Ssz1 and Zuo1 experiments, I became concerned that the peaks observed for $Zuo1_{\Delta chg}$ may also be background. It is interesting to note, however, that I also acquired "negative control" data from three other labs and from additional data collected in our lab using different antibodies. Though some genes associated with PDR did show some background signal, many did not show any background in any of these data sets. Though these data do not represent proper controls for the $Ssz1_{S295F}$ and $Zuo1_{\Delta chg}$ experiments, they do suggest that many PDR genes are not simply unsuitable for this type of analysis because of consistent background signal. These findings reiterate the importance of repeating the proper negative controls in order to validate or disregard the $Ssz1_{S295F}$ and $Zuo1_{\Delta chg}$ data.

Table A-3. $Zuo1_{\Delta chg}$ and $Ssz1_{S295F}$ bind to a significant number of Pdr1 target genes

Genes bound by Pdr1*	Contains PDRE	Upregulated by ZuoC	Bound by $Zuo1_{\Delta chg}$	Bound by $Ssz1_{S295F}$
ICT1/YLR099W-A	**yes**	**yes**	no	no
PDR10/SNC2	**yes**	no	no	no
PDR16	**yes**	no	no	**yes**
PDR3/YBL006C	**yes**	no	no	no
PDR5/YOR152C	**yes**	**yes**	no	**yes**
RPN4	**yes**	no	no	no
RSB1	**yes**	no	no	**yes**
SNQ2	**yes**	no	no	**yes**
TPO1	**yes**	no	no	no
VHR1	**yes**	no	**yes**	**yes**
YGR035C/YGR035W-A	**yes**	**yes**	no	no
YMR102C	**yes**	no	no	no
ADH1	no	no	no	**yes**
CCW12/HOG1	**yes**	no	no	**yes**
CWP2	**yes**	no	no	**yes**
ENO1/PUP2	no	no	no	**yes**
GLN1/VMA13	no	no	**yes**	**yes**
GLY1/IES6	no	no	no	**yes**
MNN4	**yes**	no	no	**yes**
PMA1	no	no	**yes**	**yes**
PUT4/PYK2	**yes**	no	no	no
ROX1/YPR063C	no	no	no	**yes**
RPS5	no	no	no	no
SNA2	no	no	no	**yes**
TDH1/YJL051W	no	no	no	**yes**
TDH2	no	no	no	**yes**
TEF1	no	no	no	**yes**
UTH1	no	no	no	**yes**
UTR5/ANP1	no	no	no	**yes**
YPL068C	**yes**	no	no	no

*Based on ChIP-chip data reported in (Fardeau et al., 2007).

Figure A-2. Binding of $Zuo1_{\Delta chg}$ and $Ssz1_{S295F}$ to promoters of genes involved in PDR. Examples of binding of $Zuo1_{\Delta chg}$ and $Ssz1_{S295F}$ to promoters of genes shown or predicted to be involved in the PDR regulon. Data shown are normalized ratios of IP DNA to input DNA as observed using the software SignalMap (Roche NimbleGen, Inc.).

Figure A-2

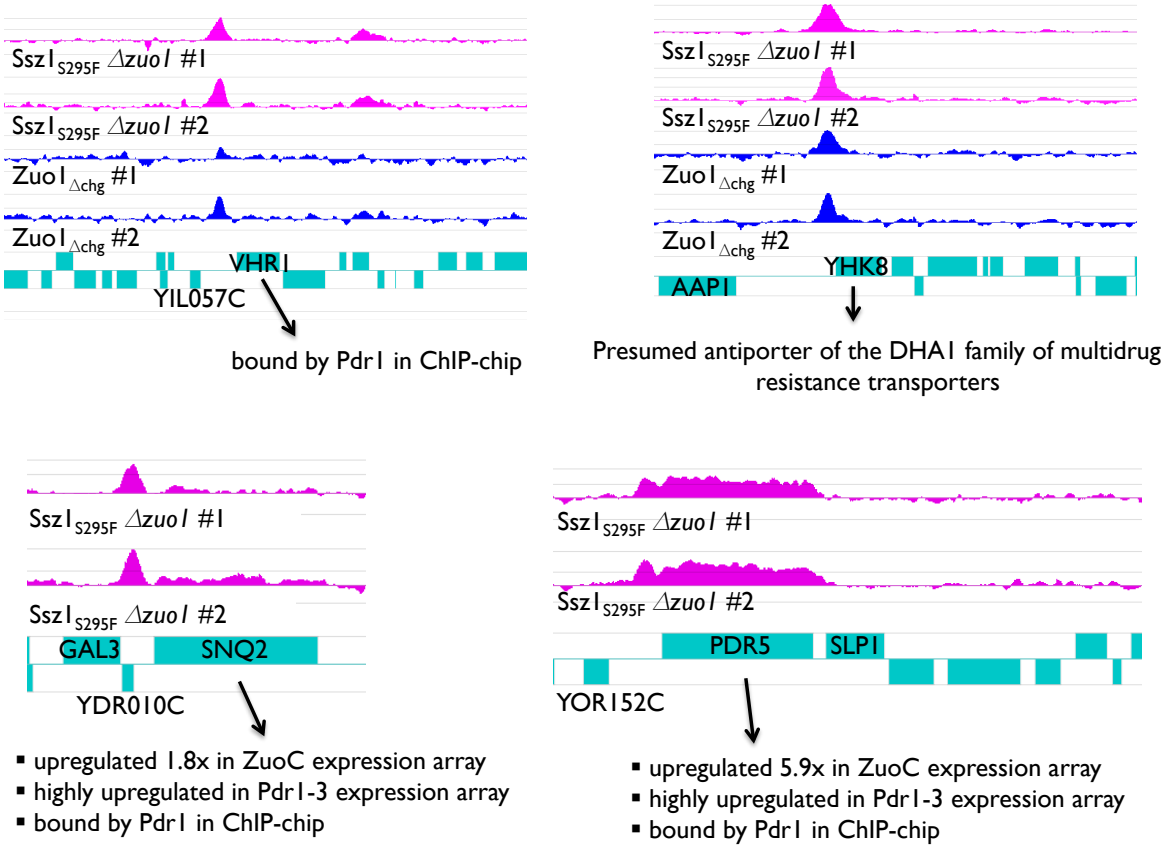
Ssz1S295F Δzuo1 #1
Ssz1S295F Δzuo1 #2
Zuo1Δchg #1
Zuo1Δchg #2
VHR1
YIL057C
bound by Pdr1 in ChIP-chip
Ssz1S295F Δzuo1 #1
Ssz1S295F Δzuo1 #2
Zuo1Δchg #1
Zuo1Δchg #2
YHK8
AAP1
Presumed antiporter of the DHA1 family of multidrug resistance transporters
Ssz1S295F Δzuo1 #1
Ssz1S295F Δzuo1 #2
GAL3
SNQ2
YDR010C
▪ upregulated 1.8x in ZuoC expression array
▪ highly upregulated in Pdr1-3 expression array
▪ bound by Pdr1 in ChIP-chip
Ssz1S295F Δzuo1 #1
Ssz1S295F Δzuo1 #2
PDR5
SLP1
YOR152C
▪ upregulated 5.9x in ZuoC expression array
▪ highly upregulated in Pdr1-3 expression array
▪ bound by Pdr1 in ChIP-chip

Figure A-3. Binding of $Ssz1_{S295F}$ to promoters of genes associated with PDR appears to be predominantly nonspecific. Examples of binding of Ssz1S295F to promoters of genes shown or predicted to be involved in the PDR regulon in Δzuo1 and Δzuo1Δpdr1 strains compared with nonspecific DNA IP-ed by the a-Ssz1 antibody in a Δssz1 strain. Data shown are normalized ratios of IP DNA to input DNA as observed using the software SignalMap (Roche NimbleGen, Inc.).

Figure A-3

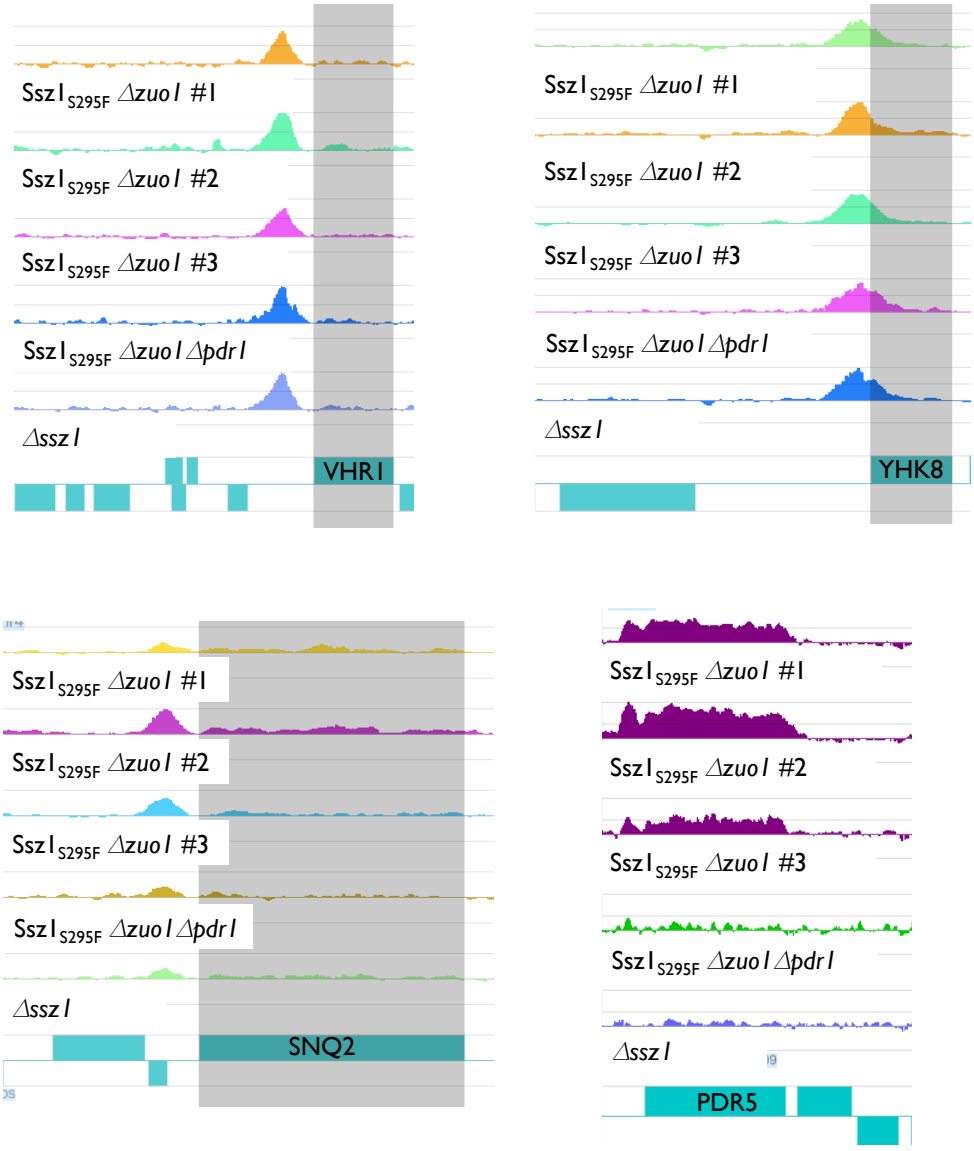
Ssz1 S295F Δzuo1 #1
Ssz1 S295F Δzuo1 #2
Ssz1 S295F Δzuo1 #3
Ssz1 S295F Δzuo1 Δpdr1
Δssz1
VHR1
Ssz1 S295F Δzuo1 #1
Ssz1 S295F Δzuo1 #2
Ssz1 S295F Δzuo1 #3
Ssz1 S295F Δzuo1 Δpdr1
Δssz1
YHK8
Ssz1 S295F Δzuo1 #1
Ssz1 S295F Δzuo1 #2
Ssz1 S295F Δzuo1 #3
Ssz1 S295F Δzuo1 Δpdr1
Δssz1
SNQ2
Ssz1 S295F Δzuo1 #1
Ssz1 S295F Δzuo1 #2
Ssz1 S295F Δzuo1 #3
Ssz1 S295F Δzuo1 Δpdr1
Δssz1
PDR5

Nucleocytoplasmic shuttling of Zuo1 and Ssz1

In an effort to determine if Ssz1 and Zuo1 activate the nuclear transcription factor Pdr1 directly, I decided to test whether Zuo1 and Ssz1 undergo nucleocytoplasmic shuttling. Using the NetNES server, I identified a predicted nuclear export signal (NES) in both the C-terminus of Zuo1 and the N-terminus of Ssz1 (la Cour et al., 2004). To test whether these proteins translocate to the nucleus, I obtained a yeast strain containing a Crm1 T539C mutation that renders the major nuclear exporter sensitive to the drug Leptomycin B (LMB) and allows Crm1-mediated nuclear export to be blocked. I crossed this strain to strains with integrated copies of GFP-tagged *SSZ1*, *ZUO1*, or *SSB1* as a control. GFP-tagged Ssz1 and Zuo1 showed predominantly cytoplasmic localization and appeared to be excluded from the nucleus even upon treatment with LMB. Ssb1, on the other hand, showed slight nuclear accumulation upon drug treatment, though it maintained much of its cytoplasmic signal. Though it is possible that small amounts of Zuo1 or Ssz1 shuttle into the nucleus or that this shuttling occurs rapidly, I was not able to trap these proteins in the nucleus using this method. It is also possible that these proteins do undergo nucleocytoplasmic shuttling, but are exported via a Crm1-independent pathway and, therefore, cannot be blocked by LMB treatment.

I next tested whether Ssz1 and Zuo1 translocate to the nucleus under PDR-inducing conditions or upon dissociation from the ribosome. I found that an mcherry fusion of Zuo1 lacking its charged ribosome binding domain showed significant nuclear accumulation, while an mcherry fusion of full-length protein did not, even upon overexpression (Figure A-4A). The mcherry-Zuo1$_{\Delta chg}$ fusion also rendered cells resistant to the drug cycloheximide, while mcherry-Zuo1 did not, suggesting that Zuo1 may translocate to the nucleus to induce PDR. As Zuo1

overexpression likely results in some protein dissociated from the ribosome (though I did not test ribosome association for this fusion), translocation may occur upon unfolding of Zuo1's C-terminal domain. It is possible that a nuclear localization signal (NLS) is sequestered in the folded C-terminal domain. I also found that a C-terminally-tagged fusion of Zuo1 lacking its charged domain was able to translocate to the nucleus, however, this construct did not induce PDR. As I have discovered that the extreme C-terminal residues of Zuo1 are required for PDR induction, I think that the mcherry fusion might be interfering with PDR induction in this context. GFP-tagged Ssz1 also showed strong nuclear accumulation when expressed in a Δ*zuo1* strain, which would result in all Ssz1 to become ribosome dissociated (Figure A-4B). Thus, both Ssz1 and Zuo1 are capable of translocation to the nucleus, consistent with a direct model of Pdr1 activation. However, the signal that causes these proteins to dissociate from the ribosome and undergo this nuclear shuttling it not known.

All fusions of Zuo1 and Ssz1 that I tested for localization are summarized in Table A-4. Lines highlighted in teal indicate constructs that showed at least some PDR induction as observed by growth of cells expressing the fusion in the presence of the drug cycloheximide. Text shown in red represents data that I collected personally. Text shown in gray represents assumptions made based on data of a similar nature that were not collected using the specific construct indicated.

Figure A-4. Zuo1 and Ssz1 translocate to the nucleus when dissociated from the ribosome. (A) An mcherry fusion of Zuo1 lacking its charged ribosome-binding domain shows strong nuclear accumulation, while full-length Zuo1 shows predominantly cytosolic localization. (B) GFP-tagged Ssz1 shows predominantly cytosolic localization in wt cells, but shows nuclear accumulation in a strain lacking Zuo1.

Figure A-4

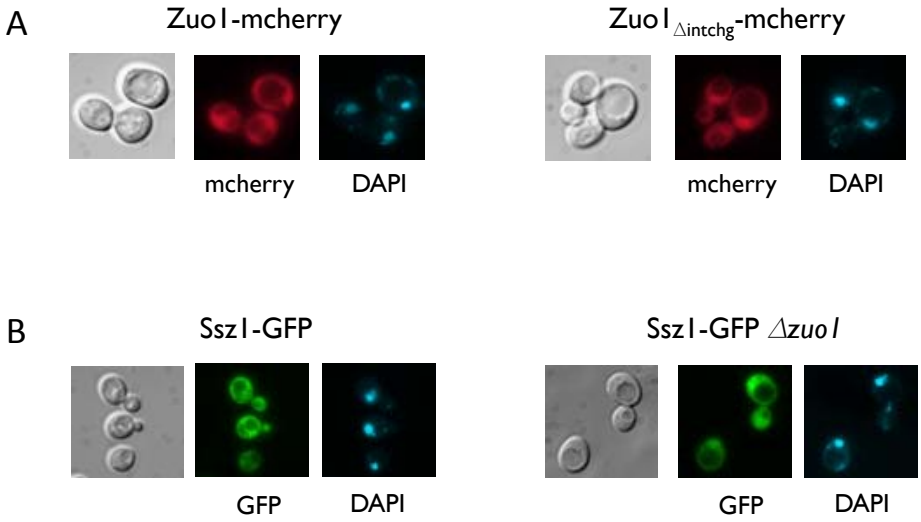
A
Zuo1-mcherry
mcherry
DAPI
Zuo1 △intchg-mcherry
mcherry
DAPI
B
Ssz1-GFP
GFP
DAPI
Ssz1-GFP Δzuo1
GFP
DAPI

Table A-4. Fluorescently tagged fusions of Ssz1 and Zuo1 tested for localization

Copy #	Promoter	Gene Name	Ribosome Association	PDR	Localization	C-terminal Fold (Zuo1)
cen	ZUO1	mcherry	-	-	cytoplasm	-
cen	ZUO1	Zuo1-mcherry	on	-	cytoplasm	folded
cen	ZUO1	$Zuo1_{\Delta intchg}$-mcherry	off	-	nucleus	unfolded
cen	ZUO1	mcherry-$Zuo1_{\Delta chg}$	off	-	nucleus	unfolded
cen	GPD	mcherry-Zuo1	partially off	-	cytoplasm	folded
cen	GPD	mcherry-$Zuo1_{\Delta chg}$	off	+	nucleus	unfolded
cen	GPD	mcherry-ZuoC	off	++		unfolded
integrated	ZUO1	Zuo1-GFP Crm1 T539C	on	-	cytoplasm	folded
integrated	SSZ1	Ssz1-GFP Crm1 T539C	on	-	cytoplasm	-
integrated	SSZ1	Δ*zuo1* Ssz1-GFP	off		nucleus	-

Δintchg = Δ174-365
Δchg = Δ285-364

Identification of a structural homolog of Zuo1's C-terminal domain

In its autoinhibited form, the C-terminal domain of Zuo1 forms a left-handed four-helix bundle. In an effort to better understand the function of this domain, I searched for structural homologs of the domain using the DALI server (Holm and Rosenstrom, 2010). The most significant structural homolog of Zuo1's C-terminus identified was the DHB (DAXX helical bundle) domain of the protein DAXX (Z-score=6.5, RMSD=2.9 Å). DAXX has been shown to have diverse roles in transcription and cell cycle regulation (Escobar-Cabrera et al., 2010; Giovinazzi et al., 2011). This is especially interesting in light of recent data implicating Pdr1 in the regulation of cellular growth during the diauxic shift and the role of higher eukaryotic orthologs of Zuo1 in cell cycle regulation. DAXX has been shown to bind to a short peptide at the N-terminus of the Ras-association domain family 1C (Rass1fC) using a hydrophobic pocket formed by helices 2 and 5 of the DHB domain (Escobar-Cabrera et al., 2010). An alignment of the structures of Zuo1's C-terminal domain and the DHB domain of DAXX indicates that this hydrophobic pocket lies in the same region as the hydrophobic residues I identified as important for interaction of Zuo1 with the TF Pdr1 (Figure A-5).

Figure A-5. Structural alignment of Zuo1's C-terminal domain and the DAXX helical bundle domain. Overlay of the ribbon diagrams of Zuo1's C-terminal domain (green) and the DAXX helical bundle (DHB) domain (pink) in complex with the Rass1fC peptide (light orange). Side chains of residues of the DHB domain and Rass1fC peptide that interact with each other are shown. Side chains of residues of Zuo1's C-terminal domain that interact with the TF Pdr1 are shown.

Figure A-5

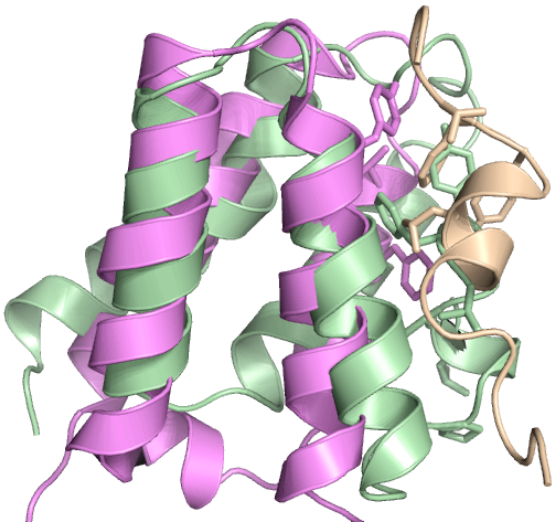

Testing the effect of the hyperactive S427G allele on Zuo1 C-terminal structure

In chapter two I presented data indicating that alteration of serine 427 to glycine results in enhanced PDR induction by $Zuo1_{365-433}$. In chapter three I show that unfolding of Zuo1's C-terminal domain has an activating effect on its transcriptional properties. I, therefore, wanted to determine if the enhanced activity of the S427G mutant is due to its ability to perturb protein structure. To test this, I compared the ^{15}N-^{1}H HSQC spectra of the folded C-terminal domain ($Zuo1_{348-433}$) with and without the S427G alteration. This analysis revealed a very similar pattern of peak dispersion between the two samples (Figure A-6A), suggesting that the structure of the C-terminal domain is not destabilized by S427G. Consistent with the model that disruption of structure is critical to activity, the S427G alteration was not sufficient to activate the folded $Zuo1_{348-433}$ fragment (Figure A-6B). These data suggest that the enhanced activity of S427G is not due to structural perturbation, but that serine 427 is likely a key residue for PDR induction. Data presented in chapter two indicate that Zuo1's C-terminus containing the S427G alteration interacts more strongly with Pdr1 in the yeast two-hybrid system. Thus, this alteration may better facilitate the interaction between Zuo1's C-terminus in its unfolded conformation and the transcription factor.

Figure A-6. The hyperactive S427G allele does not unfold Zuo1's C-terminal domain or activate the folded domain. (A) S427G does not unfold the C-terminal domain. Overlay of the ^{15}N–^{1}H HSQC spectra of Zuo1 residues 348-433 with and without the S427G alteration. (B) S427G enhances PDR activity of the unfolded $Zuo1_{365-433}$ fragment, but does not activate the folded $Zuo1_{348-433}$ fragment. Wt cells were transformed with plasmid DNA encoding TAP or TAP tag fusions of $Zuo1_{365-433}$ or $Zuo1_{348-433}$ with or without the S427G mutation. Serial dilutions of cells containing the indicated plasmids were spotted onto media without (-) or with (+) the drug cycloheximide

Figure A-6

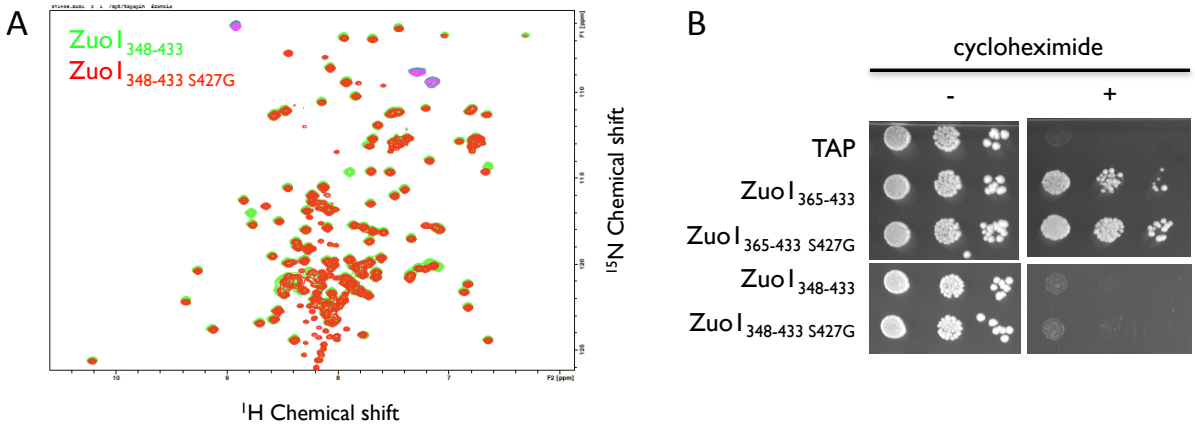
A
Zuo1 348-433
Zuo1 348-433 S427G
15N Chemical shift
1H Chemical shift
B
cycloheximide
-
+
TAP
Zuo1 365-433
Zuo1 365-433 S427G
Zuo1 348-433
Zuo1 348-433 S427G

PDR activation, ribosome association, and C-terminal fold of Zuo1 mutants

Tables A-5 through A-7 included on the following pages summarize the PDR activity, ribosome association, and C-terminal fold of the majority of mutants of Zuo1 or Zuo1 C-terminal fragments I tested. Lines highlighted in teal indicate constructs that showed at least some PDR induction as observed by growth in the presence of the drug cycloheximide and/or activation of the *PDR5-lacZ* reporter. Text shown in red represents data that I collected personally. Text in black represents data collected by another member of the lab that are either previously published or preliminary in nature. Text shown in gray represents assumptions made based on data of a similar nature that were not collected using the specific construct indicated.

Table A-5. Correlation between PDR induction, ribosome association, and C-terminal fold by Zuo1 variants

Copy #	Promoter	Gene Name	Expressed?	PDR induction	Ribosome Association	C-terminal fold
cen	ZUO1	Zuo1	yes	-	yes	folded
cen	TEF	Zuo1	yes	-	on	folded
cen	GPD	Zuo1	yes	-	partially off	folded
2μ	GPD	Zuo1	yes	-	partially off	folded
cen	ZUO1	Zuo1 L411R		-		unfolded
cen	TEF	Zuo1 L411R		+		unfolded
cen	GPD	Zuo1 L411R	yes	++		unfolded
cen	TEF	Zuo1 HPD-AAA		-		folded
cen	GPD	Zuo1 HPD-AAA		-	partially off	folded
cen	ZUO1	$Zuo1_{\Delta chg}$ / $Zuo1_{\Delta 285-364}$	yes	+	off	unfolded
cen	GPD	$Zuo1_{\Delta chg}$ / $Zuo1_{\Delta 285-364}$	yes	+	off	unfolded
cen	ZUO1	$Zuo1_{\Delta chg}$ L411R	yes	+	off	unfolded
cen	ZUO1	$Zuo1_{\Delta 282-331}$	yes	-	partially off	
cen	ZUO1	$Zuo1_{\Delta 310-337}$	yes	-	partially off	
cen	GPD	$Zuo1_{\Delta 310-337}$		-	partially off	
cen	ZUO1	$Zuo1_{\Delta 310-365}$	yes	+	off	unfolded
cen	ZUO1	$Zuo1_{\Delta 340-354}$		-		
cen	ZUO1	$Zuo1_{\Delta 285-347}$	yes	-	off	
cen	ZUO1	Zuo1 299-301Ala		-		
cen	GPD	Zuo1 299-301Ala	yes	-	partially off	
cen	ZUO1	Zuo1 351-356Ala		-		

Table A-6. Correlation between PDR induction and C-terminal fold by Zuo1 C-terminal fragments

Copy #	Promoter	Tag	Gene Name	PDR induction	Expressed?	C-terminal Fold
cen	GPD	TAP	$Zuo1_{348-433}$	-	yes	folded
cen	GPD	TAP	$Zuo1_{348-433}$ S427G	-	yes	folded
cen	GPD	TAP	$Zuo1_{348-433}$ K351A/K355A	-	yes	
cen	GPD	TAP	$Zuo1_{348-433}$ K351P/K355P	++	yes	unfolded
cen	GPD	TAP	$Zuo1_{348-433}$ D386R	-	yes	
cen	GPD	TAP	$Zuo1_{348-433}$ D390R	-	yes	
cen	GPD	TAP	$Zuo1_{348-433}$ D386R/D390R	+ (weak)	yes	unfolded
cen	GPD	TAP	$Zuo1_{348-433}$ D390W	-	yes	
cen	GPD	TAP	$Zuo1_{348-433}$ L411R	++	yes	unfolded
cen	GPD	TAP	$Zuo1_{348-433}$ S427G/K351A/K355A	-	yes	
cen	GPD	TAP	$Zuo1_{348-433}$ S427G/D386R	+	yes	
cen	GPD	TAP	$Zuo1_{348-433}$ S427G/D390R	++	yes	
cen	GPD	TAP	$Zuo1_{348-433}$ S427G/D386R/D390R	+++	yes	unfolded
cen	GPD	TAP	$Zuo1_{348-433}$ S427G/D390W	+	yes	
cen	GPD	TAP	$Zuo1_{348-433}$ S427G/L411R	+++	yes	unfolded
cen	GPD	8HT	$Zuo1_{348-433}$	-	couldn't detect	folded
cen	GPD	8HT	$Zuo1_{348-433}$ D386R/D390R	-	couldn't detect	unfolded
cen	GPD	8HT	$Zuo1_{348-433}$ L411R	-	couldn't detect	unfolded
cen	GPD	-	$Zuo1_{348-433}$	-	(no Ab)	folded
cen	GPD	TAP	$Zuo1_{354-433}$	-	runs small	
cen	GPD	TAP	$Zuo1_{358-433}$	+	yes	partially folded
cen	GPD	TAP	$Zuo1_{358-433}$ S427G	++ (not sure how high)	yes	partially folded
cen	GPD	TAP	$Zuo1_{358-433}$ L411R	++	yes	unfolded

Copy #	Promoter	Tag	Gene Name	PDR induction	Expressed?	C-terminal Fold
cen	GPD	8HT	$Zuo1_{358-433}$	+ (less than TAP)	couldn't detect	partially folded
cen	GPD	8HT	$Zuo1_{358-433}$ D386R/D390R	+ (very little)	couldn't detect	unfolded
cen	GPD	8HT	$Zuo1_{358-433}$ L411R	+ (less than TAP)	couldn't detect	unfolded
cen	GPD	-	$Zuo1_{358-433}$	-	(no Ab)	partially folded
cen	GPD	TAP	$Zuo1_{365-433}$ / ZuoC	++	yes	unfolded
2µ	GPD	TAP	$Zuo1_{365-433}$ / ZuoC	++	yes	unfolded
cen	GPD	TAP	ZuoC D370A	++	yes	unfolded
cen	GPD	TAP	ZuoC D372A	++	yes	unfolded
cen	GPD	TAP	ZuoC K373A	++	runs high	unfolded
cen	GPD	TAP	ZuoC E379A	++	yes	unfolded
cen	GPD	TAP	ZuoC L411R	++	yes	unfolded
cen	GPD	TAP	ZuoC S421A	++	yes	unfolded
cen	GPD	TAP	ZuoC G422D	-		unfolded
cen	GPD	TAP	ZuoC G422A	++	yes	unfolded
cen	GPD	TAP	ZuoC K423A	++	yes	unfolded
cen	GPD	TAP	ZuoC L424A	++	yes	unfolded
cen	GPD	TAP	ZuoC P425A	+ (weak)	yes	unfolded
cen	GPD	TAP	ZuoC S426G	+		unfolded
cen	GPD	TAP	ZuoC S426A	++ (at least)	yes	unfolded
cen	GPD	TAP	ZuoC S426D	-	yes	unfolded
cen	GPD	TAP	ZuoC S427G	+++	yes	unfolded
cen	GPD	TAP	ZuoC S427A	++	yes	unfolded
cen	GPD	TAP	ZuoC S427D	-	yes	unfolded
cen	GPD	TAP	ZuoC S427N	++		unfolded
cen	GPD	TAP	ZuoC S427F	+		unfolded
cen	GPD	TAP	ZuoC L428G	-	yes	unfolded
cen	GPD	TAP	ZuoC L428A	-	yes	unfolded
cen	GPD	TAP	ZuoC L429G	-	yes	unfolded
cen	GPD	TAP	ZuoC L429A	-	yes	unfolded
cen	GPD	TAP	ZuoC S430G	++ (at least)	yes	unfolded
cen	GPD	TAP	ZuoC S430A	++	yes	unfolded
cen	GPD	TAP	ZuoC Y431A	-	yes	unfolded
cen	GPD	TAP	ZuoC F432A	+	yes	unfolded
cen	GPD	TAP	ZuoC V433A	-	yes	unfolded

Copy #	Promoter	Tag	Gene Name	PDR induction	Expressed?	C-terminal Fold
cen	GPD	TAP	$ZuoC_{\Delta YFV}$ / $Zuo1_{365-430}$	-	yes	unfolded
cen	GPD	TAP	$ZuoC_{\Delta 13}$ / $Zuo1_{365-420}$	-	yes	unfolded
cen	GPD	8HT	$Zuo1_{365-433}$ / ZuoC	- (slight?)	couldn't detect	unfolded
cen	GPD	8HT	ZuoC D386R/D390R	-	couldn't detect	unfolded
cen	GPD	8HT	ZuoC L411R	-	couldn't detect	unfolded
cen	GPD	-	$Zuo1_{365-433}$ / ZuoC	-	(no Ab)	unfolded
cen	GPD	TAP	$Zuo1_{388-433}$	++	yes	unfolded
cen	GPD	TAP	$Zuo1_{403-433}$	++	yes	unfolded
cen	GPD	TAP	$Zuo1_{421-433}$	++	yes	unfolded
cen	GPD	TAP	$Zuo1_{421-433}$ S427G	+++	yes	unfolded
cen	GPD	TAP	$Zuo1_{421-433}$ K423A	++	yes	unfolded
cen	GPD	GST	$Zuo1_{421-433}$	same as GST-ZuoC		unfolded

Table A-7. Correlation between *in vitro* fold and stability of Zuo1 C-terminal fragments purified from *E. coli* and PDR induction *in vivo*

Vector	Tag	Gene Name	*E. coli* expression	Fold	Stability	PDR induction*
pQE30	8HT	$Zuo1_{365-433}$ / ZuoC	-	unfolded	unstable	++
pQE30	8HT	$Zuo1_{358-433}$	yes	partially folded	unstable / Tm = 35.5 ºC	+
pQE30	8HT	$Zuo1_{348-433}$	yes	folded	stable / Tm = 43.5 ºC	-
pQE30	8HT	$Zuo1_{348-433}$ S427G	yes	folded		-
pQE30	8HT	$Zuo1_{348-433}$ S427D	yes	folded		-
pQE30	8HT	$Zuo1_{348-433}$ L411R	yes	unfolded	unstable	++
pQE30	8HT	$Zuo1_{348-433}$ D386R/D390R	yes	unfolded	unstable	+
pQE30	8HT	$Zuo1_{348-433}$ K351P/K355P	yes	unfolded	unstable	++
pQE30	8HT	$Zuo1_{348-430}$ / ΔYFV	yes	unfolded	unstable	-
pQE30	8HT	$Zuo1_{335-433}$	yes	folded (no added fold)		
pQE30	8HT	$Zuo1_{306-433}$	yes	folded (no added fold)		
pGEX-TEV	GST	$Zuo1_{365-433}$ / ZuoC	yes	unfolded	unstable	++
pGEX-TEV	GST	$Zuo1_{358-433}$	yes	partially folded	unstable	+
pGEX-TEV	GST	$Zuo1_{348-433}$	yes	folded	stable	-

*PDR induction by TAP-tagged fusion in yeast

Auto-activation of yeast two-hybrid reporters by GBD fusions of Zuo1 and Ssz1

Table A-8 summarizes the auto-activation of the yeast two-hybrid *GAL1-HIS3, GAL2-ADE2,* and *GAL7-lacZ* reporters by Gal4 DNA binding domain fusions of Zuo1 and Ssz1. All constructs shown were cloned into pGBDU-C1, a 2µ plasmid containing the *ADH* promoter (James et al., 1996), and expressed as fusions to the Gal4 DNA binding domain (GBD). Auto-activation of the *GAL1-HIS3* and *GAL2-ADE2* reporters was measured by growth on minimal media lacking either histidine (and containing 2mM 3-AT as indicated) or adenine. *GAL7-lacZ* activation was measured by ß-galactosidase activity. Auto-activation of the three reporters was tested in either PJ69-4a or PJ69-4a Δ*pdr1::TRP1* cells (James et al., 1996; Prunuske et al., 2012). Because $Zuo1_{365\text{-}433}$ showed some auto-activation of all reporters except *GAL2-ADE2* in the absence of Pdr1, I tested the majority of mutants of $Zuo1_{365\text{-}433}$ for growth in the absence of adenine to determine their effect on interaction with Pdr1. Text shown in red represents data that I collected personally. Text in black represents data collected by another member of the lab that are either previously published or preliminary in nature. Text shown in gray represents assumptions made based on data of a similar nature that were not collected using the specific construct indicated.

Table A-8. Auto-activation of *GAL1-HIS3, GAL2-ADE2,* and *GAL7-lacZ* reporters of the yeast two-hybrid system by Gal4 DNA binding domain fusions of Zuo1 and Ssz1

Strain	GBD fusion	PDR*	Expressed?	Yeast Two-Hybrid Reporter Activation			
				GAL1-HIS3	*GAL1-HIS3* +3-AT	*GAL2-ADE2*	*GAL7-lacZ*
WT	Zuo1	-	yes	-	-	-	-
WT	Zuo1 L411R	++	yes	+	+	-	-
WT	$Zuo1_{\Delta chg}$ / $Zuo1_{\Delta 285-347}$	+		++	++	-	-
WT	$Zuo1_{\Delta chg}$ S427G	++		+++	+++	-	
WT	$Zuo1_{\Delta chg}$ S427D	-		+	+	-	
WT	Zuo1(charged) / $Zuo1_{283-368}$	-	yes	-		-	-
WT	ZuoC / $Zuo1_{365-433}$	++	yes	+++	+++	++	++
Δpdr1	ZuoC / $Zuo1_{365-433}$	-	yes	+++	+	-	+
WT	ZuoC S421A	++	yes			++	
WT	ZuoC G422A	++	yes			++	
WT	ZuoC K423A	++	yes			++	
WT	ZuoC L424A	++	yes			-	
WT	ZuoC P425A	+	yes			-	
WT	ZuoC S426A	++	yes			++	
WT	ZuoC S426D	-		+++	++	-	
WT	ZuoC S427A	++	yes			++	
WT	ZuoC S427G	+++	yes	+++	+++	+++	+++
Δpdr1	ZuoC S427G	-	yes	+++	+	-	+
WT	ZuoC S427D	-		+++	++	-	++
WT	ZuoC L428A	-	yes			-	
WT	ZuoC L428G	-	yes	++	-	-	+
Δpdr1	ZuoC L428G	-	yes	+	-	-	
WT	ZuoC L429A	-	yes			-	
WT	ZuoC L429G	-	yes	++	-	-	
WT	ZuoC S430A	++	yes			++	
WT	ZuoC Y431A	-	yes			-	
WT	ZuoC F432A	+	yes			-	
WT	ZuoC V433A	-	yes			-	

Strain	GBD fusion	PDR*	Expressed?	Yeast Two-Hybrid Reporter Activation			
				GAL1-HIS3	*GAL1-HIS3* +3-AT	*GAL2-ADE2*	*GAL7-lacZ*
WT	$Zuo1_{421-433}$	++	yes	+++	+++	-	+
Δpdr1	$Zuo1_{421-433}$	-	yes	-	-	-	-
WT	$ZuoC_{\Delta 13}$ / $Zuo1_{365-420}$	-	yes	-	-	-	-
Δpdr1	$ZuoC_{\Delta 13}$ / $Zuo1_{365-420}$	-	yes	-	-	-	-
WT	$Zuo1_{358-433}$	+	yes	+++	++	-	
WT	$Zuo1_{348-433}$	-	yes	-	-	-	
WT	$Zuo1_{348-433}$ L411R	++	yes	+++	+++	-	
WT	Ssz1	++		++	-	-	-
WT	$Ssz1_{1-407}$ S295F	+++	yes	+++	+++	-	+
Δpdr1	$Ssz1_{1-407}$ S295F	-	yes	-	-	-	-
WT	$Ssz1_{1-407}$ S295F/I283N	-	yes	+	-	-	
Δpdr1	$Ssz1_{1-407}$ S295F/I283N	-	yes	+	-	-	

*PDR induction in yeast by Ssz1 or TAP-tagged Zuo1 fusions

REFERENCES

Albanese, V., S. Reissmann, and J. Frydman. 2010a. A ribosome-anchored chaperone network that facilitates eukaryotic ribosome biogenesis. *The Journal of cell biology*. 189:69-81.

Albanese, V., S. Reissmann, and J. Frydman. 2010b. A ribosome-anchored chaperone network that facilitates eukaryotic ribosome biogenesis. *The Journal of cell biology*. 189:69-81.

Albanese, V., A.Y. Yam, J. Baughman, C. Parnot, and J. Frydman. 2006. Systems analyses reveal two chaperone networks with distinct functions in eukaryotic cells. *Cell*. 124:75-88.

Allen, D.L., and G.J. Pielak. 1998. Baseline length and automated fitting of denaturation data. *Protein science : a publication of the Protein Society*. 7:1262-1263.

Anfinsen, C.B. 1973. Principles that govern the folding of protein chains. *Science*. 181:223-230.

Ausubel, L.J., J.I. Krieger, and D.A. Hafler. 1997. Changes in cytokine secretion induced by altered peptide ligands of myelin basic protein peptide 85-99. *J Immunol*. 159:2502-2512.

Balzi, E., W. Chen, S. Ulaszewski, E. Capieaux, and A. Goffeau. 1987. The multidrug resistance gene PDR1 from Saccharomyces cerevisiae. *The Journal of biological chemistry*. 262:16871-16879.

Ban, N., P. Nissen, J. Hansen, P.B. Moore, and T.A. Steitz. 2000. The complete atomic structure of the large ribosomal subunit at 2.4 A resolution. *Science*. 289:905-920.

Banerjee, D., G. Lelandais, S. Shukla, G. Mukhopadhyay, C. Jacq, F. Devaux, and R. Prasad. 2008. Responses of pathogenic and nonpathogenic yeast species to steroids reveal the functioning and evolution of multidrug resistance transcriptional networks. *Eukaryot Cell*. 7:68-77.

Bauer, B.E., H. Wolfger, and K. Kuchler. 1999. Inventory and function of yeast ABC proteins: about sex, stress, pleiotropic drug and heavy metal resistance. *Biochim Biophys Acta*. 1461:217-236.

Ben-Shem, A., N. Garreau de Loubresse, S. Melnikov, L. Jenner, G. Yusupova, and M. Yusupov. 2011. The structure of the eukaryotic ribosome at 3.0 A resolution. *Science*. 334:1524-1529.

Boorsma, A., B.C. Foat, D. Vis, F. Klis, and H.J. Bussemaker. 2005. T-profiler: scoring the activity of predefined groups of genes using gene expression data. *Nucleic acids research*. 33:W592-595.

Braun, E.L., and E. Grotewold. 2001a. Fungal Zuotin proteins evolved from MIDA1-like factors by lineage-specific loss of MYB domains. *Molecular biology and evolution*. 18:1401-1412.

Braun, E.L., and E. Grotewold. 2001b. Fungal Zuotin proteins evolved from MIDA1-like factors by lineage-specific loss of MYB domains. *Molecular biology and evolution*. 18:1401-1412.

Bukau, B., E. Deuerling, C. Pfund, and E.A. Craig. 2000. Getting newly synthesized proteins into shape. *Cell*. 101:119-122.

Carvajal, E., H.B. van den Hazel, A. Cybularz-Kolaczkowska, E. Balzi, and A. Goffeau. 1997. Molecular and phenotypic characterization of yeast PDR1 mutants that show hyperactive transcription of various ABC multidrug transporter genes. *Mol Gen Genet*. 256:406-415.

Chen, H., and G.R. Fink. 2006. Feedback control of morphogenesis in fungi by aromatic alcohols. *Genes & development*. 20:1150-1161.

Chen, H., M. Fujita, Q. Feng, J. Clardy, and G.R. Fink. 2004. Tyrosol is a quorum-sensing molecule in Candida albicans. *Proceedings of the National Academy of Sciences of the United States of America*. 101:5048-5052.

Conz, C., H. Otto, K. Peisker, M. Gautschi, T. Wolfle, M.P. Mayer, and S. Rospert. 2007a. Functional characterization of the atypical Hsp70 subunit of yeast ribosome-associated complex. *The Journal of biological chemistry*. 282:33977-33984.

Conz, C., H. Otto, K. Peisker, M. Gautschi, T. Wolfle, M.P. Mayer, and S. Rospert. 2007b. Functional characterization of the atypical Hsp70 subunit of yeast ribosome-associated complex. *The Journal of biological chemistry*. 282:33977-33984.

Cornilescu, G., F. Delaglio, and A. Bax. 1999. Protein backbone angle restraints from searching a database for chemical shift and sequence homology. *J Biomol NMR*. 13:289-302.

Craig, E.A., H.C. Eisenman, and H.A. Hundley. 2003. Ribosome-tethered molecular chaperones: the first line of defense against protein misfolding? *Curr Opin Microbiol*. 6:157-162.

Craig, E.A., P. Huang, R. Aron, and A. Andrew. 2006. The diverse roles of J-proteins, the obligate Hsp70 co-chaperone. *Reviews of physiology, biochemistry and pharmacology*. 156:1-21.

Dean, M., Y. Hamon, and G. Chimini. 2001. The human ATP-binding cassette (ABC) transporter superfamily. *Journal of lipid research*. 42:1007-1017.

Decottignies, A., and A. Goffeau. 1997. Complete inventory of the yeast ABC proteins. *Nature genetics*. 15:137-145.

Delaglio, F., S. Grzesiek, G.W. Vuister, G. Zhu, J. Pfeifer, and A. Bax. 1995. NMRPipe: a multidimensional spectral processing system based on UNIX pipes. *J. Biomol. NMR*. 6:277-293.

Delahodde, A., R. Pandjaitan, M. Corral-Debrinski, and C. Jacq. 2001. Pse1/Kap121-dependent nuclear localization of the major yeast multidrug resistance (MDR) transcription factor Pdr1. *Molecular microbiology*. 39:304-312.

DeRisi, J., B. van den Hazel, P. Marc, E. Balzi, P. Brown, C. Jacq, and A. Goffeau. 2000. Genome microarray analysis of transcriptional activation in multidrug resistance yeast mutants. *FEBS letters*. 470:156-160.

DeRisi, J.L., V.R. Iyer, and P.O. Brown. 1997. Exploring the metabolic and genetic control of gene expression on a genomic scale. *Science*. 278:680-686.

Devaux, F., P. Marc, C. Bouchoux, T. Delaveau, I. Hikkel, M.C. Potier, and C. Jacq. 2001. An artificial transcription activator mimics the genome-wide properties of the yeast Pdr1 transcription factor. *EMBO reports*. 2:493-498.

Dickinson, J.R. 1996. 'Fusel' alcohols induce hyphal-like extensions and pseudohyphal formation in yeasts. *Microbiology*. 142 (Pt 6):1391-1397.

Eisenman, H.C., and E.A. Craig. 2004. Activation of pleiotropic drug resistance by the J-protein and Hsp70-related proteins, Zuo1 and Ssz1. *Molecular microbiology*. 53:335-344.

Ellis, R.J. 2001. Macromolecular crowding: obvious but underappreciated. *Trends Biochem Sci*. 26:597-604.

Erbse, A., M.P. Mayer, and B. Bukau. 2004. Mechanism of substrate recognition by Hsp70 chaperones. *Biochem Soc Trans*. 32:617-621.

Escobar-Cabrera, E., D.K. Lau, S. Giovinazzi, A.M. Ishov, and L.P. McIntosh. 2010. Structural characterization of the DAXX N-terminal helical bundle domain and its complex with Rassf1C. *Structure*. 18:1642-1653.

Fardeau, V., G. Lelandais, A. Oldfield, H. Salin, S. Lemoine, M. Garcia, V. Tanty, S. Le Crom, C. Jacq, and F. Devaux. 2007. The central role of PDR1 in the foundation of yeast drug resistance. *The Journal of biological chemistry*. 282:5063-5074.

Ferreira, M.E., S. Hermann, P. Prochasson, J.L. Workman, K.D. Berndt, and A.P. Wright. 2005. Mechanism of transcription factor recruitment by acidic activators. *The Journal of biological chemistry*. 280:21779-21784.

Fiaux, J., J. Horst, A. Scior, S. Preissler, A. Koplin, B. Bukau, and E. Deuerling. 2010. Structural analysis of the ribosome-associated complex (RAC) reveals an unusual Hsp70/Hsp40 interaction. *The Journal of biological chemistry*. 285:3227-3234.

Fink, A.L. 1999. Chaperone-mediated protein folding. *Physiological reviews*. 79:425-449.

Freeman, B.C., and K.R. Yamamoto. 2002. Disassembly of transcriptional regulatory complexes by molecular chaperones. *Science*. 296:2232-2235.

Gautschi, M., H. Lilie, U. Funfschilling, A. Mun, S. Ross, T. Lithgow, P. Rucknagel, and S. Rospert. 2001a. RAC, a stable ribosome-associated complex in yeast formed by the DnaK- DnaJ homologs Ssz1p and zuotin. *Proceedings of the National Academy of Sciences of the United States of America*. 98:3762-3767.

Gautschi, M., H. Lilie, U. Funfschilling, A. Mun, S. Ross, T. Lithgow, P. Rucknagel, and S. Rospert. 2001b. RAC, a stable ribosome-associated complex in yeast formed by the DnaK-DnaJ homologs Ssz1p and zuotin. *Proceedings of the National Academy of Sciences of the United States of America*. 98:3762-3767.

Gautschi, M., A. Mun, S. Ross, and S. Rospert. 2002. A functional chaperone triad on the yeast ribosome. *Proceedings of the National Academy of Sciences of the United States of America*. 99:4209-4214.

Gershenson, A., and L.M. Gierasch. 2011. Protein folding in the cell: challenges and progress. *Curr Opin Struct Biol*. 21:32-41.

Ghaemmaghami, S., W.K. Huh, K. Bower, R.W. Howson, A. Belle, N. Dephoure, E.K. O'Shea, and J.S. Weissman. 2003. Global analysis of protein expression in yeast. *Nature*. 425:737-741.

Giovinazzi, S., C.R. Lindsay, V.M. Morozov, E. Escobar-Cabrera, M.K. Summers, H.S. Han, L.P. McIntosh, and A.M. Ishov. 2011. Regulation of mitosis and taxane response by Daxx and Rassf1. *Oncogene*.

Guntert, P. 2004. Automated NMR structure calculation with CYANA. *Methods Mol Biol*. 278:353-378.

Hallstrom, T.C., D.J. Katzmann, R.J. Torres, W.J. Sharp, and W.S. Moye-Rowley. 1998. Regulation of transcription factor Pdr1p function by an Hsp70 protein in Saccharomyces cerevisiae. *Molecular and cellular biology*. 18:1147-1155.

Hallstrom, T.C., L. Lambert, S. Schorling, E. Balzi, A. Goffeau, and W.S. Moye-Rowley. 2001. Coordinate control of sphingolipid biosynthesis and multidrug resistance in Saccharomyces cerevisiae. *The Journal of biological chemistry*. 276:23674-23680.

Hallstrom, T.C., and W.S. Moye-Rowley. 2000a. Hyperactive forms of the Pdr1p transcription factor fail to respond to positive regulation by the hsp70 protein Pdr13p. *Molecular microbiology*. 36:402-413.

Hallstrom, T.C., and W.S. Moye-Rowley. 2000b. Multiple signals from dysfunctional mitochondria activate the pleiotropic drug resistance pathway in Saccharomyces cerevisiae. *The Journal of biological chemistry*. 275:37347-37356.

Harris, B.Z., and W.A. Lim. 2001. Mechanism and role of PDZ domains in signaling complex assembly. *Journal of cell science*. 114:3219-3231.

Hartl, F.U., and M. Hayer-Hartl. 2002. Molecular chaperones in the cytosol: from nascent chain to folded protein. *Science*. 295:1852-1858.

Hatzold, J., and B. Conradt. 2008. Control of apoptosis by asymmetric cell division. *PLoS Biol*. 6:e84.

Hauser, M., P. Horn, H. Tournu, N.C. Hauser, J.D. Hoheisel, A.J. Brown, and J.R. Dickinson. 2007. A transcriptome analysis of isoamyl alcohol-induced filamentation in yeast reveals a novel role for Gre2p as isovaleraldehyde reductase. *FEMS Yeast Res*. 7:84-92.

Hlavacek, O., H. Kucerova, K. Harant, Z. Palkova, and L. Vachova. 2009. Putative role for ABC multidrug exporters in yeast quorum sensing. *FEBS letters*. 583:1107-1113.

Holm, L., and P. Rosenstrom. 2010. Dali server: conservation mapping in 3D. *Nucleic acids research*. 38:W545-549.

Hornby, J.M., E.C. Jensen, A.D. Lisec, J.J. Tasto, B. Jahnke, R. Shoemaker, P. Dussault, and K.W. Nickerson. 2001. Quorum sensing in the dimorphic fungus Candida albicans is mediated by farnesol. *Applied and environmental microbiology*. 67:2982-2992.

Huang, P., M. Gautschi, W. Walter, S. Rospert, and E.A. Craig. 2005. The Hsp70 Ssz1 modulates the function of the ribosome-associated J-protein Zuo1. *Nature structural & molecular biology*. 12:497-504.

Hundley, H., H. Eisenman, W. Walter, T. Evans, Y. Hotokezaka, M. Wiedmann, and E. Craig. 2002. The in vivo function of the ribosome-associated Hsp70, Ssz1, does not require its putative peptide-binding domain. *Proceedings of the National Academy of Sciences of the United States of America*. 99:4203-4208.

Hundley, H.A., W. Walter, S. Bairstow, and E.A. Craig. 2005. Human Mpp11 J protein: ribosome-tethered molecular chaperones are ubiquitous. *Science*. 308:1032-1034.

Inoue, T., W. Shoji, and M. Obinata. 1999. MIDA1, an Id-associating protein, has two distinct DNA binding activities that are converted by the association with Id1: a novel function of Id protein. *Biochem Biophys Res Commun*. 266:147-151.

James, P., J. Halladay, and E.A. Craig. 1996. Genomic libraries and a host strain designed for highly efficient two-hybrid selection in yeast. *Genetics*. 144:1425-1436.

Jungwirth, H., and K. Kuchler. 2006. Yeast ABC transporters-- a tale of sex, stress, drugs and aging. *FEBS letters*. 580:1131-1138.

Kampinga, H.H., and E.A. Craig. 2010. The HSP70 chaperone machinery: J proteins as drivers of functional specificity. *Nature reviews. Molecular cell biology*. 11:579-592.

Katzmann, D.J., T.C. Hallstrom, Y. Mahe, and W.S. Moye-Rowley. 1996. Multiple Pdr1p/Pdr3p binding sites are essential for normal expression of the ATP binding cassette transporter protein-encoding gene PDR5. *The Journal of biological chemistry*. 271:23049-23054.

Katzmann, D.J., T.C. Hallstrom, M. Voet, W. Wysock, J. Golin, G. Volckaert, and W.S. Moye-Rowley. 1995. Expression of an ATP-binding cassette transporter-encoding gene (YOR1)

is required for oligomycin resistance in Saccharomyces cerevisiae. *Molecular and cellular biology*. 15:6875-6883.

Kliewer, S.A., B. Goodwin, and T.M. Willson. 2002. The nuclear pregnane X receptor: a key regulator of xenobiotic metabolism. *Endocr Rev*. 23:687-702.

Kolaczkowska, A., M. Kolaczkowski, A. Delahodde, and A. Goffeau. 2002. Functional dissection of Pdr1p, a regulator of multidrug resistance in Saccharomyces cerevisiae. *Mol Genet Genomics*. 267:96-106.

Kolaczkowski, M., A. Kolaczkowska, B. Gaigg, R. Schneiter, and W.S. Moye-Rowley. 2004. Differential regulation of ceramide synthase components LAC1 and LAG1 in Saccharomyces cerevisiae. *Eukaryot Cell*. 3:880-892.

Kolaczkowski, M., A. Kolaczowska, J. Luczynski, S. Witek, and A. Goffeau. 1998. In vivo characterization of the drug resistance profile of the major ABC transporters and other components of the yeast pleiotropic drug resistance network. *Microb Drug Resist*. 4:143-158.

Kolaczkowski, M., M. van der Rest, A. Cybularz-Kolaczkowska, J.P. Soumillion, W.N. Konings, and A. Goffeau. 1996. Anticancer drugs, ionophoric peptides, and steroids as substrates of the yeast multidrug transporter Pdr5p. *The Journal of biological chemistry*. 271:31543-31548.

la Cour, T., L. Kiemer, A. Molgaard, R. Gupta, K. Skriver, and S. Brunak. 2004. Analysis and prediction of leucine-rich nuclear export signals. *Protein Eng Des Sel*. 17:527-536.

Lee, H.S., R.D. Dimla, and P.G. Schultz. 2009. Protein-DNA photo-crosslinking with a genetically encoded benzophenone-containing amino acid. *Bioorg Med Chem Lett*. 19:5222-5224.

Lelandais, G., and F. Devaux. 2010. Comparative functional genomics of stress responses in yeasts. *Omics : a journal of integrative biology*. 14:501-515.

Li, J., X. Qian, and B. Sha. 2009. Heat shock protein 40: structural studies and their functional implications. *Protein Pept Lett*. 16:606-612.

Linge, J.P., M.A. Williams, C.A. Spronk, A.M. Bonvin, and M. Nilges. 2003. Refinement of protein structures in explicit solvent. *Proteins*. 50:496-506.

Liu, H., C.A. Styles, and G.R. Fink. 1996. Saccharomyces cerevisiae S288C has a mutation in FLO8, a gene required for filamentous growth. *Genetics*. 144:967-978.

Lu, X., A.Z. Ansari, and M. Ptashne. 2000. An artificial transcriptional activating region with unusual properties. *Proceedings of the National Academy of Sciences of the United States of America*. 97:1988-1992.

Lu, Z., A.Z. Ansari, X. Lu, A. Ogirala, and M. Ptashne. 2002. A target essential for the activity of a nonacidic yeast transcriptional activator. *Proceedings of the National Academy of Sciences of the United States of America*. 99:8591-8596.

Lytle, B.L., F.C. Peterson, S.H. Qiu, M. Luo, Q. Zhao, J.L. Markley, and B.F. Volkman. 2004. Solution structure of a ubiquitin-like domain from tubulin-binding cofactor B. *The Journal of biological chemistry*. 279:46787-46793.

MacPherson, S., M. Larochelle, and B. Turcotte. 2006. A fungal family of transcriptional regulators: the zinc cluster proteins. *Microbiol Mol Biol Rev*. 70:583-604.

Mahe, Y., Y. Lemoine, and K. Kuchler. 1996. The ATP binding cassette transporters Pdr5 and Snq2 of Saccharomyces cerevisiae can mediate transport of steroids in vivo. *The Journal of biological chemistry*. 271:25167-25172.

Majmudar, C.Y., L.W. Lee, J.K. Lancia, A. Nwokoye, Q. Wang, A.M. Wands, L. Wang, and A.K. Mapp. 2009. Impact of nonnatural amino acid mutagenesis on the in vivo function and binding modes of a transcriptional activator. *J Am Chem Soc*. 131:14240-14242.

Malkin, L.I., and A. Rich. 1967. Partial resistance of nascent polypeptide chains to proteolytic digestion due to ribosomal shielding. *J Mol Biol*. 26:329-346.

Mamnun, Y.M., R. Pandjaitan, Y. Mahe, A. Delahodde, and K. Kuchler. 2002. The yeast zinc finger regulators Pdr1p and Pdr3p control pleiotropic drug resistance (PDR) as homo- and heterodimers in vivo. *Molecular microbiology*. 46:1429-1440.

Markley, J.L., A. Bahrami, H.R. Eghbalnia, F.C. Peterson, E.L. Ulrich, W.M. Westler, and B.F. Volkman. 2009. Macromolecular Structure Determination by NMR Spectroscopy. *In* Structural Bioinformatics. J. GU and P.E. Bourne, editors. John Wiley. 93-142.

Nelson, R.J., T. Ziegelhoffer, C. Nicolet, M. Werner-Washburne, and E.A. Craig. 1992. The translation machinery and 70 kd heat shock protein cooperate in protein synthesis. *Cell*. 71:97-105.

Nourani, A., D. Papajova, A. Delahodde, C. Jacq, and J. Subik. 1997. Clustered amino acid substitutions in the yeast transcription regulator Pdr3p increase pleiotropic drug resistance and identify a new central regulatory domain. *Mol Gen Genet*. 256:397-405.

Otto, H., C. Conz, P. Maier, T. Wolfle, C.K. Suzuki, P. Jeno, P. Rucknagel, J. Stahl, and S. Rospert. 2005. The chaperones MPP11 and Hsp70L1 form the mammalian ribosome-associated complex. *Proceedings of the National Academy of Sciences of the United States of America*. 102:10064-10069.

Palecek, S.P., A.S. Parikh, and S.J. Kron. 2000. Genetic analysis reveals that FLO11 upregulation and cell polarization independently regulate invasive growth in Saccharomyces cerevisiae. *Genetics*. 156:1005-1023.

Panchal, S.C., D.A. Kaiser, E. Torres, T.D. Pollard, and M.K. Rosen. 2003. A conserved amphipathic helix in WASP/Scar proteins is essential for activation of Arp2/3 complex. *Nat Struct Biol*. 10:591-598.

Pappas, V., and S.M. Miller. 2009. Functional analysis of the Volvox carteri asymmetric division protein GlsA. *Mech Dev*. 126:842-851.

Peisker, K., D. Braun, T. Wolfle, J. Hentschel, U. Funfschilling, G. Fischer, A. Sickmann, and S. Rospert. 2008. Ribosome-associated complex binds to ribosomes in close proximity of Rpl31 at the exit of the polypeptide tunnel in yeast. *Molecular biology of the cell*. 19:5279-5288.

Pfund, C., P. Huang, N. Lopez-Hoyo, and E.A. Craig. 2001. Divergent functional properties of the ribosome-associated molecular chaperone Ssb compared with other Hsp70s. *Molecular biology of the cell*. 12:3773-3782.

Pfund, C., N. Lopez-Hoyo, T. Ziegelhoffer, B.A. Schilke, P. Lopez-Buesa, W.A. Walter, M. Wiedmann, and E.A. Craig. 1998. The molecular chaperone Ssb from Saccharomyces cerevisiae is a component of the ribosome-nascent chain complex. *Embo J*. 17:3981-3989.

Pohl, A., P.F. Devaux, and A. Herrmann. 2005. Function of prokaryotic and eukaryotic ABC proteins in lipid transport. *Biochim Biophys Acta*. 1733:29-52.

Prunuske, A.J., J.K. Waltner, P. Kuhn, B. Gu, and E.A. Craig. 2012. Role for the molecular chaperones Zuo1 and Ssz1 in quorum sensing via activation of the transcription factor Pdr1. *Proceedings of the National Academy of Sciences of the United States of America*. 109:472-477.

Raue, U., S. Oellerer, and S. Rospert. 2007. Association of protein biogenesis factors at the yeast ribosomal tunnel exit is affected by the translational status and nascent polypeptide sequence. *The Journal of biological chemistry*. 282:7809-7816.

Resto, V.A., O.L. Caballero, M.R. Buta, W.H. Westra, L. Wu, J.M. Westendorf, J. Jen, P. Hieter, and D. Sidransky. 2000. A putative oncogenic role for MPP11 in head and neck squamous cell cancer. *Cancer research*. 60:5529-5535.

Richly, H., L. Rocha-Viegas, J.D. Ribeiro, S. Demajo, G. Gundem, N. Lopez-Bigas, T. Nakagawa, S. Rospert, T. Ito, and L. Di Croce. 2010. Transcriptional activation of polycomb-repressed genes by ZRF1. *Nature*. 468:1124-1128.

Robinson, M.D., J. Grigull, N. Mohammad, and T.R. Hughes. 2002. FunSpec: a web-based cluster interpreter for yeast. *BMC bioinformatics [electronic resource]*. 3:35.

Sahi, C., and E.A. Craig. 2007. Network of general and specialty J protein chaperones of the yeast cytosol. *Proceedings of the National Academy of Sciences of the United States of America*. 104:7163-7168.

Sahi, C., T. Lee, M. Inada, J.A. Pleiss, and E.A. Craig. 2010. Cwc23, an essential J protein critical for pre-mRNA splicing with a dispensable J domain. *Molecular and cellular biology*. 30:33-42.

Sarkadi, B., L. Homolya, G. Szakacs, and A. Varadi. 2006. Human multidrug resistance ABCB and ABCG transporters: participation in a chemoimmunity defense system. *Physiological reviews*. 86:1179-1236.

Schwieters, C.D., J.J. Kuszewski, N. Tjandra, and G. Marius Clore. 2003. The Xplor-NIH NMR molecular structure determination package. *J Magn Reson*. 160:65-73.

Shahi, P., and W.S. Moye-Rowley. 2009. Coordinate control of lipid composition and drug transport activities is required for normal multidrug resistance in fungi. *Biochimica et biophysica acta*. 1794:852-859.

Shoji, W., T. Inoue, T. Yamamoto, and M. Obinata. 1995. MIDA1, a protein associated with Id, regulates cell growth. *The Journal of biological chemistry*. 270:24818-24825.

Sietsma, H., R.J. Veldman, and J.W. Kok. 2001. The involvement of sphingolipids in multidrug resistance. *The Journal of membrane biology*. 181:153-162.

Simonics, T., Z. Kozovska, D. Michalkova-Papajova, A. Delahodde, C. Jacq, and J. Subik. 2000. Isolation and molecular characterization of the carboxy-terminal pdr3 mutants in Saccharomyces cerevisiae. *Curr Genet*. 38:248-255.

Souid, A.K., C. Gao, L. Wang, E. Milgrom, and W.C. Shen. 2006. ELM1 is required for multidrug resistance in Saccharomyces cerevisiae. *Genetics*. 173:1919-1937.

Spellman, P.T., G. Sherlock, M.Q. Zhang, V.R. Iyer, K. Anders, M.B. Eisen, P.O. Brown, D. Botstein, and B. Futcher. 1998. Comprehensive identification of cell cycle-regulated genes of the yeast Saccharomyces cerevisiae by microarray hybridization. *Molecular biology of the cell*. 9:3273-3297.

Taylor, E.J., S.G. Campbell, C.D. Griffiths, P.J. Reid, J.W. Slaven, R.J. Harrison, P.F. Sims, G.D. Pavitt, D. Delneri, and M.P. Ashe. 2010. Fusel alcohols regulate translation initiation by inhibiting eIF2B to reduce ternary complex in a mechanism that may involve altering the integrity and dynamics of the eIF2B body. *Molecular biology of the cell*. 21:2202-2216.

Thakur, J.K., H. Arthanari, F. Yang, S.J. Pan, X. Fan, J. Breger, D.P. Frueh, K. Gulshan, D.K. Li, E. Mylonakis, K. Struhl, W.S. Moye-Rowley, B.P. Cormack, G. Wagner, and A.M. Naar. 2008. A nuclear receptor-like pathway regulating multidrug resistance in fungi. *Nature*. 452:604-609.

Tietjen, J.R., D.W. Zhang, J.B. Rodriguez-Molina, B.E. White, M.S. Akhtar, M. Heidemann, X. Li, R.D. Chapman, K. Shokat, S. Keles, D. Eick, and A.Z. Ansari. 2010. Chemical-genomic dissection of the CTD code. *Nature structural & molecular biology*. 17:1154-1161.

Uesugi, M., O. Nyanguile, H. Lu, A.J. Levine, and G.L. Verdine. 1997. Induced alpha helix in the VP16 activation domain upon binding to a human TAF. *Science*. 277:1310-1313.

von Plehwe, U., U. Berndt, C. Conz, M. Chiabudini, E. Fitzke, A. Sickmann, A. Petersen, D. Pfeifer, and S. Rospert. 2009. The Hsp70 homolog Ssb is essential for glucose sensing via the SNF1 kinase network. *Genes & development*. 23:2102-2115.

Walsh, P., D. Bursac, Y.C. Law, D. Cyr, and T. Lithgow. 2004. The J-protein family: modulating protein assembly, disassembly and translocation. *EMBO reports*. 5:567-571.

Waltner, J.K., F.C. Peterson, B.L. Lytle, and B.F. Volkman. 2005. Structure of the B3 domain from Arabidopsis thaliana protein At1g16640. *Protein Sci*. 14:2478-2483.

Willis, K.A., K.E. Barbara, B.B. Menon, J. Moffat, B. Andrews, and G.M. Santangelo. 2003. The global transcriptional activator of Saccharomyces cerevisiae, Gcr1p, mediates the response to glucose by stimulating protein synthesis and CLN-dependent cell cycle progression. *Genetics*. 165:1017-1029.

Willson, T.M., and S.A. Kliewer. 2002. PXR, CAR and drug metabolism. *Nature reviews. Drug discovery*. 1:259-266.

Winzeler, E.A., D.D. Shoemaker, A. Astromoff, H. Liang, K. Anderson, B. Andre, R. Bangham, R. Benito, J.D. Boeke, H. Bussey, A.M. Chu, C. Connelly, K. Davis, F. Dietrich, S.W. Dow, M. El Bakkoury, F. Foury, S.H. Friend, E. Gentalen, G. Giaever, J.H. Hegemann, T. Jones, M. Laub, H. Liao, N. Liebundguth, D.J. Lockhart, A. Lucau-Danila, M. Lussier, N. M'Rabet, P. Menard, M. Mittmann, C. Pai, C. Rebischung, J.L. Revuelta, L. Riles, C.J. Roberts, P. Ross-MacDonald, B. Scherens, M. Snyder, S. Sookhai-Mahadeo, R.K. Storms, S. Veronneau, M. Voet, G. Volckaert, T.R. Ward, R. Wysocki, G.S. Yen, K. Yu, K. Zimmermann, P. Philippsen, M. Johnston, and R.W. Davis. 1999. Functional characterization of the S. cerevisiae genome by gene deletion and parallel analysis. *Science*. 285:901-906.

Wolfger, H., Y.M. Mamnun, and K. Kuchler. 2004. The yeast Pdr15p ATP-binding cassette (ABC) protein is a general stress response factor implicated in cellular detoxification. *The Journal of biological chemistry*. 279:11593-11599.

Wu, Z., G. Belanger, B.B. Brennan, J.K. Lum, A.R. Minter, S.P. Rowe, A. Plachetka, C.Y. Majmudar, and A.K. Mapp. 2003. Targeting the transcriptional machinery with unique artificial transcriptional activators. *J Am Chem Soc*. 125:12390-12391.

Wuster, A., and M.M. Babu. 2010. Transcriptional control of the quorum sensing response in yeast. *Mol Biosyst*. 6:134-141.

Yan, W., and E.A. Craig. 1999. The glycine-phenylalanine-rich region determines the specificity of the yeast Hsp40 Sis1. *Mol. Cell. Biol.* 19:7751-7758.

Yan, W., B. Schilke, C. Pfund, W. Walter, S. Kim, and E.A. Craig. 1998a. Zuotin, a ribosome-associated DnaJ molecular chaperone. *EMBO J*. 17:4809-4817.

Yan, W., B. Schilke, C. Pfund, W. Walter, S. Kim, and E.A. Craig. 1998b. Zuotin, a ribosome-associated DnaJ molecular chaperone. *EMBO J*. 17:4809-4817.

Yang, S., C.R. Lopez, and E.L. Zechiedrich. 2006. Quorum sensing and multidrug transporters in Escherichia coli. *Proceedings of the National Academy of Sciences of the United States of America*. 103:2386-2391.

Yoshida, M., T. Inoue, W. Shoji, S. Ikawa, and M. Obinata. 2004. Reporter gene stimulation by MIDA1 through its DnaJ homology region. *Biochem Biophys Res Commun*. 324:326-332.

Young, J.C. 2010. Mechanisms of the Hsp70 chaperone system. *Biochemistry and cell biology = Biochimie et biologie cellulaire*. 88:291-300.

Young, J.C., J.M. Barral, and F. Ulrich Hartl. 2003. More than folding: localized functions of cytosolic chaperones. *Trends Biochem Sci*. 28:541-547.